

MESA+

INSTITUTE FOR NANOTECHNOLOGY

UNIVERSITEIT TWENTE.

Surface Modification of Silicon Nanowire Field-effect Devices with Si-C and Si-N bonded Monolayers

Muhammad Nasir Masood



The research described within this thesis was carried in the BIOS Lab-on-a-chip group at the MESA⁺ Institute for Nanotechnology at the University of Twente, Enschede, the Netherlands. The project was financially supported by Higher Education Commission of Pakistan (HEC) and the University of Twente, the Netherlands.

Committee members:

Chairman

Prof. dr. ir. A. J. Mouthaan

University of Twente

Promotor

Prof. dr. ir. A. van. den Berg

University of Twente

Assistant Promotor

Dr. Edwin T. Carlen

University of Twente

Members

Prof. dr. ir. J.G.E. Gardeniers

University of Twente

Prof. dr. ir. J. Huskens

University of Twente

Prof. dr. Jurrian Schmitz

University of Twente

Prof. dr. H. J. Zuilhof

University of Wageningen

Title: Surface Modification of Silicon Nanowire Field-effect Devices with Si-C and Si-N bonded Monolayers

Author: Muhammad Nasir Masood

ISBN: 978-90-365-3283-9

DOI: 10.3990/1.9789036532839

Publisher: Woormann Print Service, Zutphen, the Netherlands

About the Cover: 3D nanowire device and 3D image of Si-N monolayer on Si (111) by Nymus3D

Copyright © 2011 by Muhammad Nasir Masood, Enschede, the Netherlands

Surface Modification of Silicon Nanowire Field-effect Devices with Si-C and Si-N bonded Monolayers

DISSERTATION

to obtain

the degree of doctor at the university of Twente

on the authority of the rector magnificus,

prof. dr. H. Brinksma,

on account of the decision of the graduation

committee, to be publicly defended on Thursday the

24th of November 2011 at 16:45 hrs

By

Muhammad Nasir Masood
Born on November 25th 1976
in Khair-pur Mirs, Pakistan.

بِسْمِ اللَّهِ الرَّحْمَنِ الرَّحِيمِ

Dedicated to my parents, family and all those who love me

TABLE OF CONTENTS

1. GENERAL INTRODUCTION.....	1
1.1. SELF-ASSEMBLED MONOLAYERS.....	2
1.2. AIMS OF THE THESIS	4
1.3. THESIS OUTLINE	4
1.4. BIBLIOGRAPHY	6
2. SILICON NANOWIRE BIOSENSORS.....	7
2.1. INTRODUCTION	8
2.2. APPLICATION OF Si-NW FET BIOSENSORS.....	10
2.3. SILICON NANOWIRE DEVICE FABRICATION	12
2.4. BIOFUNCTIONALIZATION SCHEMES	16
2.5. Si-NW BIOSENSOR: SENSITIVITY IN AQUEOUS MEDIA.....	19
2.6. ELECTROCHEMICAL CELL AND MICROFLUIDICS.....	23
2.7. CONCLUSION	24
2.8. BIBLIOGRAPHY	25
3. SI-ALKYL MONOLAYERS: A FUNCTIONALIZATION TOOL FOR NANOSENSORS	29
3.1. INTRODUCTION	30
3.2. SI-ALKYL FUNCTIONALIZATION METHODOLOGIES.....	34
3.3. SILICON NANOWIRE MODIFIED WITH SI-ALKYL MONOLAYERS	42
3.4. REACTION MECHANISM.....	44
3.5. FURTHER FUNCTIONALIZATION OF MODIFIED SURFACES	46
3.6. CONCLUSION	47
3.7. BIBLIOGRAPHY	48
4. SURFACE PREPARATION OF ACTIVE GATE REGIONS FOR SILICON FIELD-EFFECT DEVICES	54
4.1. INTRODUCTION	55
4.2. EXPERIMENTAL.....	56
4.3. RESULTS AND DISCUSSIONS.....	59
4.4. CONCLUSION	70
4.5. BIBLIOGRAPHY	70
5. SELECTIVE BIOFUNCTIONALIZATION OF ALL-(111) SURFACE SILICON NANOWIRES	72
5.1. INTRODUCTION	73
5.2. EXPERIMENTAL.....	76
5.3. RESULTS AND DISCUSSION	79
5.4. CONCLUSION	85
5.5. BIBLIOGRAPHY	85
6. MATHEMATICAL MODELING OF THIN GATE DIELECTRICAL LAYERS	

OF SILICON NANOWIRES AND THEIR SENSITIVITY	88
6.1. INTRODUCTION	89
6.2. EXPERIMENTAL.....	90
6.3. RESULTS AND DISCUSSION.....	90
6.4. CONCLUSION	95
6.5. BIBLIOGRAPHY	96
7. MULTIFUNCTIONAL SYMMETRIC PRECURSOR: SELECTIVE FUNCTIONALIZATION WITH SI-N BONDED MONOLAYER	97
7.1. INTRODUCTION	98
7.2. EXPERIMENTAL.....	100
7.3. RESULTS AND DISCUSSION.....	103
7.4. CONCLUSION	117
7.5. BIBLIOGRAPHY	118
8. CONCLUSIONS AND FUTURE RECOMMENDATIONS.....	123
9. SUMMARY	127
10. PUBLICATIONS.....	130
11. ACKNOWLEDGEMENTS	131
12. CURRICULUM VITAE.....	134

Chapter 1

General Introduction

This chapter briefly introduces surface modifications using self-assembled monolayers and gives an outline to the various chapters of the thesis.

1.1. Self-assembled monolayers

The functionalization of silicon surfaces through self-assembled monolayers (SAM) is an important way to introduce new surface characteristics to be used for different applications such as biosensing, wettability and molecular electronics. Self assembled monolayers become more valuable and interesting when dealing with nano-devices such as silicon nanowire field effect transistor (Si-NW FETs) devices because of the high surface to volume ratio of these structures and the possibility of tuning characteristics of a device by surface amendments. It is a very exciting and emerging field to integrate molecular based devices and solid state inorganic structures with biologically active interfaces as well.¹ These SAM layers have a number of advantages and applications: i) low leakage current and tunneling current density ($10^{-8} \text{ A cm}^{-2}$)² for a thin well packed monolayer as compared to a conventional 3 nm Si/SiO₂; ii) the ability to improve carrier mobility and the transconductance of silicon nanowires;³ iii) ability to further conjugate biomolecules for biosensor applications⁴ and iv) wettability control.⁵ Figure 1.1 shows a schematic diagram of a SAM on a substrate with the different parts indicated.

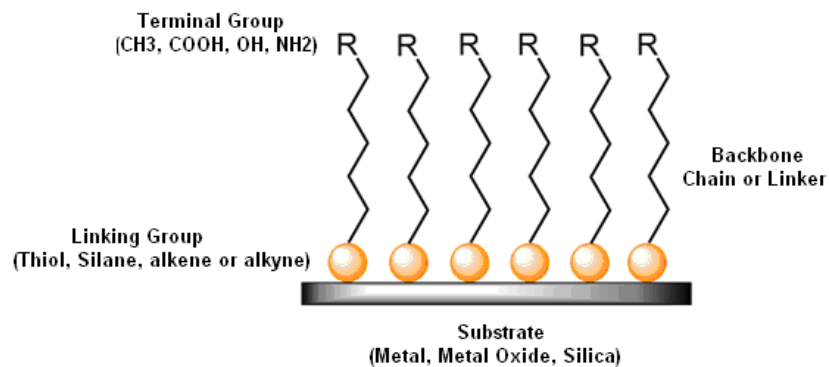


Figure 1.1 Diagram of SAM showing substrate (grey) linking group (orange), backbone chain (black) and terminal group (R).⁶

The use of organic molecules as a precursor for SAM fabrication usually involves two functional groups at the both ends of the molecule having different preferences for reaction. Silanes, thiols and alkenyl groups also known as the head groups or linking groups can be used for bonding to silicon oxide, gold and hydrogen terminated silicon surfaces, respectively. The amine (-NH₂), aldehyde (-COH) and carboxylic acid (COOH) groups are known as tail or terminal groups, at the top of the monolayer that can be used to conjugate biological entities.⁶ The most commonly reported precursor molecule for a self assembled monolayer on silicon oxide surfaces is 3-aminopropyl triethoxy silane (APTES). A monolayer fabricated on a bare silicon or hydrogen terminated silicon surface by UV irradiation, heating or sonication reaction bonded via the Si-C bond directly has a number of advantages as compared to monolayers fabricated on conventional silicon oxide or native oxide interfaces: i) intervening oxide undermines the real potential of SAMs to tune surface characteristics for electronic devices in terms of mobility, recombination velocities, flat band potentials, but these all can be much improved with the help of Si-C or silicon-alkyl monolayers; ii) unexpected surface density, polymerization and degradation in acidic or basic environments and short life times of silane based monolayers can be replaced by stoichiometric, one to one silicon bonded, highly stable and resistant to boiling, acidic and basic environments and crystalline in nature monolayers can become a real nanotechnological advancement; iii) selective functionalization of nanowires and nanostructures with the help of monolayers on bare silicon is possible in addition to others, increasing the sensitivity of a biosensors;⁴ iv) acceptor-ligand couple comes closer to the sensor surface due to a thin monolayer (2 nm) without any intervening oxide layer (10-20 nm) thus improving the extent of the field-effect and Debye length constraints which are well known and limit the performance of silicon biosensor devices.

1.2. Aims of the Thesis

In order to utilize emerging functionalization strategies involving a direct Si-C bond to silicon nanowires surfaces, research was carried out to answer the questions:

1. Are the claims made by so many scientific reports regarding Si-alkyl monolayers on planar silicon samples true in terms of their stability and resistance to oxidation? Are these layers workable truly for an electrical based label free biosensor?
2. Is it possible to improve nanowire device characteristics by using thinner monolayers (1-2 nm) as compared to a thick oxide layer (10-20 nm)?
3. What are the optimized conditions and possibilities to use Si-alkyl monolayers as a tool to selectively functionalize the active gate regions of silicon nanowire biosensors?
4. Is there a better approach to make well packed functional monolayer on silicon nanowires without involving a protecting group to avoid steric hindrances and degradation of the monolayer quality?
5. Is it possible to use commercially available relatively short chain (C_1 to C_6) functional precursor molecules such as vinyl phthalimide, tert butyl allyl carbamate, etc., to get good functional monolayers without doing lengthy synthesis in an organic laboratory?

1.3. Thesis Outline

The thesis is divided into eight chapters including an introductory chapter. The following is a brief description of the different chapters.

Chapter 2: This chapter introduces silicon nanowire field effect transistors configured as biosensors. In this chapter, an attempt was made to explore the potential of Si-NW devices to use as a sensor device for biological species such as DNA, proteins and viruses etc. Different factors that are involved in improving or deteriorating the

efficiency of detection are discussed.

Chapter 3: The modification of nanowire surfaces is crucial for selective bimolecular conjugation as well as for enhanced electrical performances of the nanowire devices. Si-alkyl monolayers have the potential to address both factors due to the fact that they offer biomolecular conjugation at one side and improvement in the carrier mobility and transconductance values on the other side. Si-alkyl monolayers as a functionalization tool for nanosensors have been reviewed in this chapter.

Chapter 4: Control of morphology of the silicon surface during etching and hydrogen termination is very crucial for the formation of high quality self-assembled monolayers. Surface roughness, adsorption of impurities and oxidation undermine the efficiency and usability of devices. X-ray photoelectron spectroscopy (XPS), Atomic force microscopy (AFM) and scanning electron microscopy (SEM) along with electrical measurements were used to characterize the surfaces and devices.

Chapter 5: The selective functionalization of Si-NW FET via functional Si-alkyl monolayers was carried out using UV based hydrosilylation. XPS was used to characterize the modified surfaces. Bioconjugation was carried out and monitored with SEM. Electrical measurements showed enhanced device characteristics after modifications.

Chapter 6: An analytical model is presented to demonstrate the improvement in detection sensitivity of alkyl and alkenyl passivated silicon nanowire biosensor compared to conventional nanowire biosensor geometries and silicon dioxide passivation layers as well as interface design and electrical biasing guidelines for depletion mode sensors.

Chapter 7: Silicon nanowires were functionalized with a new, direct and efficient method by using Si-N bonded monolayer for the first time in solution phase by UV-hydrosilylation. Modified surfaces were characterized fully by XPS and fluorescence studies and biosensing was demonstrated electrically by using electrolyte insulator semiconductor (EIS) sensor configuration in capacitance-voltage mode of operation.

Chapter 8: This is a concluding chapter along with future recommendations.

1.4. Bibliography

1. Li, M., Modification of Silicon by self-assembled monolayers for Application in nano-electronics and biology, PhD Thesis, Graduate School—New Brunswick Rutgers, The State University of New Jersey, New Jersey, USA, **2007**.
2. Collet, J.; Tharaud, O.; Chapoton, A.; Vuillaume, D., Low-voltage, 30 nm channel length, organic transistors with a self-assembled monolayer as gate insulating films. *Appl Phys Lett* **2000**, 76, (14), 1941-1943.
3. Cui, Y.; Zhong, Z.; Wang, D.; Wang, W. U.; Lieber, C. M., High Performance Silicon Nanowire Field Effect Transistors. *Nano Lett* **2003**, 3, (2), 149-152.
4. Masood, M. N.; Chen, S.; Carlen, E. T.; van den Berg, A., All-(111) Surface Silicon Nanowires: Selective Functionalization for Biosensing Applications. *ACS App Mater Interfaces* **2010**, 2, (12), 3422-3428.
5. Akram Raza, M.; Kooij, E. S.; van Silfhout, A.; Poelsema, B., Superhydrophobic Surfaces by Anomalous Fluoroalkylsilane Self-Assembly on Silica Nanosphere Arrays. *Langmuir* **2010**, 26, (15), 12962-12972.
6. Driscoll, P. F. Bioanalytical applications of chemically modified surfaces, a PhD dissertation, Faculty of the Worcester Polytechnic Institute, Worcester, Massachusetts, USA, 2009.

Chapter 2

Silicon nanowire biosensors

The chapter reviews the silicon nanowire field effect transistor (Si-NW FET) biosensor for different biomedical applications. The aim is to understand the potential of Si-NW FET devices in screening biomedically important analytes such as disease biomarkers proteins, DNA and RNA etc. Si-NW FET biosensors are label free, sensitive, and responsive in real time because of a change in the electric field in the vicinity of silicon nanowire body by a charged analyte which modulates the current flowing in the body of the device. The detection process involves the transport of analytes to the surface of the sensor, binding of analyte with the surface bonded receptors and modulation in conductance and response. The detection sensitivity is dependant on the nanowire fabrication method, dimensions, doping concentration, functionalization procedure for receptors, mode of operation (i.e. accumulation, depletion and inversion), concentration of buffer and sample delivery system. In this chapter, a review of the technologies involved in nanowire fabrication, pros and cons in their operation in aqueous solution and their application will be made.

2.1. Introduction

One and two dimensional nanostructures, namely carbon nanotubes and silicon nanowires, have gained attention due to their potential applications as highly sensitive, real time and label free sensors in aqueous solutions.¹ Si-NWs have a unique place in biosensor research because silicon is one of the most characterized materials with structure, size and electronic properties reproducibly controlled.² There are two principal driving forces that promote the exploration of Si-NWs for a sensitive detector. First, silicon nanowires are comparable in size with most biological entities, such as proteins, nucleic acids, cells and viruses, etc, making them good interfacial materials between biological molecules and scientific instruments. Secondly, due to their small size, Si-NWs have high surface to volume ratio and a major fraction of the atoms are at the surface, therefore, a binding event taking place at the surface can be fully sensed in the bulk.³ Being small in size also provides fast response times because small areas have smaller electrostatic capacitances.⁴

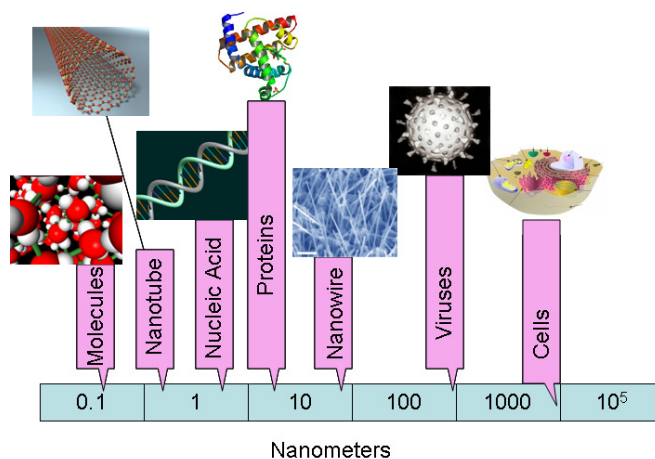


Figure 2.1 Size of several nano-materials is compared to the size of some biological entities, such as nucleic acids, proteins, virus, and cells.³

Normally, Si-NW biosensors are configured as field-effect devices for their efficient

operation. In comparison with the conventional ion-selective field effect transistor (ISFET), the mode of operation of Si-NW FETs is simple as they do not require the formation of a conduction channel and have minimal leakage currents as they are formed on silicon-on-insulator (SOI) substrate. The Si-NWs having ultra small size and can be gated radially and symmetrically from all sides and have high surface to volume ratio which is a reason for their greater sensitivity compared to their predecessors.⁵ SiNW-FET sensors exhibit a conductivity change in response to the variation in the electric field or potential at the nanowire surface. In a typical Si-NW FET device, a semiconductor such as p-type silicon (p-Si), is physically connected to metal source and drain electrodes through which a current is injected and collected, and the conductance of the semiconductor device is controlled by a third gate electrode capacitively coupled through a dielectric layer. In the case of p-Si, applying a positive gate potential/voltage depletes carriers and reduces the conductance, while applying a negative gate voltage leads to accumulation of carriers and increase in conductance, see Figure 2.2.

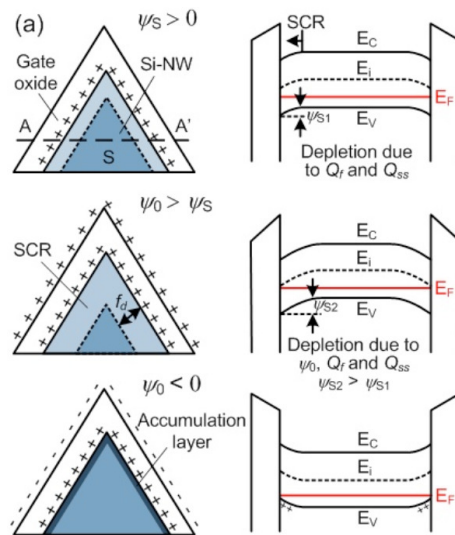


Figure 2.2 Changes in surface charge density on the surface of a p-type silicon nanowire change its conductivity in accumulation mode of gating.⁵

The dependence of the Si-NW FET conductance on gate voltage also enables direct, electrical sensing since the electric field resulting from binding of charged molecules on the sensor surface is analogous to applying a voltage using a gate electrode. The Si-NW drain to source current (I_{DS}) can be modulated by the interaction of ions like hydronium ion H_3O^+ by varying the solution pH due to the presence of native oxide or thermally grown oxide coating as is known from the ISFET sensor. A selective sensor can be configured with Si-NW devices by linking receptor groups to the surface. The native silicon dioxide coating on silicon nanowires make it simple and straightforward since extensive data exists for chemical modification of silicon oxide or glass surfaces from planar chemical and biological sensor literature. When the sensor device, with surface receptors, is exposed to a solution containing a macromolecule such as a protein, which has a net negative (or positive) charge in aqueous solution, specific binding will lead to an increase (or decrease) in surface negative charge and an increase (or decrease) in conductance for a p-type nanowire devices.²

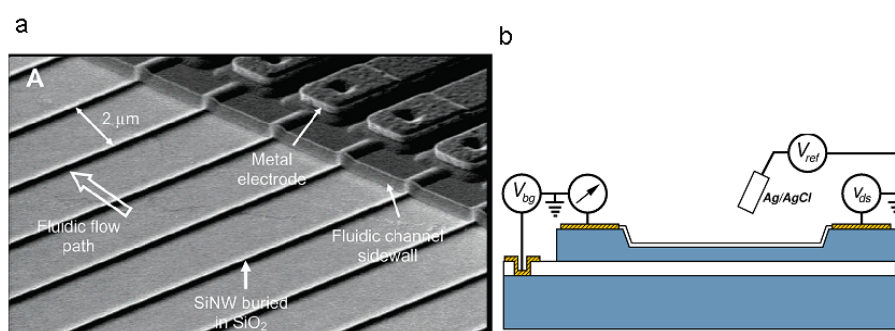


Figure 2.3 Si-NW FET configuration for biosensing; a) SEM image of Si-NW FET¹⁹; b) measurement set-up.

2.2. Application of Si-NW FET biosensors

2.2.1. Protein detection

Various types of proteins including biomarker proteins for different diseases have been

detected selectively, in real time, and label free by various groups using Si-NW FET biosensors. In the field of medical diagnostics, the detection of cancer biomarker proteins, which occur in blood or tissue associated with cancer and whose detection is very crucial for early diagnostics or clinical management is an excellent example of using Si-NW biosensors.⁶ For example, Lieber and co-workers have reported a highly sensitive and multiplexed detection of cancer marker proteins using Si-NW FET.⁷ Modification of the Silicon nanowire arrays with cancer marker antibodies allowed real-time multiplexed detection of free protein specific antigen (f-PSA), PSA-a-antichymotrypsin (PSA-ACT) complex, carcinoembryonic antigen (CEA) and mucin-1 with good sensitivity down to the 50- to 100-fg/mL level. High selectivity and sensitivity to sample concentrations down to 0.9 pg/mL of the targeted cancer markers was achieved in undiluted serum samples. The incorporation of PSA antibody functionalized p- and n-type Si-NWs in a single sensor chip enabled discrimination of possible electrical cross-talk and/or false-positive signals in the detection of PSA by correlating the response versus time from the two types of device elements. Real and selective binding events showed complementary responses in the p- and n-type devices.⁶ Biotin-functionalized Si-NWs have been utilized for the label-free detection of streptavidin and monoclonal antibiotin (m-antibiotin) down to 10 pM.⁸ The use of Si-NW FET devices was extended to the detection of small molecules. For example, the detection of small molecular inhibitors of ATP binding to Abelson protein (Abl) was achieved by covalently linking it to Si-NWs.

2.2.2. DNA detection

Si-NW FET sensors have also been used for the direct detection of DNA. In the first case, the surfaces of the Si-NW devices were modified with peptide nucleic acid (PNA) receptors, and the identification of fully complementary versus mismatched DNA was carried out with a limit of detection in the tens of femtomolar range.⁹ In the second case, single stranded (ss) probe DNA was covalently immobilized on the Si-NWs for detection of up to 25 pM of label-free complimentary (target) ss-DNA in sample solutions.¹⁰ Many other examples of direct DNA detection using Si-NW FET biosensor

have been reported.

2.2.3. Virus detection

Viruses are among the most important causes of human disease and are of increasing concern as possible agents of bio warfare and bioterrorism. Lieber and co-worker have used Si-NWs for the real-time electrical detection of single virus particles with high selectivity.¹¹ Measurements made with Si-NWs functionalized with antibodies specific to influenza A virus showed the detection of influenza A virus but not paramyxovirus or adenovirus. Further, they demonstrated the selective detection of multiple viruses in parallel with Si-NWs functionalized with antibodies specific for influenza virus or adenovirus.

2.3. Silicon nanowire device fabrication

Si-NW-FETs used as biosensor have been fabricated by various approaches and resulted in different dimensions, doping concentration, surface crystal planes, contact resistances and contact doping, operating regime (accumulation, depletion and inversion), number density of addressable nanowires per unit area and all these variations have crucial effect on the performance of a biosensor system.³ The increase in sensitivity results from a decrease in diameter due to the fact that the surface to volume ratio becomes larger resulting into an efficient gating control of surface charges to conduction, It has been shown that a Si-NW having a diameter greater than 150 nm behaves like a planar sensor.^{12, 13} The device sensitivity dependence on the channel dimensions and doping concentration was also demonstrated in other studies.¹⁴ These studies favor the importance of small dimensions in order to achieve high levels of sensitivity to the environment necessary to detect the effects brought about by analyte binding. Several NW characteristics that can be altered during NW preparation, such as dimension and doping levels have been shown to control device performance. A decrease in the minimum amount of analyte necessary to get a sufficiently high and

detectable signal can be achieved by using Si-NW devices of less than 10 nm diameter as indicated by mathematical simulations.³ Moreover, impurity doping concentration plays a more crucial role for the detection sensitivity for Si-NW FETs sensors in aqueous buffer solutions as compared to doping type (p- or n- type).^{15, 16, 17} It was demonstrated experimentally that lightly doped silicon nanowires are expected to exhibit greater sensitivity than highly doped or undoped devices.¹⁴ In a large array of devices with very small diameter and with very low doping level, device to device reproducibility will be a challenge.¹⁷ Silicon-alkyl monolayers or silicon-carbon monolayers on surfaces behaving as molecular switches can overcome these challenges and fine tuning of device properties will be possible.¹⁸

2.3.1. Top-down fabrication

The top-bottom fabrication approach utilizes industrially available materials of high quality (e.g. silicon wafers) to etch, pattern and shape nanostructures.¹⁹ Clean room techniques such as photolithography, wet and dry etching, e-beam lithography and micromachining are used to configure nanostructures into working devices. Nanowires fabricated by top-down techniques are uniformly identical and well aligned. Top-down devices are easy to integrate into functional systems due to their high yield, well oriented and predetermined positions on a substrate. The control of device dimensions (diameter/channel depth and length) are very easy with top-down approaches which result into controllable biosensors as well.¹⁷ Usually the top down fabrication of Si-NWs FET employs silicon-on-insulator (SOI) wafers as a substrate. Silicon on insulator technology refers to the use of a layered silicon-insulator-silicon substrate in place of conventional silicon substrates in semiconductor manufacturing, especially microelectronics/nanoelectronics, to reduce parasitic device capacitance and thereby improve performance. SOI-based devices differ from conventional silicon-built devices in that the silicon junction is above an electrical insulator, typically silicon dioxide or sapphire (These types of devices are called silicon on sapphire, or SOS, and are less common). The choice of insulator depends largely on the intended application, with sapphire being used for radiation-sensitive applications and silicon dioxide preferred

for improved performance and diminished short channel effects in micro/nanoelectronics devices. The insulating layer and topmost silicon layer also vary widely with application. The first industrial implementation of SOI was announced by IBM in August 1998. SOI is a three-layer substrate where the bottom silicon layer can be used as a gate electrode. The middle layer, a 50- to 200-nm-thick silicon oxide is commonly referred as the buried oxide (Box) layer. The Si-NWs are etched from a top layer (30–200 nm thick) made of single-crystal silicon. This top layer can be thinned to the desired thickness, typically the approximate thickness of the NWs, using oxidation and/or wet etching techniques. The Si top layer can also be doped by several techniques in order to produce n-type or p-type NWs. Presently, this technique has been used to fabricate only Si-NWs because of the ready availability of SOI wafers. Top-down techniques have been the preferred method for Si-NW production for biosensors.

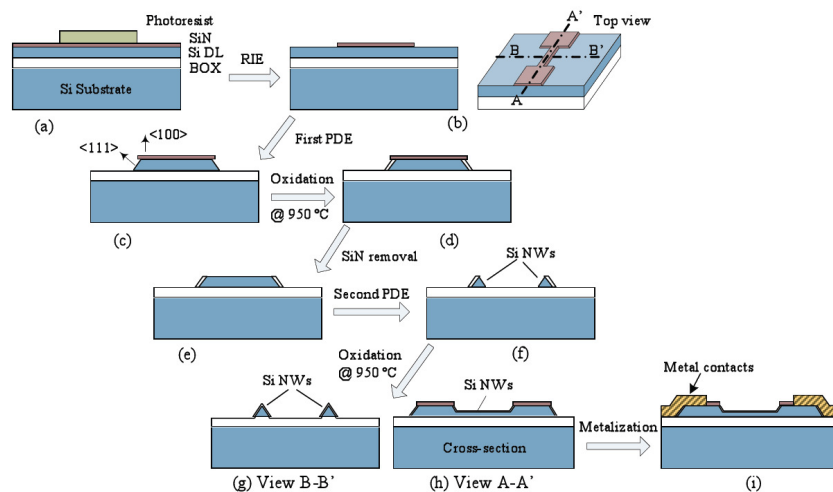


Figure 2.4 Top-down Si-NW microfabrication procedure (not to scale): (a) first lithography and etch steps for SiN layer patterning (BOX: buried oxide layer and Si DL: silicon device layer of the SOI substrate); (b) two dimensional top view; (c, & d) silicon device layer PDE and local oxidation; (e & f) second PDE and size reduction; (g, to i) gate oxidation and contact metalization.²⁰

Electron beam lithography is a top-down approach used to fabricate Si-NW biosensors where an electron beam is used to pattern the substrate surface and dimensions of the resulting nanowire devices can be defined. The devices made by the e-beam lithography might have dimensions in the range down to 50 nm in diameter and up to several micrometers in length.^{13, 14, 10, 21} A combination of deep ultraviolet lithography with a size-reduction strategy (self-limiting oxidation) was used to produce Si-NW with widths smaller than e-beam NWs, ranging from 5 to 50 nm.^{19, 22} Figure 2.4 shows a simple method to produce highly reproducible Si-NW FET devices with all (111) silicon surfaces using conventional photolithography and plane dependant wet etchings (PDE).²⁰ Another top-down technique is the superlattice nanowire pattern transfer (SNAP) method used by Heath and coworkers.^{23, 24} This method uses molecular beam epitaxy to create a physical template for NW patterning on GaAs/AlGaAs superlattice. This pattern for NW is then transferred on a previously n- or p-doped SOI, resulting in the production of highly aligned, 20-nm-wide Si-NWs.

2.3.2. Bottom-up fabrication

The bottom-up approach involves preparing Si-NWs from molecular precursors, rather than starting with the bulk semiconductor. Bottom-up methods are used to produce both group IV semiconductor Si-NWs and metal oxide NWs. Bottom-up techniques can be used to produce high-quality Si-NWs; however, these Si-NWs grow with random orientation on the substrate and are characterized by a distribution of lengths and diameters.¹⁹ The variation in Si-NW dimension, relative to top-down-based devices, can impose limits on bottom-up sensors because of poor device uniformity and low fabrication yields.²³ Bottom-up techniques allow the growth of Si-NWs on a wide range of substrates, limited only by the temperature of the process used to form the Si-NWs, which is typically in the 800–1000 °C range. The most common substrate is a silicon wafer; however, the choice of substrates can be expanded to low-temperature materials by growing the Si-NWs on a thermally stable substrate and transferring them to a second, less thermally stable substrate, such as plastic or glass.²⁵ NWs produced by bottom-up techniques for use in nano biosensing can be grouped into two main

synthetic approaches: vapor–liquid–solid (VLS) synthesis and laser ablation VLS. During VLS, Si-NWs are synthesized in an “atom by atom” fashion. Catalyst nanoparticles are uniformly dispersed on the substrate. A stream of carrier gas, containing the NW molecular precursors, is flowed over the substrate at elevated temperatures. These precursors (for instance, SiH_4 to make Si-NWs) initially decompose on the catalyst nanoparticles and dissolve the molten catalyst, forming an alloy in liquid state. Continuous decomposition of the gas-phase precursors ultimately saturates the catalyst particle and the semiconductor precipitates, leading to the NW growth with a random orientation on the substrate surface. The catalyst defines the diameter of the growing NWs, which will retain the same diameter as the catalyst nanoparticle. An advantage of the VLS method is the possibility to selectively dope the growing NWs by adding dopant precursor.

2.4. Biofunctionalization schemes

Si-NW FETs are sensitive to local environment but non-specific in response without proper functionalization of their surfaces with appropriate biomolecular or chemical receptors. The selectivity for a particular analyte is typically achieved by anchoring a specific recognition group to the surface of the Si-NW. A bifunctional linker molecule with two chemically different termini is used to help anchor the receptor molecules to the Si-NW surface. In the case of Si NWs, the linker molecule of choice depends on whether or not the wire has an oxide coating. After covalent attachment of the receptor molecules, unreacted sites are usually deactivated with other highly reactive molecules, such as ethanamine, butyl amine, or 2-mercaptoethanol.

2.4.1. Functionalization of “oxidized-surface” silicon nanowires

Si-NW surfaces might have a native oxide or a thermal oxide layer which can be used to functionalize these surfaces. A variety of linker molecules have been designed to bind to the native oxide coating on the Si-NWs. Alkoxy-silane derivatives are the most

widely used linkers. The Si-methoxide or Si-ethoxide reacts with the surface OH group, anchoring the linker molecule to the silicon oxide surface. A very common linker for Si/SiO₂ NW functionalization is 3-(trimethoxysilyl) propyl aldehyde (APTMS). This linker produces an aldehyde-rich surface that can be directly used to covalently immobilize monoclonal antibodies.^{7, 26, 11} Another linker molecule is 3-aminopropyl triethoxy silane (APTES).

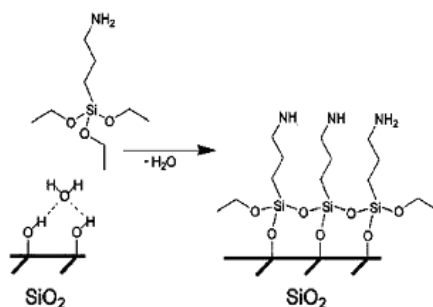


Figure 2.5 Functionalization of silicon oxide surface by 3-amino propyl triethoxy silane (APTES).

An amine terminated surface monolayer can be obtained by using APTES and results in surface exposed -NH_2 (amine) groups that can be bioconjugated by using the proper coupling reagent like glutaraldehyde to produce a surface that is reactive toward amine groups present in the chemical structure of the proteins and antibodies like monoclonal antibody prostate-specific antigen (PSA) in order to immobilize the receptor on the surface.¹⁴ Biotinylated PNA was immobilized on Si-NW surfaces having a layer of avidin which was already conjugated to silicon nanowire surface via biotinylated p-nitrophenyl ester.⁹ Another useful linker is 3-mercaptopropyltrimethoxysilane (MPTMS) which makes thiol terminated monolayers on the oxide surface and is used to couple DNA probes modified with acrylic phosphoramidite at the 5'-end.¹⁰ This method placed the receptor molecule distant from the sensing surface.

2.4.2. Functionalization of “hydrogen terminated” silicon nanowires

The intervening native oxide (1–2 nm thick) or a thermally grown oxide passivation layer (10–20 nm) on the Si-NW surfaces may limit sensor performance due to a number of reasons: i) interfacial trapped states causes hysteresis in response (native oxide); ii) receptor-analyte binding event takes place far way from Si-NW channel imparting only a small field effect for conductance modulation and small response (thermal oxide); iii) oxide surface chemistry (Alkoxy-Silane) is hydrolysable under different buffer pH ranges (thermal and native); iv) gate-oxide thickness is a major constraint in future devices in accordance to the Moore’s law.²⁷ The etching of the silicon oxide layer with the help of HF or NH₄F leaves silicon surface hydrogen terminated which is stable to air oxidation for tens of minutes, but is easily photo-dissociate able with UV light to generate surface radicals that react efficiently with ω -functionalized 1-alkene or 1-alkyne under inert atmosphere resulting into very stable and dense Si-Alkyl monolayer.²⁸

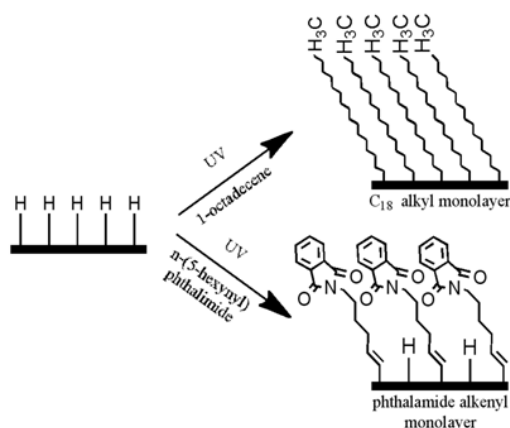


Figure 2.6 Silicon Functionalization via Si-alkyl Monolayer under UV reaction.

This photochemical hydrosilylation treatment selectively functionalizes the Si NWs,²⁹ but does not react with the underlying SiO₂ layer (Box) of the substrate. Selectively

functionalized devices can detect analyte in trace amounts. Heath et al.²³ used this photo-hydrosilylation treatment using an olefin derivative of an easily cleavable carbamate, followed by deprotection, which results in Si NWs coated with amino groups. The $-NH_2$ groups can then be used to physically adsorb probe single-stranded (ssDNA) on the Si NWs, and attach several biotin derivatives, antibodies,¹³ and probe ssPNA.²²

2.5. Si-NW biosensor: sensitivity in aqueous media

The detection of a biological analyte needs a proper media for sending the analyte to the sensor surface. Appropriate pH buffers providing sufficient physiological conditions for sensing like phosphate buffer saline (1 x PBS) having pH 7.4 and 0.14M electrolyte concentration is used and it is similar to the human serum. Binding affinities of antibodies-antigen and DNA are the best under these conditions. Si-NW sensing, however, is dependent on the field-effect that is caused by the electrostatic charge of biological entities binding in the vicinity of Si-NW body and in the presence of high concentration of counter ions in the buffer, this electrical field might be screened and even nullified resulting into very weak or no sensing signal at all. Such a screening effect of counter-ions is known as Debye screening and the Debye length (λ_D) is the maximum distance at which an external charge can influence the NW carrier concentration to change signal. The value of Debye length (in nanometers) in water can be calculated with good approximation using the formula $\lambda_D = 0.32(I)^{-1/2}$, where I is the ionic strength of the buffer solution in moles.³⁰ In aqueous media, the accumulation of carriers inside the NW occurs when ligand-analyte binding takes place on the Si-NW surface within the Debye length λ_D set by the ionic strength of the solvent buffer; however, the Debye length decreases rapidly with an increase in the ionic strength and vice versa.³¹ Probe molecules must therefore be attached as close as possible to the NW surface, yet still retain their biological activity. The Debye length plays an important role during immunological experiments where “large,” relatively-low-charged

biomolecules, such as antibodies, capture their target proteins. When operating at the electrolyte concentration of serum, the $\lambda_D \approx 0.7$ nm is much smaller than the size of many antibodies (10–15 nm) and many proteins (5–10 nm). Therefore, at such a short λ_D , the electrolytes present in the buffer screen the charges carried by the analyte. So, pH and especially the electrolyte concentration are critical experimental variables to be considered see Figure 2.7.

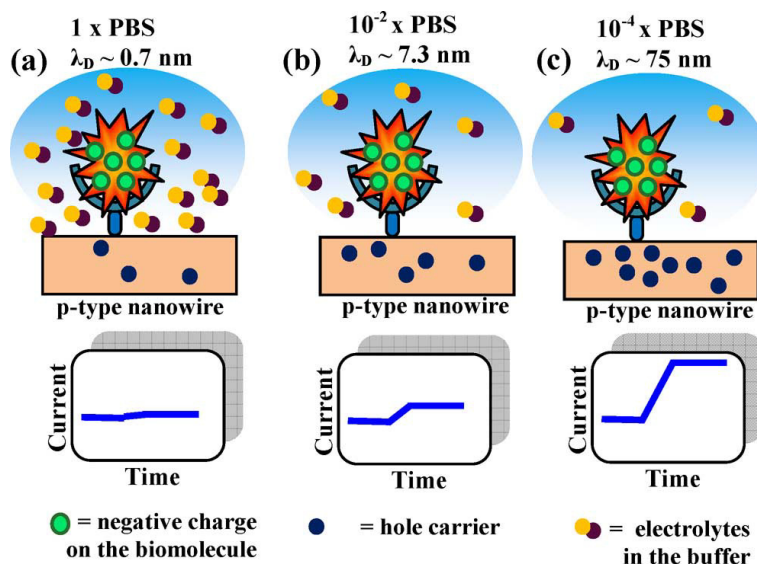


Figure 2.7 Effect of the buffer electrolyte concentration (Debye Length) on the sensitivity of Si-NW FET sensor shown for p-type Si-NW device and a negatively charged analyte molecule. (a) At high electrolyte concentration (1 x PBS, short Debye length), most of the charge carried by the captured analyte is screened by ions present in the buffer. This screening causes the analyte charge to have little effect on the accumulation that would provide an increase in device conductance. (b) Operating at lower analyte concentration (0.01 x PBS), the charge carried by the analyte is poorly screened, and thus, a larger change in conductance can be observed. (c) In very dilute buffers, charges located far away from the wire can still exert an influence on the carrier density of the wire, resulting in extreme sensitivities.³

Computational models for the response time of a nanobiosensor in a diffusion-capture regime were examined in order to study the effects of electrostatic screening caused by buffer solutions.¹⁶ These calculations predict that the sensor response varies linearly

with pH and logarithmically with electrolyte concentration and were in good agreement with data available in the literature, which indeed show that Si-NW FET sensors respond linearly to pH variation (which is crucial for protein detection) but nonlinearly to electrolyte concentration and concluded to develop analyte binding schemes at low ionic strength, in order to reduce the time taken to obtain a detectable signal change.³ However, such a scheme might present problems related to the necessity of meeting certain minimum electrolyte concentrations in order to retain a strong binding affinity between probes and target molecules. Decreasing the salt concentration in the analyte solution allows for detection of larger biomolecules. At longer Debye lengths, charged residues on the analyte located several nanometers away from the NW will still exert an effect on the charge carriers in the NW. One way to ensure longer Debye lengths is to use dilute buffer solutions with low electrolyte concentrations. However, this practice could be problematic due to complications caused by the necessary dilutions when preparing the sample.³ A second problem with excessive dilutions is the fact that a minimum salt concentration is necessary to retain biological activity of some proteins and is indispensable for DNA hybridization.³¹ To demonstrate the effect of the Debye length on the nanosensor sensitivity, Stern et al. used the well-studied biotin–streptavidin (SA) couple. Binding of this ligand–receptor system was monitored with p-type Si-NW FET sensors using different buffer ionic strengths, but at constant SA concentration.²¹ This system is ideal for this study, as the biotin–SA binding affinity is known to be unaffected by variations in buffer salt concentrations.²¹ A stable baseline signal was established with biotin immobilized on the NW surface in 0.01×PBS buffer ($\lambda_D \sim 7.3$ nm). Addition of 10 nM SA in the same buffer caused the negatively charged SA to bind to the biotinylated device and increased conductance with respect to the baseline.³ These results imply that the majority of the protein's charge is unscreened and thus influences the carrier density in the NW. When the buffer ionic strength was increased tenfold ($\lambda_D \sim 2.3$ nm), the protein's charge was partially screened by the stronger buffer and the conductance decreased due to a weaker chemical gating effect of the bound SA. A further tenfold increase (now, 1×PBS, $\lambda_D \sim 0.7$ nm) screened most of the protein's charge, leading to a negligible change in device conductance with

respect to the initial baseline. A parallel experiment with a non-biotinylated device showed no response. This experiment clearly demonstrates that the electrolyte concentration of buffers is a critical variable influencing the sensitivity of these nano-biosensors.³ This sensitivity dependence on the buffer composition is an important limitation for future applications of nano-biosensors when fast detection is required. Other immunological assays based on optical detection, such as enzyme linked immunosorbent assay (ELISA), can comfortably operate at serum's electrolyte concentrations. In the Stern et al.'s study, it was demonstrated that by carefully choosing λ_D , it is possible to operate in such a way that only bound analytes would produce a signal while the presence of unbound molecules is screened, thus significantly reducing false positive results. For instance, at 0.05 x PBS, DNA-modified devices were shown to respond only to the target DNA and to be insensitive to non-target DNA, whereas in more dilute buffers, false positives were observed.³ The relationship between the spatial location of charge and chemical gating effects was also investigated by Zhang et al.²² They used the hybridization of ssDNA to a ssPNA probe immobilized on the NW surface, at constant buffer ionic strength (constant λ_D) and fixed length of DNA (constant DNA charge). The only variable was the number of complementary DNA bases with respect to the PNA receptor.³ This number changed from fully complementary (22 nucleotides) to non complementary by decreasing three bases at a time. Using this strategy, the distance of the charge layer produced by the bound target DNA to the Si-NW surface was varied by controlling the location of the hybridization sites. The PNA–DNA hybrid and partial hybrid were assumed to stand normal to the NW surface. As the complementary segment became shorter and the DNA charge layer moved away from the sensor surface, the ability of the NW device to signal the hybridized DNA was progressively diminished. These results confirm that the detection sensitivity of Si-NW devices is strongly dependent on the location and strength of the electric field produced by analyte molecules on the NW surface.

2.6. Electrochemical cell and microfluidics

An important factor to be taken into consideration is the system used to deliver the analyte solution. The analyte must reach the active sensing surface in order to interact with the capture agent. The time a receptor takes to capture its target molecule is affected by the delivery strategy. Since fast responses are highly desirable, rapid analyte delivery is crucial to the development of nanobiosensors. So far, two main methods have been utilized for such sample delivery: microfluidic channels^{7, 8, 19, 14, 23, 2, 26, 11, 9} and mixing cells^{13, 10, 21, 22} each having its advantages and disadvantages. A microfluidics channel is usually made of molded elastomer such as polydimethylsiloxane (PDMS) with injection and drain channels (Figure 2.8). The microfluidics devices are placed on the top of the nanosensor so that the solution can be directed over the Si-NWs.

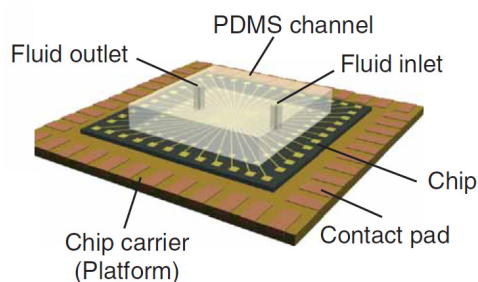


Figure 2.8 Microfluidic channel on Si-NW chip.²

A key benefit of a microfluidics device is that it allows the analysis to be conducted using exceedingly small samples, on the order of a nanoliter. The flow within the central part of the channel is laminar and has a higher flux than at the periphery. When a sample is injected into the channel, in order for the analyte to reach the sensor surface, the analyte has to diffuse normal to the flow, from the middle of the channel to the bottom where the Si-NWs are located. Laminar microfluidic flow thus partially restricts the ability of molecules to reach the nanosensor surface,³² especially for

molecules with high molecular weights (above 100 kD_a) that are known to diffuse an order of magnitude slower than smaller biomolecules such as oligonucleotides.³ Several computational models of the sensing phenomena suggest that the analyte delivery to the sensor surface might be the limiting step toward the detection of analytes at ultralow concentrations.^{17, 32} Simulations indicate that limits imposed by analyte transport in microfluidic systems will prevent nanoscale sensors from reaching detection in the femtomolar range, for assays performed in minutes, unless novel methods to actively direct biomolecules to a sensor surface are developed. Also, another disadvantage of PDMS channels is caused by the highly hydrophobic sidewalls present in these devices.³ Hydrophobic biomolecules with low solubility in buffers are likely to adsorb and deposit along the PDMS walls. A passivation strategy, using the protein repelling properties of polyethylene glycol, was developed by Wang et al., thus reducing undesirable, nonspecific adsorption of biomolecules.²⁶ The other popular delivery method utilizes a mixing cell (also called solution chamber). This cell, typically a cone shaped, plastic sample holder, is placed over the nanosensor chip and allows the solution to be delivered from the top aperture. For simple cells, where there is no continuous flow, different solutions are delivered by replacement methods and the analyte diffuses isotropically until it reaches the sensor surface. A more advanced mixing cell setup, has been designed by Stern et al.¹³ In this setup, injection of the solution tangential to the Si-NW FET sensor significantly decreased the detection response times compared to those observed in Si-NW FETs that used microchannels for the detection of similar target molecules.^{23, 9}

2.7. Conclusion

Si-NW FET biosensors have been used by many groups to detect bio-analytes of medical interests like disease biomarkers proteins, nucleic acids because these nanobiosensors are cheap, efficient, highly sensitive, label free and give response in real time. Top-down fabrication approaches can produce these sensors in bulk however,

biofunctionalization of receptors, choice of biosensing buffers with appropriate concentrations, sample delivery system, and operation regime of the sensor are the factors which decide the ultimate sensitivity and selectivity of these devices.

2.8. Bibliography

1. Tong, H. D.; Chen, S.; van der Wiel, W. G.; Carlen, E. T.; van den Berg, A., Novel Top-Down Wafer-Scale Fabrication of Single Crystal Silicon Nanowires. *Nano Lett* **2009**, 9, (3), 1015-1022.
2. Patolsky, F.; Zheng, G. F.; Lieber, C. M., Fabrication of silicon nanowire devices for ultrasensitive, label-free, real-time detection of biological and chemical species. *Nature Protoc* **2006**, 1, (4), 1711-1724.
3. Curreli, M.; Zhang, R.; Ishikawa, F. N.; Chang, H. K.; Cote, R. J.; Zhou, C.; Thompson, M. E., Real-Time, Label-Free Detection of Biological Entities Using Nanowire-Based FETs. *IEEE Trans Nanotech* **2008**, 7, (6), 651-667.
4. Knopfmacher, O.; Tarasov, A.; Fu, W. Y.; Wipf, M.; Niesen, B.; Calame, M.; Schonenberger, C., Nernst Limit in Dual-Gated Si-Nanowire FET Sensors. *Nano Lett* **10**, (6), 2268-2274.
5. Carlen, E. T.; van den Berg, A., Nanowire electrochemical sensors: can we live without labels? *Lab Chip* **2007**, 7, (1), 19-23.
6. Wanekaya, A. K.; Chen, W.; Myung, N. V.; Mulchandani, A., Nanowire-based electrochemical biosensors. *Electroanal* **2006**, 18, (6), 533-550.
7. Zheng, G. F.; Patolsky, F.; Cui, Y.; Wang, W. U.; Lieber, C. M., Multiplexed electrical detection of cancer markers with nanowire sensor arrays. *Nature Biotech* **2005**, 23, (10), 1294-1301.
8. Cui, Y.; Wei, Q. Q.; Park, H. K.; Lieber, C. M., Nanowire nanosensors for highly sensitive and selective detection of biological and chemical species. *Science* **2001**, 293, (5533), 1289-1292.
9. Hahm, J.; Lieber, C. M., Direct ultrasensitive electrical detection of DNA and

- DNA sequence variations using nanowire nanosensors. *Nano Lett* **2004**, 4, (1), 51-54.
10. Li, Z.; Chen, Y.; Li, X.; Kamins, T. I.; Nauka, K.; Williams, R. S., Sequence-specific label-free DNA sensors based on silicon nanowires. *Nano Lett* **2004**, 4, (2), 245-247.
 11. Patolsky, F.; Zheng, G. F.; Hayden, O.; Lakadamyali, M.; Zhuang, X. W.; Lieber, C. M., Electrical detection of single viruses. *P. Nat. Acad. Sci USA* **2004**, 101, (39), 14017-14022.
 12. Elfstrom, N.; Juhasz, R.; Sychugov, I.; Engfeldt, T.; Karlstrom, A. E.; Linnros, J., Surface charge sensitivity of silicon nanowires: Size dependence. *Nano Lett* **2007**, 7, (9), 2608-2612.
 13. Stern, E.; Klemic, J. F.; Routenberg, D. A.; Wyrembak, P. N.; Turner-Evans, D. B.; Hamilton, A. D.; LaVan, D. A.; Fahmy, T. M.; Reed, M. A., Label-free immunodetection with CMOS-compatible semiconducting nanowires. *Nature* **2007**, 445, (7127), 519-522.
 14. Kim, A.; Ah, C. S.; Yu, H. Y.; Yang, J. H.; Baek, I. B.; Ahn, C. G.; Park, C. W.; Jun, M. S.; Lee, S., Ultrasensitive, label-free, and real-time immunodetection using silicon field-effect transistors. *App Phys Lett* **2007**, 91, (10), 3.
 15. Nair, P. R.; Alam, M. A., Performance limits of nanobiosensors. *App Phys Lett* **2006**, 88, (23), 3.
 16. Nair, P. R.; Alam, M. A., Screening-limited response of nanobiosensors. *Nano Lett* **2008**, 8, (5), 1281-1285.
 17. Nair, P. R.; Alam, M. A., Design considerations of silicon nanowire biosensors. *IEEE Trans Electron Devices* **2007**, 54, (12), 3400-3408.
 18. He, T.; He, J.; Lu, M.; Chen, B.; Pang, H.; Reus, W. F.; Nolte, W. M.; Nackashi, D. P.; Franzon, P. D.; Tour, J. M., Controlled modulation of conductance in silicon devices by molecular monolayers. *J Am Chem Soc* **2006**, 128, (45), 14537-14541.
 19. Gao, Z. Q.; Agarwal, A.; Trigg, A. D.; Singh, N.; Fang, C.; Tung, C. H.; Fan, Y.; Buddharaju, K. D.; Kong, J. M., Silicon nanowire arrays for label-free detection of DNA. *Anal Chem* **2007**, 79, (9), 3291-3297.
 20. Chen, S. Y.; Bommer, J. G.; van der Wiel, W. G.; Carlen, E. T.; van den Berg, A., Top-Down Fabrication of Sub-30 nm Monocrystalline Silicon Nanowires Using Conventional Microfabrication. *ACS Nano* **2009**, 3, (11), 3485-3492.

21. Stern, E.; Wagner, R.; Sigworth, F. J.; Breaker, R.; Fahmy, T. M.; Reed, M. A., Importance of the debye screening length on nanowire field effect transistor sensors. *Nano Lett* **2007**, 7, (11), 3405-3409.
22. Zhang, G. J.; Zhang, G.; Chua, J. H.; Chee, R. E.; Wong, E. H.; Agarwal, A.; Buddharaju, K. D.; Singh, N.; Gao, Z. Q.; Balasubramanian, N., DNA sensing by silicon nanowire: Charge layer distance dependence. *Nano Lett* **2008**, 8, (4), 1066-1070.
23. Bunimovich, Y. L.; Shin, Y. S.; Yeo, W. S.; Amori, M.; Kwong, G.; Heath, J. R., Quantitative real-time measurements of DNA hybridization with alkylated nonoxidized silicon nanowires in electrolyte solution. *J Am Chem Soc* **2006**, 128, (50), 16323-16331.
24. Heath, J. R., Superlattice Nanowire Pattern Transfer (SNAP). *Account Chem Res* **2008**, 41, (12), 1609-1617.
25. McAlpine, M. C.; Ahmad, H.; Wang, D. W.; Heath, J. R., Highly ordered nanowire arrays on plastic substrates for ultrasensitive flexible chemical sensors. *Nat Mater* **2007**, 6, (5), 379-384.
26. Wang, W. U.; Chen, C.; Lin, K. H.; Fang, Y.; Lieber, C. M., Label-free detection of small-molecule-protein interactions by using nanowire nanosensors. *P. Nat. Acad. Sci USA* **2005**, 102, (9), 3208-3212.
27. Weldon, M. K.; Queeney, K. T.; Eng Jr, J.; Raghavachari, K.; Chabal, Y. J., The surface science of semiconductor processing: gate oxides in the ever-shrinking transistor. *Surf Sci* **2002**, 500, (1-3), 859-878.
28. Sun, X. H.; Wang, S. D.; Wong, N. B.; Ma, D. D. D.; Lee, S. T.; Teo, B. K., FTIR spectroscopic studies of the stabilities and reactivities of hydrogen-terminated surfaces of silicon nanowires. *Inorg Chem* **2003**, 42, (7), 2398-2404.
29. Masood, M. N.; Chen, S.; Carlen, E. T.; van den Berg, A., All-(111) Surface Silicon Nanowires: Selective Functionalization for Biosensing Applications. *ACS Appl Mater Interfaces* **2**, (12), 3422-3428.
30. Maehashi, K.; Katsura, T.; Kerman, K.; Takamura, Y.; Matsumoto, K.; Tamiya, E., Label-free protein biosensor based on aptamer-modified carbon nanotube field-effect transistors. *Anal Chem* **2007**, 79, (2), 782-787.
31. Heitzinger, C.; Klimeck, G., Computational aspects of the three-dimensional feature-scale simulation of silicon-nanowire field-effect sensors for DNA detection. *J*

Comput Electron **2007**, 6, (1-3), 387-390.

32. Sheehan, P. E.; Whitman, L. J., Detection limits for nanoscale biosensors. *Nano Lett* **2005**, 5, (4), 803-807.

Chapter 3

Si-Alkyl monolayers: a functionalization tool for nanosensors

The potential of highly stable, uniform and densely packed Si-C bounded Si-alkyl monolayers as a surface modification and biomolecular conjugation tool is reviewed here. Special emphasis apart from general considerations such as fabrication, reaction mechanism and characterization is given on their application for the surface bio-modification of silicon based sensors such as the silicon nanowire field effect transistor (Si-NW-FET) devices and understanding their advantages (disadvantages) for the enhancement (deterioration) of device sensitivity and problems that might hinder their use as a modified surface of an electrical sensing device in solution. Various functionalization possibilities leading to near ideal surface passivation and bio-immobilization are presented. Effects of precursor choice such as alkene or alkyne, impurity doping type (n- or p-) and effects of doping on tethering feasibility, heating and UV irradiation and mild approaches for fabrication have been considered.

3.1. Introduction

3.1.1. Pros and cons for using oxide as a dielectric layer

The most common way of functionalizing a silicon sensor is silane based chemistry on the silicon oxide surface. Most commonly 3-aminopropyl triethoxy silane (APTES) molecules are reacted with hydroxyl groups of silicon oxide under solution phase or vacuum desiccation and subsequent curing at elevated temperatures to induce cross linking^{1, 2} results in amine (-NH₂) terminated monolayers that are expected to be attached intermittently covalently to silicon oxide surface via silicon-oxygen bonds. In the case of silicon based biosensors such as Si-NW FET biosensor, receptors can be conjugated to amine terminated (APTES) monolayers of such kind by using different schemes for different type of biomolecules and many previous reports demonstrates APTES/Silane grafted platforms for the detection of biomolecules³ however, there are several fundamental physical reasons that these modification schemes are not optimal for Si-NW sensors. That is why, exposure of silicon oxide surfaces to these ions should be avoided.^{4, 5} Higher electrostatic responses can be achieved from the sensor when insulator capacitance (C_{ins}) is high enough, and however, silicon oxide layer is an extra dielectric layer between active channel and the receptors causing reduction in C_{ins} .⁵ The sensor response is also affected by the presence of interface traps. A silicon oxide surface which is functionalized can have these traps at oxide and silicon interface, within oxide or at the receptor-oxide interface. Such availability of interface traps at all oxide interfaces favors strongly to remove the oxide layer for better performance of the Si-NW sensor. Additionally, buffer solutions used in biosensing experiments usually have small ions such as sodium that are also mobile in silicon oxide layers.⁶ These mobile ions are the cause of major threshold shifts and hysteresis in electrical response which jeopardizes Si-NW biosensor performance.

3.1.2. Pros and cons for using Si-alkyl monolayer as dielectric layer

A solution to the above problem is deposition of organic monolayers directly onto the bare silicon surface using silicon-carbon attachment chemistry. A variety of approaches including thermal, ultraviolet, free radical, and electrochemical methods have been demonstrated on single crystal (111) and (100) silicon surfaces as well as on porous silicon.^{7, 8, 9, 10} Many reports in the literature show successful covalent grafting of small aliphatic and aromatic species to silicon surfaces and have been characterized chemically. Etching of native silicon oxide layer in HF or NH₄F leave the silicon surface terminated with hydrogen which is stable for some time but susceptible to oxidation in ambient conditions.¹¹ Grafted alkyl monolayers of longer chain lengths have steric hindrances and full surface coverage with a densely packed monolayer passivating every surface site can not be achieved, however, each silicon site capped with a methyl group can provide nearly 100% passivation.¹² In spite of lower surface coverage (50%), using capacitance and conductance measurements, interface trap densities as low as $3 \times 10^9 \text{ cm}^{-2} \text{ eV}^{-1}$ and trap densities of $1.7 \times 10^{11} - 3 \times 10^{11} \text{ cm}^{-2} \text{ eV}^{-1}$ have been measured from surface recombination velocity measurements from modified methyl and alkenyl modified silicon (111) surfaces in air respectively.^{13, 14} Exceptional electrical passivation can be thus achieved with small alkyl molecules. Efficient grafting of high quality alkyl monolayers with the help of hydrosilylation on silicon surfaces and their substantial characterization by different physical techniques results into surfaces with low interface trap-density. Direct attachment of receptor molecules with linker aliphatic chains onto silicon nanowire biosensors is not favorable in many ways. Receptor molecules are usually very bulky and cause steric hindrance resulting into poorly packed monolayers with surface voids and holes and poor passivation. Problems that can arise from a non-ideal monolayer formation are shown in Figure 3.1.

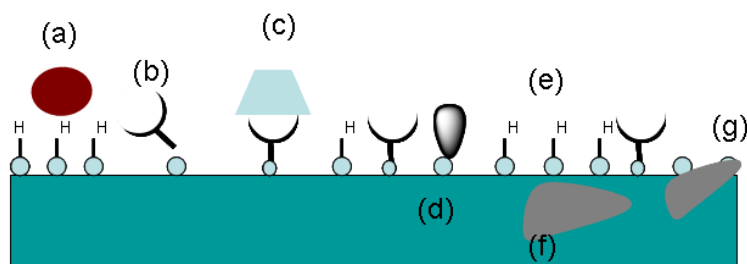


Figure 3.1 Silicon surface in case of non-ideal monolayer formation. Steric hindrances do not let complete coverage of all active sites on the surface leaving many surface atoms with termination such as hydrogen. (a) & (c) non-specific interaction of surface with analytes (b) non-specific interaction of receptor with the surface (d) surface dangling bond (e) surface voids (uncovered surface) (f) sub-surface oxidation (g) surface oxidation.

The voids (Figure 3.1e) created by loose packing of bulky receptor groups might cause bio-fouling with the surface (Figure 3.1a) or uncovered sites get oxidized in ambient aqueous environment and both of these factors have deteriorating effects on nanowire biosensor electrical response. The selection and design of bio-receptor/biorecognition groups should be such that they should only recognize/accept analyte molecules specifically and their bonding to the semiconducting surface should be strong enough to not to interact with surface non-specifically (Figure 3.1b). Formation of sub-surface oxide (Figure 3.1f) and surface dangling bonds (Figure 3.1d) should also be avoided in a perfectly covered surface.^{15, 16}

3.1.3. Improvement possibilities

Characterization of an as-passivated surface that is going to be used for sensing is very crucial so that defects and their effects on the sensor response can be minimized. The most common method for immobilization of biomolecules onto the sensor surface is the sequential attachment of different components including formation of a well packed non-functional monolayer, generation of functional sites, attachment of a linker and subsequent attachment of bio-molecules. The resulting sensor surface can better achieve both chemical and electrical requirements for sensing as compared to direct functionalization and Figure 3.2 shows one possible example.^{17, 18}

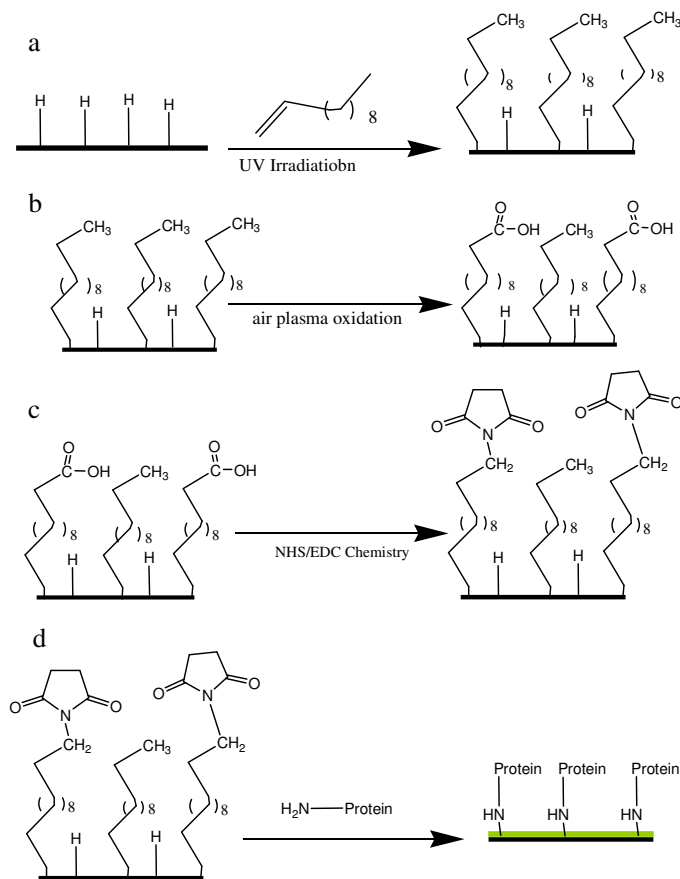


Figure 3.2 a) Sequential functionalization of Si (111) surface: via hydrosilylation reaction with 1-Undecene; b) generation of surface functional groups with mild plasma oxidation; c) NHS/EDC chemistry to activate carboxylic acid groups; (d) attachment of receptor protein.

Receptor molecules are the focus of biosensor functionality, however, the choice of the linker molecular layer (Si-C monolayer, Figure 3.2a) often plays a very crucial role in overall biosensor performance, which depends on packing density, bond stability and the electric and electrochemical properties. Intrinsic dipole moments of different kinds of linker molecules affect semiconductor band gap upon their interaction with semiconductor surfaces and can be used to tune electrical properties in a controllable way and can also be used to overcome doping difficulties for sensors with dimensions

below 10 nm.¹⁹ Bulky receptor groups when immobilized onto surfaces with inappropriate linker molecules result in poor packing and thus produce voids at the surface where small molecules in buffer can interact with exposed surface sites giving rise to spurious signals. Careful choice of the linker chain, however, can prevent “false positive” signals due to minimal steric hindrance, maximum surface coverage, and unavailability of non-reacted surface sites along with efficient bioimmobilization of bulky receptor groups. A clever approach to cope with surface voids and to cover most of reactive/dangling bonds and to still functionalize surfaces directly in a single step is to use a mixture of precursor molecules having both functional (bulky, -COOCH₃, -NH-CO-C(CH₃)₃, Phthalimide, Succinimidyl-) and inert (small, -CH₃) terminal groups and selecting the ratio in such a way that small molecules cover most of the reactive sites but functional groups should also be there in a sufficient surface density. Another challenge is to solve degradation problems of bulky functional groups due to UV exposure or extensive heating (up to 200 °C) demanding extremely mild hydrosilylation methods. However, receptors such as DNA, antibodies, proteins, and carbohydrates have been attached to appropriate aliphatic modified silicon surfaces.^{20, 21, 22, 23} Sensitive, label-free detection of biological material has also been demonstrated using oxide free silicon NW-FET structures.^{24, 25} Such devices showed improved sensitivity compared to oxide-based interfaces.²⁶

3.2. Si-alkyl functionalization methodologies

3.2.1. Wet chemical methods

3.2.1.1. Hydrosilylation via 1-alkene and 1-alkyne

Si-alkyl monolayer can be prepared by using a number of different routes and the easiest and technologically important/promising method is probably the hydrosilylation of alkene/ alkynes on hydrogen terminated surfaces. Hydrogen terminated surfaces can

be efficiently prepared by dipping the silicon wafer with native oxide in a solution of (1-5) % HF or 40% NH_4F in water. The prepared surfaces are stable and oxide free for tens of minutes and can be used in Schlenk flasks or in glove boxes for further reaction. Hydrosilylation chemistry involves 1-alkenes or 1-alkynes as precursor molecules grafted onto hydrogen terminated silicon which is also appropriate and a method of choice.⁹

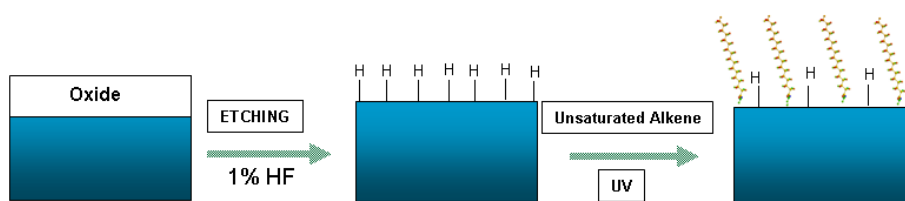


Figure 3.3 General scheme for Hydrosilylation reaction.

Hydrosilylation while using hydrogen terminated surface can be carried out under UV irradiation,²⁷ free radical initiation,⁷ heating, chemo mechanical scribing²⁸ and sonication.²⁸

3.2.2. Different approaches for biomolecular immobilizations through alkenyl chemistry

In order to get functionalized surfaces which are densely packed, stable and provide sufficient chemical flexibility for further biomolecular conjugation different approaches have been made by different groups as summarized in Table 3-1. Yang et al. used a mixed monolayer approach to get a densely packed functionalized surface in a single step and were able to successfully immobilized biotin hydrazide onto as prepared surfaces,²⁹ as shown in Figure 3.4. Monolayer fabrication by using a mixture of precursor molecules where one has functional bulky group and the other having a methyl terminal group is very handsome in the sense that i) Sterically hindered sites can be covered by small methyl terminated chains resulting into maximum surface coverage, ii) by controlling the ratio of both precursor molecules, the surface density

Table 3-1 Functionalization approaches suitable for Si-NW FET biosensors.

No	Wafer type, doping and resistivity	Precursor Molecule and availability	Terminal group and reactivity	Hydrosilylation Method	Characterization Method	Ref
1	Si (111) n-type, 1-2 Ωcm^{-1}	N-Succinimidyl undecyl-1-enate (synthesis)	(Direct) N-Succinimidyl ester biotin attachment	$h\nu = 447 \text{ nm}$, $t = 16 \text{ hours}$.	(IR-RA-S) (XPS), (AFM) Density functional Theory (DFT)	29
2	Si (100) n-type or p-type,	10-undecylenic Acid Methyl Ester (synthesized)	(Deprotected) Carboxylic acid	Heating , 200 $^{\circ}\text{C}$	X-ray reflectivity and contact angle	30
3	VLS grown silicon nanowires	10-N-Boc-amino-dec-1-ene (commercially available)	(Deprotected) primary amine DNA sensing	$h\nu = 254 \text{ nm}$ $t = 3 \text{ hours}$	(XPS) Fluorescence imaging	25
4	Si (100), n-type, 0.1-0.01 Ωcm^{-1}	10-undecynoic acid (commercially available)	(Direct) carboxylic group DNA sensing	Cathodic Electrografting current 0.6mA.	XPS, Quantitative Fluorescence analysis	31, 32
5	Si(100) n-type, arsenic doped,	N-1-BOC-amino-3-cyclopentene (commercially available)	Free amine group DNA attachment and sensing	$h\nu = 254 \text{ nm}$ $t = 1.5-2 \text{ hours}$	XPS, Fluorescence	33
6	Si (111) n-type 0.005-0.01 Ωcm^{-1} SOI : Si(100) n-type 9-18 Ωcm^{-1} dL=50nm, Box=150 nm	2-(4-(tetrahydro-2H-pyran-2-yloxy)phenoxy)-tetrahydro-2H-pyran (synthesis)	Electrically reversible hydroquinone-quinone moiety reactive to thiol group	$h\nu = 254 \text{ nm}$ $t = 2 \text{ hrs}$	Cyclic voltammetry, XPS, AFM	34
7	Si-NW n-type, p-type (VLS) $8 \times 10^{18} / \text{cm}^3$	tert-butyl allylcarbamate (commercially available)	(Deorotected) Free amine groups	UV irradiation	XPS, SPR, Fluorescence, electrical detection of ssDNA, Sensitivity.	26
8	Si(001)	t-Boc protected 10-amino-dec-ene	Free amine SSMC+ thiolated DNA conjugation	UV irradiation	XPS, Contact Angle, Fluorescence	35

of functional groups (Succinimidyl groups) can be fine tuned, resulting in proportional number density of receptor groups on the surface, and iii) their functionalization scheme is a direct and single step and does not involve any extra deprotection step which can deteriorates monolayer quality by loose packing and non-uniformity. Streifer et al.²⁵ functionalized their vapor-liquid-solid (VLS) grown silicon nanowires covalently by using tertiary butyloxy carbonyl (t-BOC) protected amine and subsequent functionalization of thiol terminated DNA after deprotection using a hetrobiofunctional cross linker known as SSMCC (sulfo-succinimidyl 4-(N-meleimidomethyl) cyclohexane-1-carboxylate). Their functionalization scheme is shown in Figure 3.5.²⁵

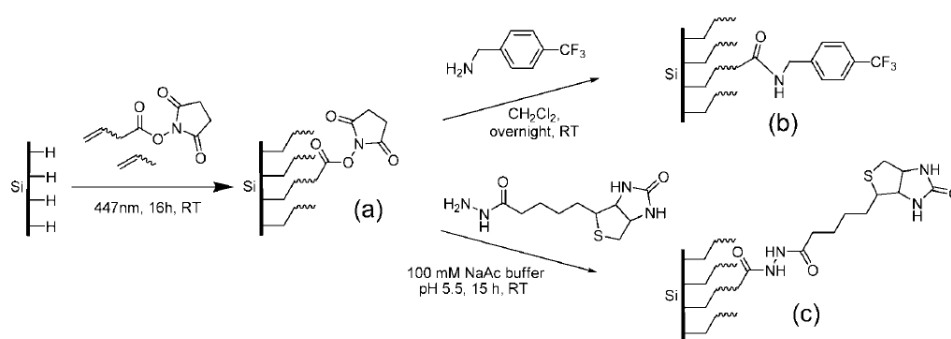


Figure 3.4 a) Schematic representation of the formation of a mixed monolayer terminated with NHS-ester moieties and b) subsequent substitution of the NHS-ester moiety by para-trifluoromethyl benzylamine (TFBA) or c) biotin hydrazide.²⁹

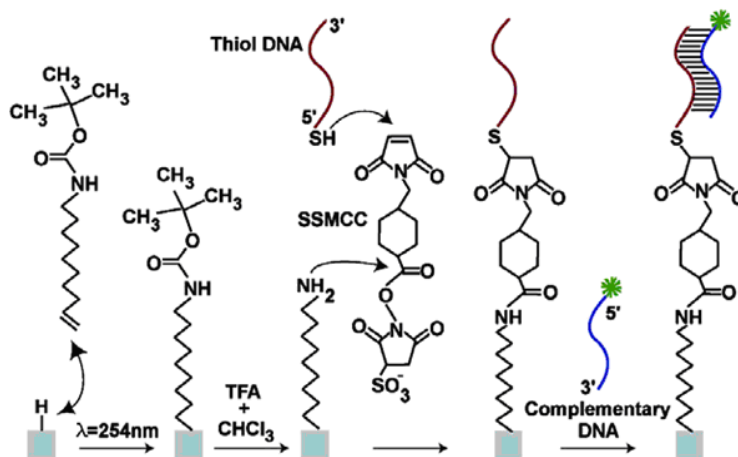


Figure 3.5 Schematic representation of selective functionalization of silicon nanowire biosensor using t-BOC protected amine (10-N-Boc-Amino-dec-1-ene), deprotection through trifluoroacetic acid (TFA) getting free amines, conjugation with hetero-bio-functional cross linker (SSMCC) and thiol ended DNA, subsequent hybridization with complementary DNA with fluorescence tag for detection.²⁶

Bunimovich et al.³⁴ developed a new method for the spatially selective biofunctionalization of silicon micro and nanostructures on single crystal silicon (111) or (100) surfaces. An electroactive monolayer of hydroquinone was formed on a hydrogen terminated electrode by hydrosilylation reaction using UV irradiation. Thiol ended biomolecules as well as cyclopentadiene can be preferentially and selectively immobilized in the regions where hydroquinone gets oxidized electrochemically. This reaction scheme is shown in Figure 3.6.

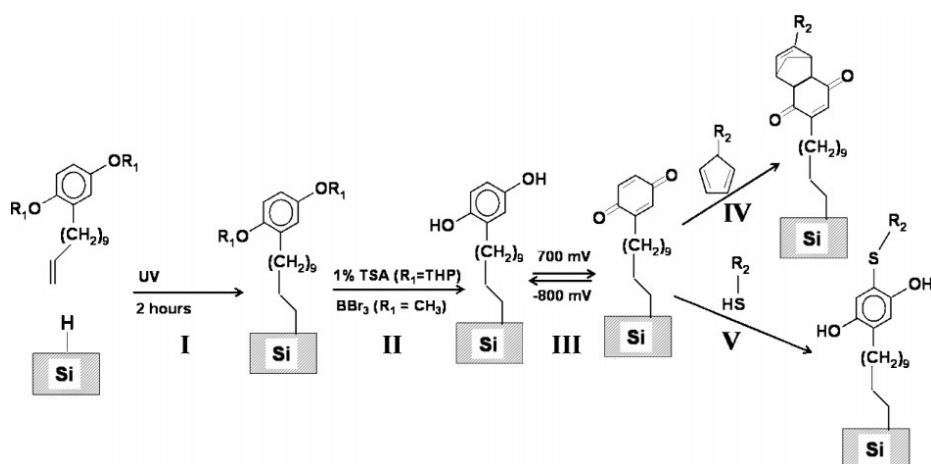


Figure 3.6 Electrically interactive monolayer for selective functionalization of micro and naoelectrodes.³⁴

It has been realized that silicon wafer doping type, its concentration and crystal orientation has effects in the efficiency of monolayer assembly. The order of ease with which surface grafting takes place is highly doped n > lowly doped n-type > lowly doped p-type > highly doped p-type. Maximum contact angle achievable by 1-Hexadecene monolayer was 109° and it was achieved in 5 hour for Si (111) surface and in 10 hours for Si (100) surface using same visible light intensity and wavelength and doping. Hydrogen terminated n-type surface is also more stable to oxidation as compare to p-type surface.³⁶

3.2.3. Alkylation via Grignard reagents (R-Mg-X)

Another wet chemical strategy to obtain alkylated silicon surfaces is to use Grignard reagents such as (R-Mg-X) having methyl, ethyl or butyl moiety. Hydrosilylation by using hydrogen terminated surfaces and 1-alkenes/alkynes is preferable due to following reasons: i) Alkene and alkynes are environment friendly and are not toxic as compare to Grignard reagents; ii) The method is single step as reaction directly proceed on hydrogen terminated surface as compare to a double step procedure in case of Grignard chemistry where a chloride/ halogenated surface is first prepared in gas phase

under UV-irradiation⁹ or a solution phase reaction with PCl_5 ³⁷ and resulting in chloride terminated surfaces are less stable to air/ambient oxidation see Figure 3.7.^{38,39}

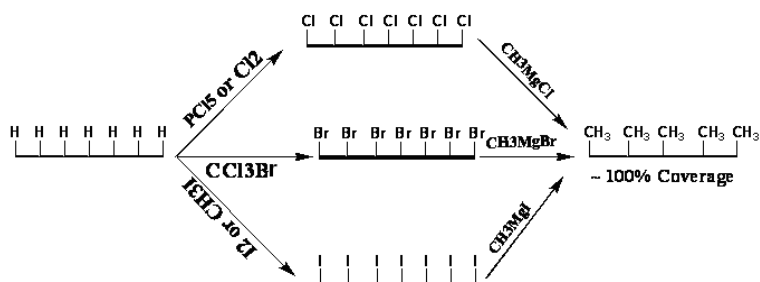


Figure 3.7 Two step hydrosilylation reactions through Grignard chemistry give nearly 100% coverage.

The methyl terminal is not more reactive/flexible for further molecular conjugations in case of biosensor applications however controllable air plasma oxidation can be used to generate functional groups on monolayer surface for further molecular immobilization.¹⁷

3.2.4. Silicon nanowire surface modifications through Grignard's chemistry

Alkylation with the help of the Grignard's reagent is beneficial due the fact that the smallest alky moiety is a methyl group ($-\text{CH}_3$) can be attached to the halogenated surface and thus does not require a double bond involving at least two carbon atoms. The chlorination-alkylation route can give 100% surface coverage which is an ideal condition to study the effect of these monolayers on the electrical behavior of Si-NW FET devices.

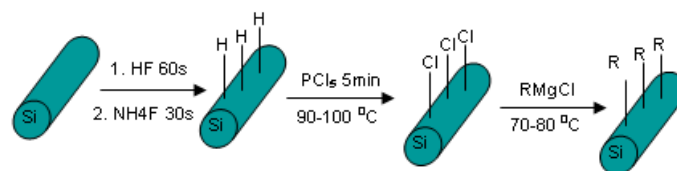


Figure 3.8 Silicon nanowire surface modification via chlorination and alkylation.⁴⁰

Si-Alkyl monolayers on silicon nanowire surfaces have shown greater stability and resistance to oxidation in ambient environments as compare to corresponding planar when exposed for several weeks. Furthermore, single carbon groups attached to silicon have greater surface coverage $\Gamma_{\text{max-alkyl}}$ (%) as shown by the Figure 3.9.⁴⁰

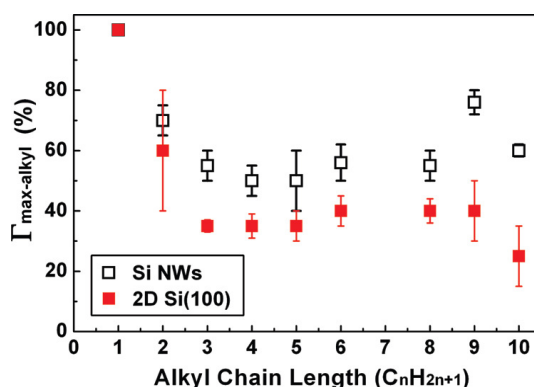


Figure 3.9 XPS Studies: $\Gamma_{\text{max-alkyl}}$ (%) [$\Gamma_{\text{max-alkyl}} = (\text{C-Si/Si2p})_{\text{max-Alkyl}} / (\text{C-Si/Si2p})_{\text{max-Cl}}$] versus alkyl chain length on n-type Si-NWs and comparison with planar/ 2D Si (100) surface.⁴⁰

It is due to the fact that increasing the number of carbon atoms increases the van der Waal diameter from 2.5 Å (in case of C1) to 4.5-5.0 Å for longer chains resulting into lower surface coverage only up to 50%. Silicon surfaces in general and silicon nanowire surfaces in particular, covered by single carbon moiety have greater resistance towards oxidation due to the fact that attractive interactions between longer alkyl chains increases by 4.6 KJ/mol per methylene unit.⁴⁰ Due to higher attractive forces, the probability is large for alkyl chains to make molecular domains and islands that leave voids and pin holes of nanometer diameters at the surface of silicon

nanowires.

3.2.5. UHV (ultra-high vacuum) approach for Si-C bond formation

Reactions under ultra-high vacuums provide experimental conditions which are well controlled even at the atomic level. At ultra-high vacuum (1×10^{-10} torr) surfaces can be heated routinely up to 1000 K without oxidation and allow access to unusual and (thermally stable) reconstructions that are otherwise unattainable even under inert atmosphere. Working under ultra high vacuum permits the scanning tunneling microscopy (STM) imaging of the surface bonded molecules.

3.3. Silicon nanowire modified with Si-alkyl monolayers

3.3.1. Improvements in device characteristics

Controlled doping of nanostructures is crucial for well defined characteristics and working domains as well as to utilize their high inherent sensitivities but uniformity and accuracy of doping profiles throughout the sensor body becomes difficult for small diameters.⁵ Electrical transport measurements show improved conductance after doping which can be fine tuned further by applying gating potential (V_g) but nanosensors need a robust solution.⁴¹ Surface modification of Si-NW FETs with carbon monolayers can be as important as the effect of its diameter and its orientation and impart dramatic improvements in device characteristics which can be fine tuned according to the intrinsic polarities of immobilized molecules provided that the surface coverage should be greater than 50%.⁴² Figure 3.10 a and b shows current-voltage (I_{ds} - V_{ds}) characteristics of SiO_2 -Si-NW and butyl-Si-NW respectively. The transconductance of Si-NW FETs of different surfaces like oxide-Si-NW, butyl-Si-NW, 1, 3-dioxane-2-ethyl-Si-NW and propyl alcohol-Si-NW (Figure 3.10c and d) indicates dependence of Si-NW characteristics on adsorbed molecules.

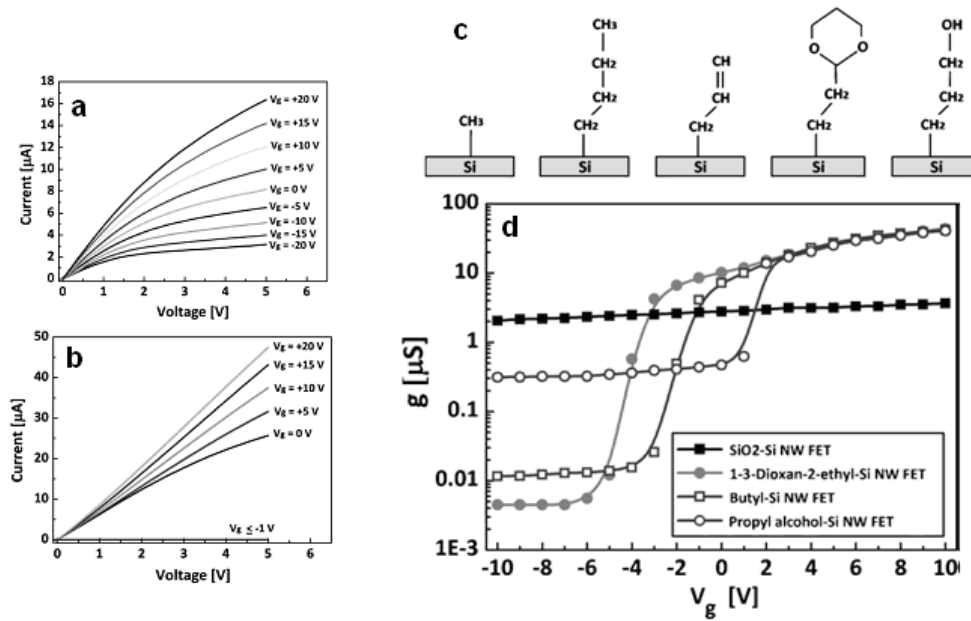


Figure 3.10 Electrical characteristics of Si-NW FETs: 1- V_{ds} curves a) SiO_2 -Si-NW FET and b) butyl-Si-NW FET at different back gate voltages (V_g), c) Different surface groups which were immobilized on silicon nanowire surfaces, d) Transconductance (g) versus back gate voltage (V_g) in SiO_2 -Si NW FET, butyl-Si-NW FET, 1,3-dioxane-2-ethyl-Si NW FET, and propyl alcohol-Si-NW FET. The transconductance values were obtained at $V_{ds}=0.2\text{V}$.⁴¹

A strong correlation of the transconductance data was observed with the corresponding change in work function $\Delta\Phi$ with respect to that of an oxide surface. Haick et al. reported a surface modified Si-NW modified with a two step chlorination and alkylation which was stable in ambient atmosphere, having small surface-defect densities and configured as an FET device with an off/on ratio of 10^5 over a relatively small voltage swing ($\pm 2\text{V}$).⁴³ These improvement in device characteristics is due to the fact that surfaces that are either hydrogen terminated or modified with methyl groups passivates surface defects near to the 100% and the probability of electron-hole pair recombination decreases causing an increase in the carrier mobilities. In response to changes in gate voltage, the same passivation of surface states allows for more effective movements of band edges in the channel compared to channels with SiO_2/Si interface or SiO_2 surface states and thus increases the on/off ratio of FETs. The

presence of hysteresis in SiO₂-Si-NW sample but not in freshly prepared H-Si-NW or CH₃-Si-NW and the observation of gradual development of hysteresis in H-Si-NWs upon increasing exposure time to air support the effects of surface states on the electrical properties of Si-NW FETs.⁴³

3.3.2. Improvements in biosensing

Heath et al. used non-oxidized silicon nanowire FETs for the detection of single stranded DNA and found two order of magnitude increase in sensitivity by using organic monolayer functionalization on nanowires surface as compared to silane based chemistry on native oxide in 1x SSC buffer (0.15 mM sodium citrate and 150 mM sodium chloride pH 7.5).²⁶

3.4. Reaction mechanism

3.4.1. Photochemical irradiation (UV-Irradiation)

Hydrosilylation under UV irradiation (~254 nm) is known to break the Si-H bond (homolysis) to create a surface free radical (dangling bond) on the silicon atop site, which reacts with α -carbon of precursor molecule in solution (1-alkene or 1-alkyne) creating a free radical at β -carbon which in turn absorbs a hydrogen atom from adjacent hydrogen terminated silicon creating second surface radical and reaction proceed forward in a sustainable way see Figure 3.11.^{44, 45, 36} UV irradiation (254 nm, 9 mW/cm²) reaction completes in about 2 hours.²⁶

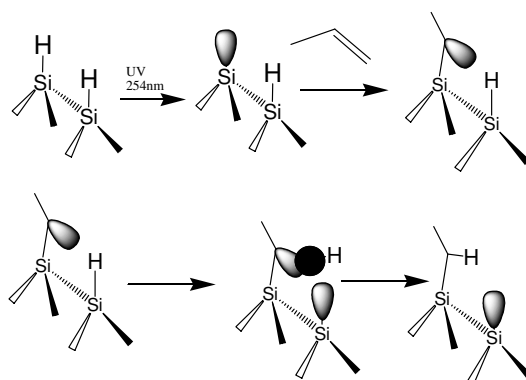


Figure 3.11 Mechanism of hydrosilylation under UV irradiation.

3.4.2. Heating

Hydrosilylation under heating at 170 - 200 °C undergoes a surface free radical reaction similar to as shown in Figure 3.11 for UV-based hydrosilylation. However, well packed, dense and very high quality monolayers have also been reported at 70 °C indicating some other reaction route for hydrosilylation.⁴⁶ One possibility might be the initiation by trace atomic oxygen by abstracting hydrogen from the surface but activation energy for this reaction have been calculated to be 130 KJ/mol implying that this possibility is only for temperatures exceeding 100 °C. STM imaging of surfaces during the early stages of the reactions at 150 °C and by UV-irradiation proved that it proceed via free radical chain reaction.^{46, 48} However, the type of reaction vessel also plays a role in the hydrosilylation reaction for example reaction is fast but results in relatively poor quality monolayer in a Pyrex Schlenk tube at 150 °C is slow, but yield high quality monolayers in inert vessel like one made of PTFE indicating a side catalytic degradation of alkenes and alkynes on glass surfaces before reacting to silicon surfaces.⁴⁷ Contradictions still exist in determining an exact mechanism for all kinds of hydrosilylation reactions.

3.5. Further functionalization of modified surfaces

3.5.1. C-H bond activation of terminal methyl group

Silicon-alkyl monolayers prepared through wet chemistry are robust and stable, passivate silicon surfaces well, reduce surface defects and interface traps and improve electrochemical characteristics of Si at one hand and provide a platform to do further surface-chemical changes to engineer sophisticated tasks like surface related assays, spectroscopic handles, heterogeneous catalysis and immobilization of biomolecular receptors onto sensing surfaces, on the other hand. A surface with packed monolayers with adequate number of bulky bio-receptors without any steric constraints is an ideal surface for sensing in aqueous solutions. Functionalized monolayers like amine terminated (-NH₂), carboxylic acid terminated (-COOH) or aldehyde terminated (-COH) can be prepared by using adequate protecting groups but a well packed monolayer is most often obtained via precursors having methyl terminal group. The methyl terminal is not able to conjugate biomolecular moieties directly and has to be activated first. The C-H bond can be activated by using different approaches having different efficiencies in term of density of surface generated groups available for bio-conjugation. The C-H bond of the terminal methyl groups on grafted monolayer can be activated by illuminating the modified surface for 15 minutes with a light of $\lambda \sim 350\text{nm}$ in the presence of 4'-[3-trifluoro-methyl-3H-diazirin-3-yl]-benzoic acid N-hydroxysuccinimide ester (TBDA-OSu) in carbon tetrachloride. The activation reagent is commercially available and results into a surface with amine reactive N-hydroxysuccinimide groups. This method is fast but generates a low surface coverage (10%) of functional groups leaving most of the surface hydrophobic see Figure 3.12.⁴⁸ Another route is to use photo-induced chlorosulfonation of the alkyl chain generating highly reactive sulfonylchloride head groups and subsequent reaction with an amine terminated linker such as ethylene diamine for amide (sulfonamide bond formation). Air plasma treatment or UV-Ozone⁴⁹ can produce carboxylic groups on the grafted

monolayer surfaces and bioimmobilization has been shown effectively.⁵⁰

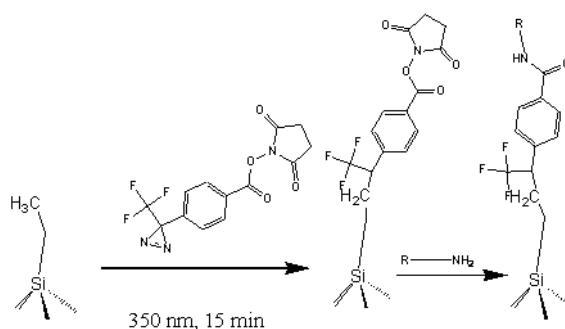


Figure 3.12 Methyl group activation to produce N-hydroxyl Succinimidyl groups on the surface and further reaction with amine terminated molecule.

3.5.2. Direct functionalization

Carboxylic acid terminated monolayers have applications and importance in biosensor development. These monolayers have been made by using a methyl ester substituted 1-Alkene/1-alkynes and yielded carboxylic acid groups on its deprotection. The ester protecting group was to avoid silyl ester formation with carboxylic group.³⁰ Another possibility is to use carboxylic functionalized 1-alkene directly to make a monolayer as double bond reacts preferentially with surface under optimized reaction conditions.^{31, 51} As prepared carboxylic terminated surfaces were reactive to amines and can be converted to amine reactive Succinimidyl groups by using EDC/NHS chemistry.⁵²

3.6. Conclusion

Silicon-alkyl monolayers grafted onto hydrogen terminated silicon by any wet chemical approach is promising in the sense that high quality interfaces become available to induce effects on both sides of the surface plane in the form of better/improved electrical characteristics due to better passivation of organic layers on

one side and availability of a very flexible interface handle for surface engineering and immobilizations on the other side. However, apart from the fact that improved nanowire characteristics due to grafted monolayers seems to be very ground breaking, realization of a robust biosensor need an ideal interface which should be void free and have least amount of leakages and imperfections due to the growth of oxide and sub-oxide. The surface based hydrosilylation reaction is not mature yet and a lot remains unknown about the reaction mechanism, however, further research will open more prospects to utilize silicon-alkyl hetrojunction for novel applications.

3.7. Bibliography

1. Kim, J.; Seidler, P.; Fill, C.; Wan, L. S., Investigations of the effect of curing conditions on the structure and stability of amino-functionalized organic films on silicon substrates by Fourier transform infrared spectroscopy, ellipsometry, and fluorescence microscopy. *Surf Sci* **2008**, 602, (21), 3323-3330.
2. Pasternack, R. M.; Amy, S. R.; Chabal, Y. J., Attachment of 3-(Aminopropyl)triethoxysilane on Silicon Oxide Surfaces: Dependence on Solution Temperature. *Langmuir* **2008**, 24, (22), 12963-12971.
3. Patolsky, F.; Zheng, G. F.; Lieber, C. M., Fabrication of silicon nanowire devices for ultrasensitive, label-free, real-time detection of biological and chemical species. *Nat Protoc* **2006**, 1, (4), 1711-1724.
4. Sze, S. M., *Physics of Semiconductor Devices*. 2nd ed.;1982.
5. Lee, K.; Nair, P. R.; Scott, A.; Alam, M. A.; Janes, D. B., Device considerations for development of conductance-based biosensors. *J App Phys* **2009**, 105, (10).
6. http://www.enigmaticconsulting.com/semiconductor_processing/selected_shorts/Getterin
7. Linford, M. R.; Fenter, P.; Eisenberger, P. M.; Chidsey, C. E. D., Alkyl monolayers on silicon prepared from 1-alkenes and hydrogen-terminated silicon. *J Am Chem Soc* **1995**, 117, (11), 3145-3155.
8. Boukherroub, R., Chemical reactivity of hydrogen-terminated crystalline silicon

surfaces. *Curr Opin Solid Stat Mater Sci* **2005**, 9, (1-2), 66-72.

9. Buriak, J. M., Organometallic chemistry on silicon surfaces: formation of functional monolayers bound through Si-C bonds. *Chem Commun* **1999**, (12), 1051-1060.
10. Allongue, P.; Henry De Villeneuve, C.; Pinson, J.; Ozanam, F.; Chazalviel, J. N.; Wallart, X., Organic monolayers on Si(111) by electrochemical method. *Electrochim Acta* **1998**, 43, (19-20), 2791-2798.
11. Higashi, G. S.; Chabal, Y. J.; Trucks, G. W.; Raghavachari, K., Ideal hydrogen termination of the Si (111) surface. *App Phys Lett* **1990**, 56, (7), 656-658.
12. Sieval, A. B.; Van den Hout, B.; Zuilhof, H.; Sudholter, E. J. R., Molecular modeling of covalently attached alkyl monolayers on the hydrogen-terminated Si(111) surface. *Langmuir* **2001**, 17, (7), 2172-2181.
13. Royea, W. J.; Juang, A.; Lewis, N. S., Preparation of air-stable, low recombination velocity Si(111) surfaces through alkyl termination. *App Phys Lett* **2000**, 77, (13), 1988-1990.
14. Kar, S., Study of silicon-organic interfaces by admittance spectroscopy. *App Surf Sci* **2006**, 252, (11), 3961-3967.
15. McGuinness, C. L.; Blasini, D.; Masejewski, J. P.; Uppili, S.; Cabarcos, O. M.; Smilgies, D.; Allara, D. L., Molecular self-assembly at bare semiconductor surfaces: Characterization of a homologous series of n-alkanethiolate monolayers on GaAs(001). *ACS Nano* **2007**, 1, (1), 30-49.
16. Scott, A.; Hacker, C. A.; Janes, D. B., In situ structural characterization of metal-molecule-silicon junctions using backside infrared spectroscopy. *J Phys Chem C* **2008**, 112, (36), 14021-14026.
17. Rosso, M.; Giesbers, M.; Schroen, K.; Zuilhof, H., Controlled Oxidation, Biofunctionalization, and Patterning of Alkyl Monolayers on Silicon and Silicon Nitride Surfaces using Plasma Treatment. *Langmuir* 26, (2), 866-872.
18. Liao, W.; Wei, F.; Qian, M. X.; Zhao, X. S., Characterization of protein immobilization on alkyl monolayer modified silicon(111) surface. *Sens & Actuat B-Chemical* **2004**, 101, (3), 361-367.
19. He, T.; He, J. L.; Lu, M.; Chen, B.; Pang, H.; Reus, W. F.; Nolte, W. M.; Nackashi, D. P.; Franzon, P. D.; Tour, J. M., Controlled modulation of conductance in silicon devices

by molecular monolayers. *J Am Chem Soc* **2006**, 128, (45), 14537-14541.

20. Rohde, R. D.; Agnew, H. D.; Yeo, W. S.; Bailey, R. C.; Heath, J. R., A non-oxidative approach toward chemically and electrochemically functionalizing Si(111). *J Am Chem Soc* **2006**, 128, (29), 9518-9525.

21. De Smet, L. C. P. M.; Pukin, A. V.; Sun, Q. Y.; Eves, B. J.; Lopinski, G. P.; Visser, G. M.; Zuilhof, H.; Sudholter, E. J. R., Visible-light attachment of SiC linked functionalized organic monolayers on silicon surfaces. *App Surf Sci* **2005**, 252, (1 SPEC. ISS.), 24-30.

22. Eves, B. J.; Fan, C. Y.; Lopinski, G. P., Sequential reactions with amine-terminated monolayers and isolated molecules on H/Si(111). *Small* **2006**, 2, (11), 1379-1384.

23. Strother, T.; Cai, W.; Zhao, X. S.; Hamers, R. J.; Smith, L. M., Synthesis and characterization of DNA-modified silicon (111) surfaces. *J Am Chem Soc* **2000**, 122, (6), 1205-1209.

24. Stern, E.; Klemic, J. F.; Routenberg, D. A.; Wyrembak, P. N.; Turner-Evans, D. B.; Hamilton, A. D.; LaVan, D. A.; Fahmy, T. M.; Reed, M. A., Label-free immunodetection with CMOS-compatible semiconducting nanowires. *Nature* **2007**, 445, (7127), 519-522.

25. Streifer, J. A.; Kim, H.; Nichols, B. M.; Hamers, R. J., Covalent functionalization and biomolecular recognition properties of DNA-modified silicon nanowires. *Nanotechnology* **2005**, 16, (9), 1868-1873.

26. Bunimovich, Y. L.; Shin, Y. S.; Yeo, W. S.; Amori, M.; Kwong, G.; Heath, J. R., Quantitative real-time measurements of DNA hybridization with alkylated nonoxidized silicon nanowires in electrolyte solution. *J Am Chem Soc* **2006**, 128, (50), 16323-16331.

27. Terry, J.; Linfood, M. R.; Wigren, C.; Cao, R. Y.; Pianetta, P.; Chidsey, C. E. D., Determination of the bonding of alkyl monolayers to the Si(111) surface using chemical-shift, scanned-energy photoelectron diffraction. *App Phys Lett* **1997**, 71, (8), 1056-1058.

28. Niederhauser, T. L.; Jiang, G. L.; Lua, Y. Y.; Dorff, M. J.; Woolley, A. T.; Asplund, M. C.; Berges, D. A.; Linfood, M. R., A new method of preparing monolayers on silicon and patterning silicon surfaces by scribing in the presence of reactive species. *Langmuir* **2001**, 17, (19), 5889-5900.

29. Yang, M.; Teeuwen, R. L. M.; Giesbers, M.; Baggerman, J.; Arafat, A.; de Wolf, F. A.; van Hest, J. C. M.; Zuilhof, H., One-step photochemical attachment of NHS-terminated monolayers onto silicon surfaces and subsequent functionalization. *Langmuir* **2008**, 24,

(15), 7931-7938.

30. Sieval, A. B.; Demirel, A. L.; Nissink, J. W. M.; Linford, M. R.; van der Maas, J. H.; de Jeu, W. H.; Zuilhof, H.; Sudholter, E. J. R., Highly stable Si-C linked functionalized monolayers on the silicon (100) surface. *Langmuir* **1998**, 14, (7), 1759-1768.

31. Cattaruzza, F.; Cricenti, A.; Flamini, A.; Girasole, M.; Longo, G.; Mezzi, A.; Prospero, T., Carboxylic acid terminated monolayer formation on crystalline silicon and silicon nitride surfaces. A surface coverage determination with a fluorescent probe in solution. *J Mater Chem* **2004**, 14, (9), 1461-1468.

32. Cattaruzza, F.; Cricenti, A.; Flamini, A.; Girasole, M.; Longo, G.; Prospero, T.; Andreano, G.; Cellai, L.; Chirivino, E., Controlled loading of oligodeoxyribonucleotide monolayers onto unoxidized crystalline silicon; fluorescence-based determination of the surface coverage and of the hybridization efficiency; parallel imaging of the process by Atomic Force Microscopy. *Nucl Acid Research* **2006**, 34, (4).

33. Lin, Z.; Strother, T.; Cai, W.; Cao, X. P.; Smith, L. M.; Hamers, R. J., DNA attachment and hybridization at the silicon (100) surface. *Langmuir* **2002**, 18, (3), 788-796.

34. Bunimovich, Y. L.; Ge, G. L.; Beverly, K. C.; Ries, R. S.; Hood, L.; Heath, J. R., Electrochemically programmed, spatially selective biofunctionalization of silicon wires. *Langmuir* **2004**, 20, (24), 10630-10638.

35. Strother, T.; Hamers, R. J.; Smith, L. M., Covalent attachment of oligodeoxyribonucleotides to amine-modified Si (001) surfaces. *Nucl Acid Resea* **2000**, 28, (18), 3535-3541.

36. Sun, Q. Y.; de Smet, L.; van Lagen, B.; Giesbers, M.; Thune, P. C.; van Engelenburg, J.; de Wolf, F. A.; Zuilhof, H.; Sudholter, E. J. R., Covalently attached monolayers on crystalline hydrogen-terminated silicon: Extremely mild attachment by visible light. *J Am Chem Soc* **2005**, 127, (8), 2514-2523.37.

37. Wallart, X.; de Villeneuve, C. H.; Allongue, P., Truly quantitative XPS characterization of organic monolayers on silicon: Study of alkyl and alkoxy monolayers on H-Si (111). *J Am Chem Soc* **2005**, 127, (21), 7871-7878.

38. Webb, L. J.; Michalak, D. J.; Biteen, J. S.; Brunschwig, B. S.; Chan, A. S. Y.; Knapp, D. W.; Meyer, H. M.; Nemanick, E. J.; Traub, M. C.; Lewis, N. S., High-resolution

soft X-ray photoelectron spectroscopic studies and scanning auger microscopy studies of the air oxidation of alkylated silicon(111) surfaces. *J Phys Chem B* **2006**, 110, (46), 23450-23459.

39. Sieval, A. B.; Opitz, R.; Maas, H. P. A.; Schoeman, M. G.; Meijer, G.; Vergeldt, F. J.; Zuilhof, H.; Sudholter, E. J. R., Monolayers of 1-alkynes on the H-terminated Si(100) surface. *Langmuir* **2000**, 16, (26), 10359-10368.

40. Bashouti, M. Y.; Stelzner, T.; Christiansen, S.; Haick, H., Covalent Attachment of Alkyl Functionality to 50 nm Silicon Nanowires through a Chlorination/Alkylation Process. *J Phy Chem C* **2009**, 113, (33), 14823-14828.

41. Bashouti, M. Y.; Tung, R. T.; Haick, H., Tuning the Electrical Properties of Si Nanowire Field-Effect Transistors by Molecular Engineering. *Small* **2009**, 5, (23), 2761-2769.

42. Leu, P. W.; Shan, B.; Cho, K. J., Surface chemical control of the electronic structure of silicon nanowires: Density functional calculations. *Phy Rev B* **2006**, 73, (19), 195320-I.

43. Haick, H.; Hurley, P. T.; Hochbaum, A. I.; Yang, P. D.; Lewis, N. S., Electrical characteristics and chemical stability of non-oxidized, methyl-terminated silicon nanowires. *J Am Chem Soc* **2006**, 128, 8990-8991.

44. Buriak, J. M., Organometallic chemistry on silicon and germanium surfaces. *Chem Rev* **2002**, 102, (5), 1271-1308.

45. Lee, M. V.; Scipioni, R.; Boero, M.; Silvestrelli, P. L.; Ariga, K., The initiation mechanisms for surface hydrosilylation with 1-alkenes. *Phys Chem* 13, (11), 4862-4867.

46. Scheres, L.; Arafat, A.; Zuilhof, H., Self-assembly of high-quality covalently bound organic monolayers onto silicon. *Langmuir* **2007**, 23, (16), 8343-8346.

47. Mischki, T. K.; Lopinski, G. P.; Wayner, D. D. M., Evidence for Initiation of Thermal Reactions of Alkenes with Hydrogen-Terminated Silicon by Surface-Catalyzed Thermal Decomposition of the Reactant. *Langmuir* **2009**, 25, (10), 5626-5630.

48. Wagner, P.; Nock, S.; Spudich, J. A.; Volkmuth, W. D.; Chu, S.; Cicero, R. L.; Wade, C. P.; Linford, M. R.; Chidsey, C. E. D., Bioreactive self-assembled monolayers on hydrogen-passivated Si(111) as a new class of atomically flat substrates for biological scanning probe microscopy. *J Struct Biolog* **1997**, 119, (2), 189-201.

49. Uosaki, K.; Quayum, M. E.; Nihonyanagi, S.; Kondo, T., Decomposition processes of an organic monolayer formed on Si(111) via a silicon-carbon bond induced by exposure to UV irradiation or ozone. *Langmuir* **2004**, 20, (4), 1207-1212.
50. Zuilhof, H.; Rosso, M.; Giesbers, M.; Schroen, K., Controlled Oxidation, Biofunctionalization, and Patterning of Alkyl Monolayers on Silicon and Silicon Nitride Surfaces using Plasma Treatment. *Langmuir* **2010**, 26, (2), 866-872.
51. Voicu, R.; Boukherroub, R.; Bartzoka, V.; Ward, T.; Wojtyk, J. T. C.; Wayner, D. D. M., Formation, characterization, and chemistry of undecanoic acid-terminated silicon surfaces: Patterning and immobilization of DNA. *Langmuir* **2004**, 20, (26), 11713-11720.
52. Fischer, M. J. E., Amine Coupling Through EDC/NHS: A Practical Approach. *Surface Plasmon Resonance: Method & Protocol*, **2010**, 627 55-73, ISBN10: 1607616696.

Chapter 4

Surface preparation of active gate regions for silicon field-effect devices

Silicon surfaces play a key role in the operation and sensitivity of field-effect devices, especially when used for biosensing. Being a surface sensitive electrical device, silicon nanowire biosensors create many challenges on the laboratory-scale surface preparation modifications. Hydrogen terminated surfaces form ideal interfaces because they are reported to have low recombination velocities due to smaller interface state density as compared to native/thermal oxide, however, their stability remains a question mark. Top-down and bottom-up silicon nanowire fabrication approaches facilitate the production of well ordered devices but the opportunity of using conventional surface analysis techniques such as commercially available X-ray photoelectron spectroscopy (XPS), is not possible. Atomic force microscopy (AFM) and scanning electron microscopy (SEM) can be used to characterize morphological properties of the surfaces and reveal differences for different surface treatments. Electrical and electrochemical measurements characterize the efficiency of as-prepared surfaces and are crucial for the choice of working regime and calibrations. Hydrogen terminated surfaces can be used to do further surface modifications for biosensor applications; however, controlled environments are crucial for making surfaces reproducibly.

4.1. Introduction

Silicon nanowire field-effect transistor (Si-NW FET) sensors hold significant promise as highly sensitive sensors for chemical and biological species.¹ The high sensitivity characteristics are mainly due to the high surface to volume ratio where a large fraction of the overall atoms in the device are surface atoms and that is why can sense a minute change in surface physical, chemical or biological environment.² A high surface to volume ratio on the other hand might offer restrictions towards the lateral growth of dielectric passivation layer around sensor surface in respect to its quality (purity, stoichiometry) and thickness as both factors that can significantly alter the device characteristics and its sensing capability.³ Native oxide or grown thermal oxide on silicon can have some charges imbedded deep inside the silicon shell or they might be present near the Si-SiO₂ interface. The charges inside the silicon oxide shell are oxide trapped charges Q_{ot} and mobile oxide charges Q_m where as those at, or in close vicinity of the Si-SiO₂ interface, are the fixed oxide charge density Q_F and interface state density Q_{it} which have a stronger influence on the electric properties of a silicon field effect devices by affecting the mobile charge density inside the silicon nanowire channel.⁴ Replacing the silicon oxide interface with an ideal interface (free of all sorts of charges and interface states) will greatly enhance the characteristics of the semiconductor devices in terms of carrier mobilities, recombination velocities and flat band voltage. The hydrogen terminated silicon surface is a chemically passivated surface where the native oxide has been removed by etching in aqueous hydrofluoric acid (HF) or ammonium fluoride (NH₄F) solutions leaving the silicon surface covalently attached with hydrogen. Since all surface Si atoms are fully coordinated, hydrogen termination leads to enhanced stability in ambient environments unlike a “clean surface” having un-passivated surface atoms, or dangling bonds. Hydrogen terminated surfaces get oxidize in an ambient atmosphere. A hydrogen-terminated silicon surface has another excellent property: it can be flattened at the atomic level by etching. For example, to etch a hydrogen-terminated silicon (111) surface, ammonium

fluoride aqueous solution is usually used. Like other silyl groups of organic compounds, the H-Si groups on the surface react with molecules that have terminal unsaturated bonds or diazo groups. The reaction is called hydrosilylation. Many types of organic compounds with various functionalities can be introduced onto the silicon surface by the hydrosilylation reaction. Consequently, ideal hydrogen-terminated defect free surfaces are very crucial for the fabrication of defect free monolayers.⁵ Wet chemical surface preparations in an inert environment such as bubbling argon, Schlenk flasks and cannula based manipulations are preferable in comparison to ultra-high vacuum (UHV) techniques because they are inexpensive, fast and allow laboratory based preparations. In this chapter, AFM and XPS studies were used to characterize silicon surfaces prepared after etching with 1 % HF and nitrogen purged/non-purged 40% NH₄F solution in terms of surface morphology and chemistry. The hydrogen terminated surfaces of Si-NW FET devices were characterized electrically in air by back gating the devices (V_{bg} - I_{ds}) where as stability of hydrogen terminated surfaces were determined by front gating the device in an aqueous electrolyte solution using a reference electrode.

4.2. Experimental

Surface preparations involving cleaning and hydrogen termination of planar silicon samples as well as Si-NWs was carried out. X-ray photoelectron spectroscopy was used to verify the cleanliness and the chemistry of the surface of planar samples where as atomic force microscopy (AFM) was used to determine the morphology of as-prepared planar as well as Si-NW sample surfaces. Hydrogen terminated silicon nanowire (H-Si-NW) device characteristics were monitored electrically after etching away the thermal oxide (10-20 nm) passivation layer with the help of 1% HF or 40% NH₄F for one to two minutes of etching and rinsing with deionized (DI) water and

drying in pure compressed nitrogen. All experiments were performed in an ambient environment (room temperature and in air).

4.2.1. Silicon samples

Single side polished planar Si (111) samples were cut from 100 mm diameter wafers into a dimension of $1 \times 1 \text{ cm}^2$. Si-NW samples were fabricated in MESA⁺ clean room and a full description can be found in the published paper by Chen et al.⁶

4.2.2. Chemicals

HF and NH_4F etching solutions used were of VSLI grade and were used as received. Milli-Q DI water ($18.2 \text{ M}\Omega\cdot\text{cm}^{-1}$ resistivity) was used to rinse the sample after each etch step. Sulfuric acid H_2SO_4 (98%), hydrogen peroxide H_2O_2 (30%) potassium chloride (KCl) was purchased from Sigma Aldrich.

4.2.3. Surface etching

The planar Si (111) samples were surface cleaned with the help of sonication with organic solvents such as acetone, ethanol, and iso-propanol, treated with piranha solution (3:1) H_2SO_4 : H_2O_2 at 90°C for 30 minutes while etching with HF and rinsing with DI water. The contact angle of the samples after cleaning / before final etch was less than 5° . Silicon nanowire samples were UV-ozone treated for 5 minutes and were directly used for measurements. However, some silicon nanowire samples were noticed to have residual polyimide (passivation layer on the sensing windows) coverage at sensor sites which was removed by an air plasma treatment for 10 minutes.

4.2.4. XPS characterization

XPS studies/surface characterization has been conducted with a monochromatic X-ray beam (Al KR, 1486.6 eV, 100W, Quantero, Physical Electronics). Mapping was done at

3×10^{-9} Torr and detector angle of 45° . Silicon (Si 2p $3/2$) was taken as a reference. Data was analyzed and fitted with the help of the software PHI Multipak, and CasaXPS.

4.2.5. Electrochemical measurements

UV-Ozone (Procleaner™ plus Bioforce Nanosciences) was used for cleaning and surface treatments. A multimeter (2400, Keithley) with Software (Labtracer 2.0, Keithley) was used for electrical data acquisition. All measurements were done with the help of probe station (PM8, Karl Süss) inside a faraday cage. A platinum wire (0.25 mm diameter, 99.99%, Sigma Aldrich) was used as a pseudo reference electrode where required.

4.2.6. AFM imaging

A Digital Instruments Dimension 3100 was used for AFM images. All AFM images performed in tapping mode with ultra sharp (average tip diameter ~ 2 nm) single crystal silicon tips (SSH-NCH-10, NanoandMore, GmbH). Silicon nanowire devices used for etching studies were made by top-bottom approach involving two plane dependant wet etchings and two photolithography steps for defining sensor areas and contact pads see Figure 2.4.⁶

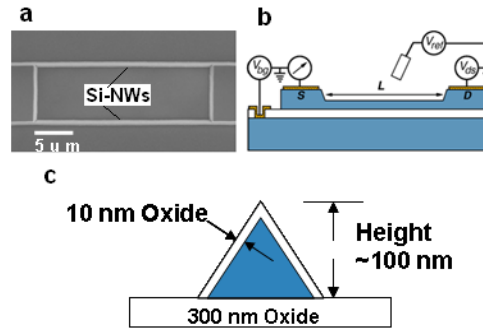


Figure 4.1 Silicon nanowire device configuration a) high resolution SEM image; b) schematic for electrical measurements with front gating V_{ref} , back gating V_{bg} and drain-source bias V_{ds} ; c) cross section of Si-NW showing height, thickness of buried oxide layer and of gate oxide.

The nanowires were p-type boron doped ($\sim 10^{17}$ - 10^{18} cm^{-3}), $L= 20$ - 40 μm , $h= 100$ nm and $W= 150$ nm , unless otherwise stated.

4.3. Results and discussions

Silicon nanowire devices were used to study the different surface treatments on their current-voltage (I-V) characteristics including UV-ozone cleaning/exposure, etching and hydrogen termination and re-oxidation where as XPS was used to study the planar samples etched via different etchants.

4.3.1. Etching: SEM, AFM and XPS studies

X-ray photoelectron spectroscopy was used to monitor the surface chemistry of Si (111) samples treated with different etchants for equal time intervals to determine the extent of oxidation on the surface for each surface treatment. All samples were etched for the same time and were analyzed with XPS after 10-20 minutes of ambient exposure. Figure 4.2a shows measured XPS results of a sample treated with piranha, which have a chemically grown native oxide that shows a peak at the binding energy of 103 eV for silicon oxide. Figures 4.2b, 4.2c and 4.2d show silicon samples etched with

aqueous 40% NH_4F solution purged with nitrogen, with aqueous 1% HF and a non-purged NH_4F solution respectively. The sample etched with nitrogen purged NH_4F solution (Figure 4b) has the least amount of silicon bonded with oxygen where as a sample etched with non-purged NH_4F solution (Figure 4.2d) has the highest amount of silicon as oxide. Etching with 1% HF solution (Figure 4.2c) however, has a less percentage of surface silicon oxide as compared to the sample shown in Figure 4.2d, but oxide is fully developed and is probably in the form of SiO_2 .

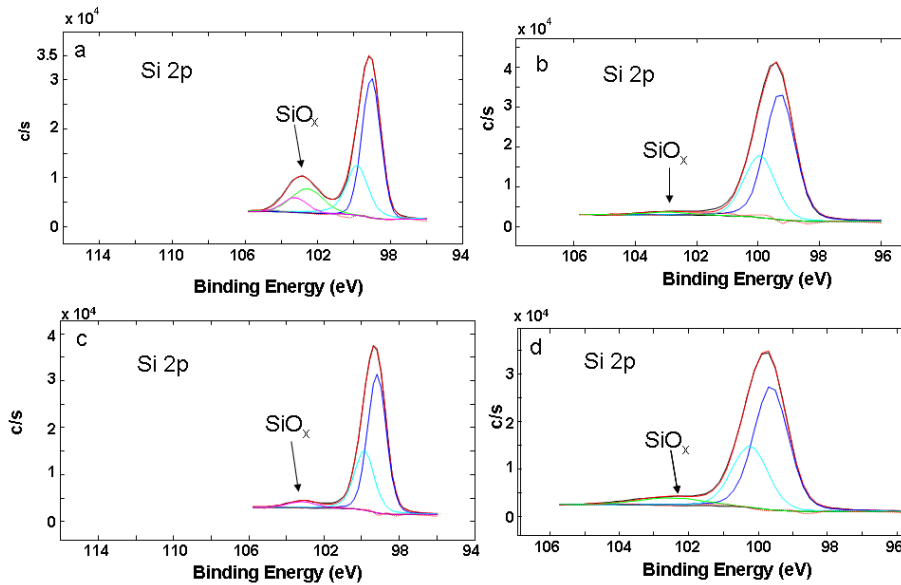


Figure 4.2 Etching planar silicon samples with different etchants: a) piranha cleaned sample having chemically grown native oxide, b) silicon sample etched with nitrogen purged 40% NH_4F solution, c) silicon sample etched with 1 % HF solution, d) silicon sample etched with NH_4F solution without nitrogen purge. The peak fits are shown in colors representing Si^0 2p^{1/2}, Si^0 2p^{3/2}, Si^{+4} 2p etc.

Etching with nitrogen purged NH_4F is efficient for producing flat Si (111) hydrogen terminated surfaces where each silicon atom is terminated with a single hydrogen atom perpendicular to the surface. Purging of dissolved oxygen from the solution ensures the least oxidation of the surface and NH_4F etch results in a smooth atomic plane with the least surface roughness. Oxygen rich NH_4F solutions or even partially purged etchant

solutions can cause etch-pit generation in the silicon.^{7, 8} Figure 4.3 shows a SEM picture of silicon nanowire etched with an oxygen rich ammonium fluoride solution.

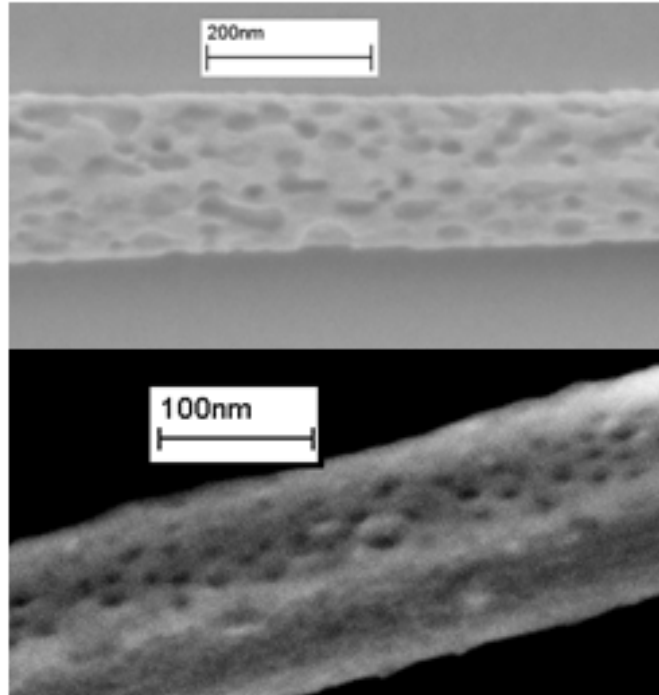


Figure 4.3 High resolution SEM of Si-NW etched with oxygen rich NH_4F solution.

Figure 4.4a is a high resolution scanning electron microscopy image of a Si-NW after 1 minute of HF etching. Figure 4.4b shows a high resolution AFM image of a Si-NW after etching with 1 % HF for 1 and 2 minutes. Striations on the side walls of the Si-NW can be seen after 2 minute of etch which are AFM imaging artifacts as per confirmation by SEM studies.

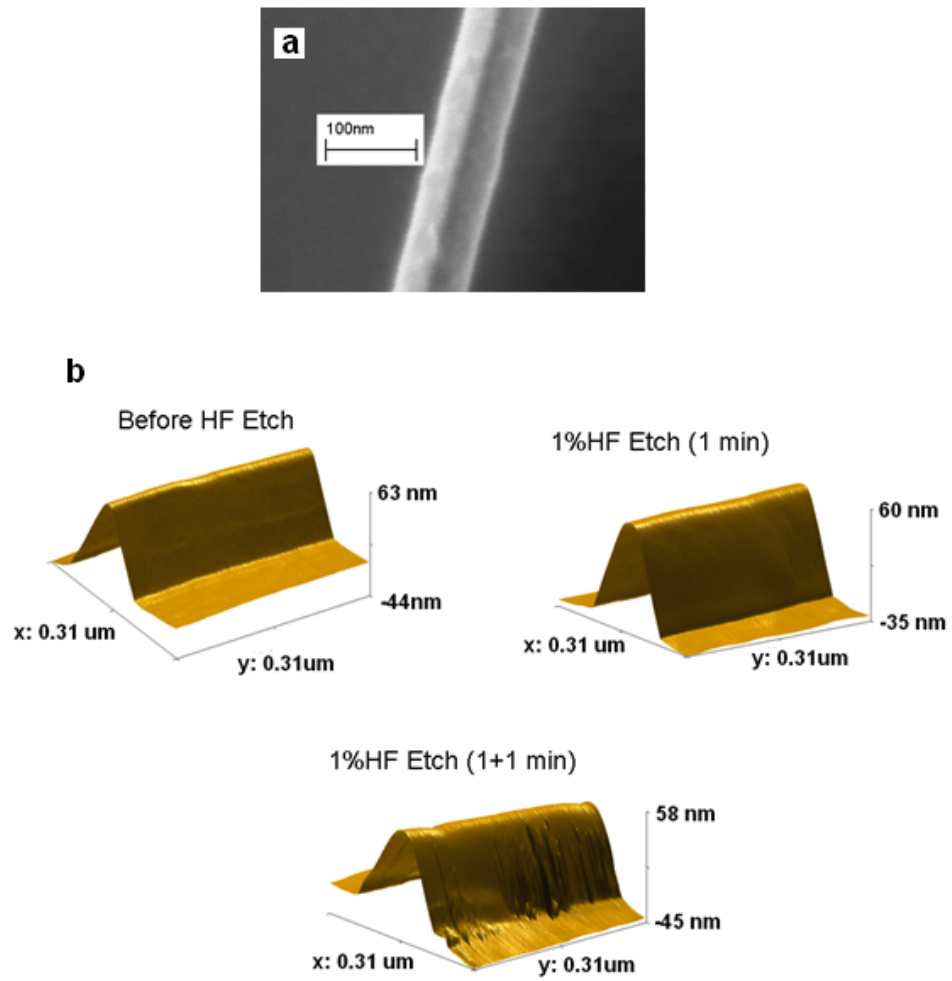


Figure 4.4 Etched silicon nanowire a) high resolution SEM image after 1 minute etch b) AFM images of Si-NW before and after etching for 1 and 2 minutes with 1% HF.

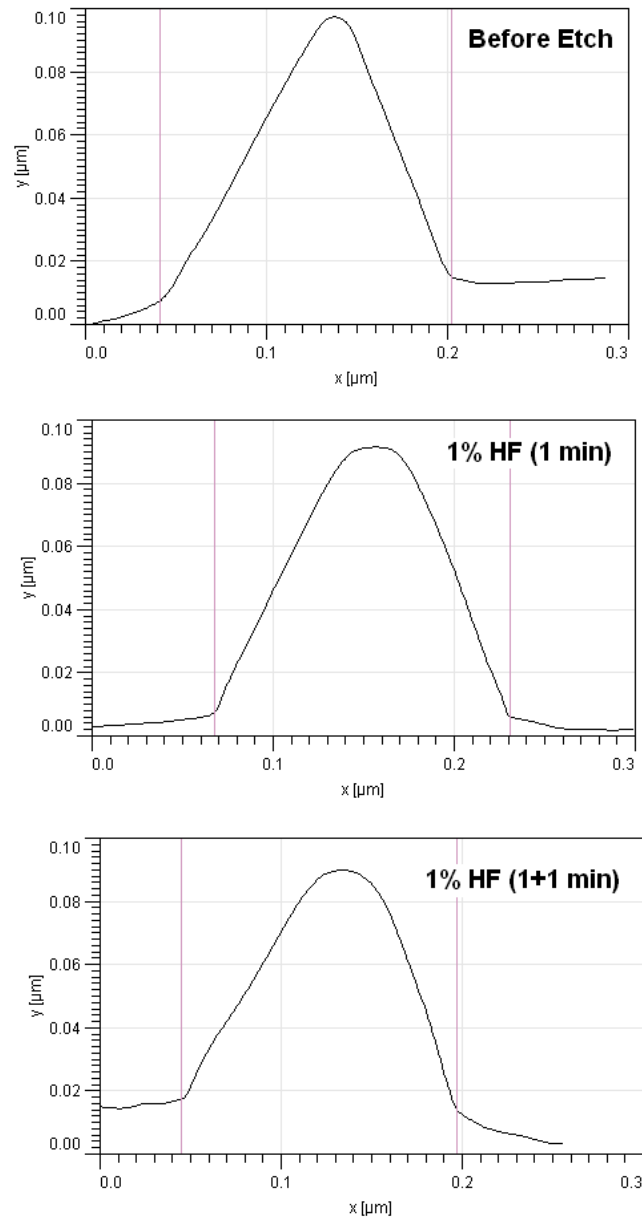


Figure 4.5 AFM profiling of Si-NW surfaces before and after HF dip for different times.

Figure 4.5 shows the profile plots of the Si-NW surface after etching with 1% HF for

different times. It can be seen that etching rate is higher for the triangular tip of the nanowire which is probably Si(100) as compare to Si (111) planes in accordance to the fact that etch rate is higher for Si (100) orientation. The top of the Si-NW becomes increasingly rounded for longer HF etch times.

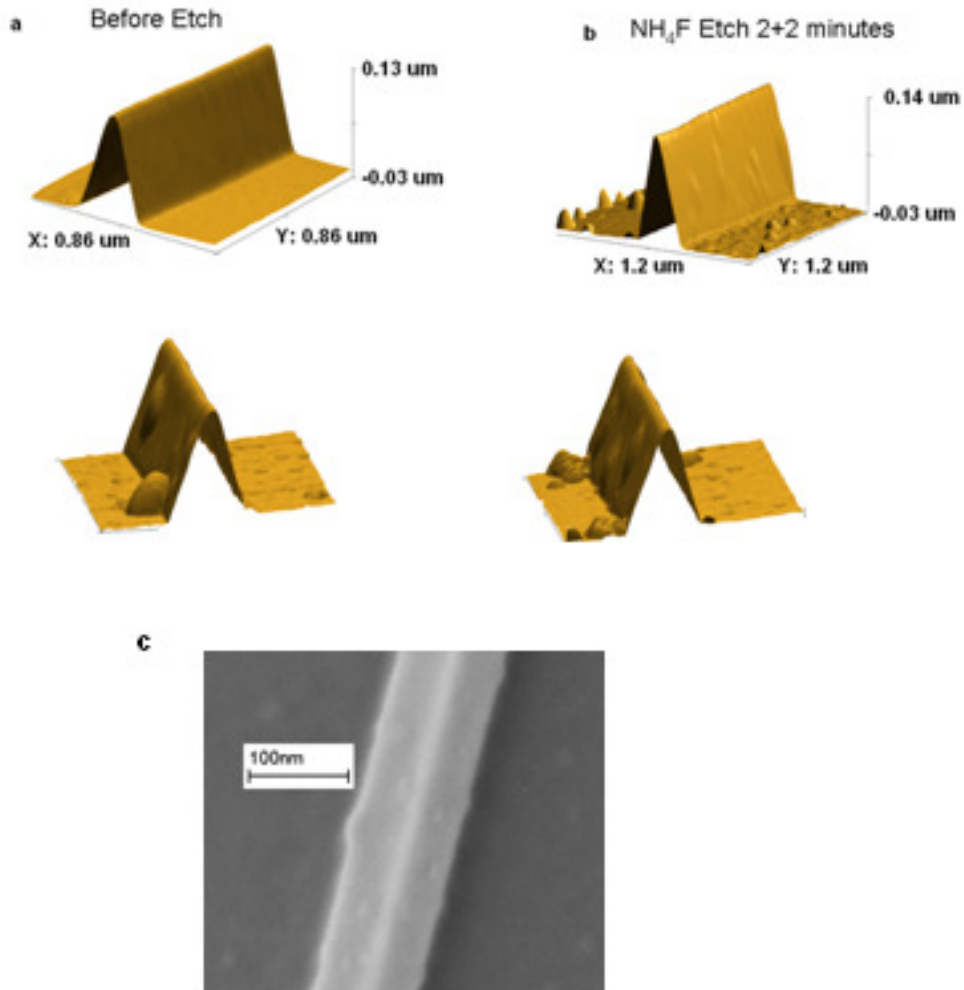


Figure 4.6 AFM profiles of NH₄F etched Si-NWs a) before and b) after etching with nitrogen purged 40% NH₄F solution showing deposition of residual crystals after a rinse/fast dip with DI water and drying with pure compressed nitrogen c) SEM image.

Figures 4.6a and 4.6b shows an AFM image of a Si-NW before and after etching with a nitrogen purged solution of 40% NH_4F . Even after a fast rinse in DI water, residual crystals get adsorbed to the surfaces so a thorough rinse is recommended to get rid of heavy residual crystal content from 40% NH_4F solution to use these surfaces for further modification (Solubility of NH_4F in water is 45g/100 ml at 25 °C, nitrogen purging causes rise in the saturation).

4.3.2. UV-Ozone surface treatment

Figure 4.7 shows electrical characteristics of Si-NW FET devices before and after UV-ozone treatment for 5 minutes. The treatment of Si-NW devices with UV-ozone is beneficial before measurements and ensures relatively clean surfaces and stable current-voltage characteristics free of capacitances due to extra charges by organic vapors and other impurities. UV-ozone treatment improves the characteristics in terms of working potential and sensitivity (Figure 4.7).

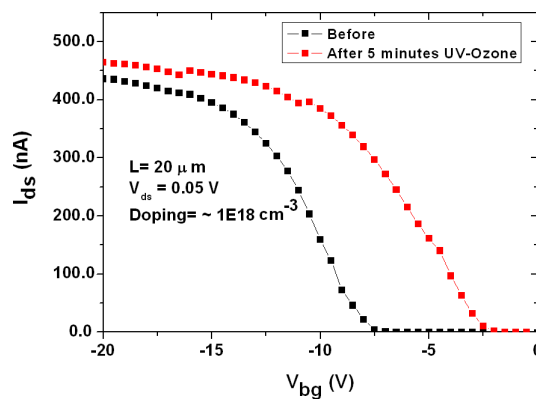


Figure 4.7 UV-ozone treatment of Si-NW oxide surface, measured in air.

Following the UV-Ozone treatment, the back gate “turn-on” voltage clearly shifts in the positive direction from $V_{bg} = -7.5 \text{ V}$ to $V_{bg} = -2.5 \text{ V}$, which we interpret as a reduction in oxide surface charge due to contamination and UV irradiation anneals the oxide space charge; however, prolonged exposure to UV can degrade devices by creating surface

states at the Si/SiO₂⁹

4.3.3. Hydrogen termination

Etching the Si-NW surface oxide with 1% HF for 1-2 minutes terminates the surface with hydrogen atoms and the resulting surface may be stable in laboratory environment for few minutes to few hours, especially hydrogen terminated Si-NWs which can show extra stability compared to planar samples.¹ Figures 4.8a and 4.8b show Si-NW characteristics (V_{bg} - I_{ds}) before and after etching in 1% HF. After etching a small non-zero current showing a “normally on” device however, the maximum current dropped by more than two orders of magnitudes as compare to non-etched device which indicate the depletion of the channel probably due to positive surface charge density or increase in interface state density. It is reported that after an HF dip, hydrogen ions stay on the silicon nanowire surface depleting the p-type channel but after a week at room temperature or after heating the chip at 180 °C for a minute, hydrogen ion desorbs as H₂ gas with the recovery of channel conductance, see Figure 4.9.¹⁰

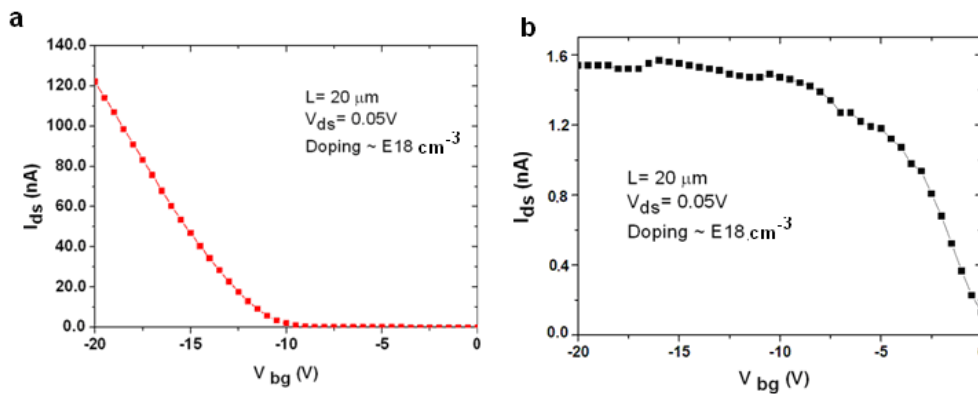


Figure 4.8 Silicon nanowire device a) before and b) after etching with 1% HF, measured in air. (Each data point in an average of 10 data points).

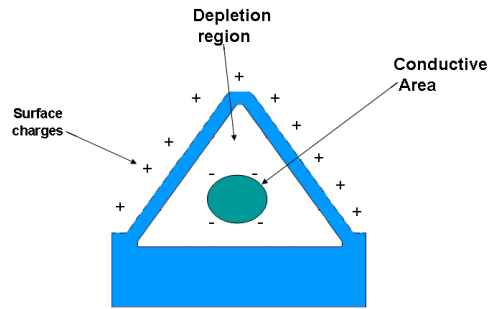


Figure 4.9 Schematic diagram of a p-doped nanowire with positive surface charges after etch and depleted region.¹⁰

Lagally's group¹¹ have studied the effect of HF etching on the charge transport properties of ultrathin films and found that after the first 13 minutes of HF etching including a substantial rinse in water for 5 minutes, a thin sheet of silicon (as thin as 27 nm, p-doped silicon 10^{-15} cm^{-3} SOI (001)) conductance increases nearly four times higher than as expected from estimated based on doping concentration. They showed that HF etching moves the Fermi level close to conduction band minimum, resulting in an inversion from the initially p-type to an n-type surface layer and this is the reason for a large drop in sheet resistance. By comparing their results to the extent of band bending caused by HF etch in thicker bulk samples; it is revealed that electronic properties of ultra thin films (less than 220 nm) are highly dependent and sensitive to the surface environments. We have measured similar effects as the Si-NW lateral dimensions are reduced below ~ 100 nm. Post etching species found on the silicon surfaces also include F and OH as well and their concentration exhibits a marked dependence of on both the HF concentration and the rinse time after the HF dip. The F and OH coverages are reduced and increased, respectively. Rinsing the samples in water after the HF treatment lowers the F coverage via substitution reaction $\text{Si-F} + \text{H}_2\text{O} \longrightarrow \text{Si-OH} + \text{HF}$, consequently increasing the number of OH groups on the surface.¹¹ Removal of moisture using a vacuum vessel during measurements was adopted serving two purposes. First, the oxidation rate of the surface is significantly reduced, allowing measurement of a large data set with only minor changes in the

surface condition. Second, a reduced pressure removes ambient water to allow comparison with the sheet resistance measurements that were taken in a dry atmosphere however, reduced the conductivity for n-type silicon which was otherwise high due to accumulation effect for carriers¹¹ where as it might substantially deplete a channel of p-type nanowire. A relatively more recent report shows that controlled adsorption of water under vacuum invert the p-type channel to n-type, however influence of HF treatment as well as pumping of moisture on conductivity is only prominent for thinner sheets/ Si-NWs and for low doping level. Figure 4.10 shows effects of different surface treatments on silicon nanowire characteristics in ambient air. It is noticed that measuring the Si-NW characteristics again and again on the same device also shifts the voltage to negative side due to charge build up in the long floating gate structure with no direct front gate electrode. It might be due to the effect of positive mobile oxide charges Q_m gathering near the surface after repeated measurements. Etching of the surface reduces the drain current; however, after two days in the laboratory environment current reappears with reduced slope. Treatment of etched surface for 10 minutes with UV-ozone also shows nearly the same effect probably due to the oxidative passivation and increased interface states due to prolonged UV treatment.^{9, 12}

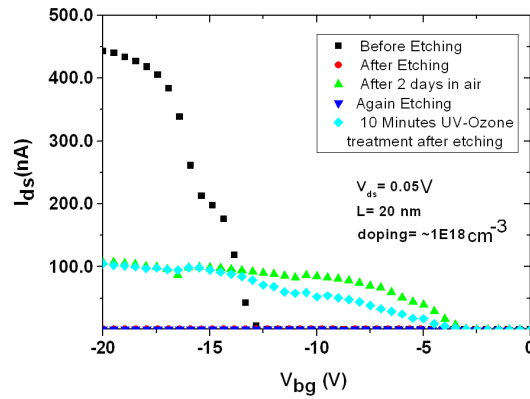


Figure 4.10 Silicon nanowire back gating in air; effect of different surface treatments on the Si-NW characteristics.

Figure 4.11 shows measured liquid front-gating (I_{ds} - V_{ref}) characteristics of a Si-NW device before and after etching in 1% HF solution for different times.

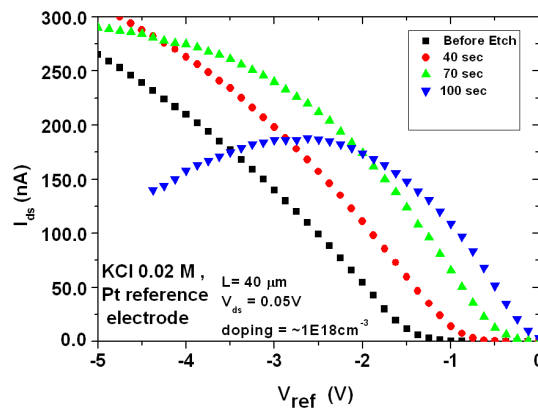


Figure 4.11 Si-NW front gating in aqueous solution before and after etching for different times.

Etching of Si-NW surface improves the characteristics in terms of drain-current (I_{ds}) and the slope up to 100 seconds of etching and device starts working at $V_{ref} = 0V$ however, scanning at larger negative voltages, the current (I_{ds}) suddenly drops probably

due to the breakdown of the hydrogen terminated surface and creation of unpassivated sites and dangling bonds or partial oxidation in aqueous solution.

4.4. Conclusion

Surface preparation of the active gate regions of Si-NW FET devices is a first step for further surface modification of the sensor. Hydrogen termination with etchants such as 1% HF, oxygen rich 40% NH_4F and nitrogen purged 40% NH_4F induce different morphologies to the silicon surface that also affect the extent of stability of as-prepared surfaces and dictate the quality of further modification and sensing performance. SEM, AFM and XPS was used to characterize silicon surfaces. The current-voltage ($I_{\text{ds}}-V_{\text{ds}}$) characteristics of Si-NW devices were studied in air (back-gating) and in aqueous solution (Front gating using a pseudo reference electrode). Different surface treatments such as UV-Ozone exposure and hydrogen termination affects device characteristics by altering the device working voltage as well as altering the slope of the curve. Surface etching of oxide depletes the Si-NW channel in air probably due to positive surface charges left behind on the surface. A controlled environment such as a glove box is recommended to make all surface preparation as clean and efficient as possible.

4.5. Bibliography

1. Peng, C.; Gao, J.; Wang, S.; Zhang, X.; Zhang, X.; Sun, X., Stability of Hydrogen-Terminated Surfaces of Silicon Nanowires in Aqueous Solutions. *J Phys Chem C* 115, (10), 3866-3871.
2. Curreli, M.; Zhang, R.; Ishikawa, F. N.; Chang, H. K.; Cote, R. J.; Zhou, C.; Thompson, M. E., Real-Time, Label-Free Detection of Biological Entities Using Nanowire-Based FETs. *IEEE Trans on Nanotech* **2008**, 7, (6), 651-667.
3. Masood, M. N.; Chen, S.; Carlen, E. T.; van den Berg, A., All-(111) Surface

Silicon Nanowires: Selective Functionalization for Biosensing Applications. *ACS Appl Mater Interfaces* **2010**, 2, (12), 3422-3428.

4. E. H. Nicollian, J. R. B., *MOS (Metal Oxide Semiconductor) Physics and Technology*. Wiley: New York, 1982.
5. Sieval, A. B.; Linke, R.; Zuilhof, H.; Sudholter, E. J. R., High-quality alkyl monolayers on silicon surfaces. *Adv Mater* **2000**, 12, (19), 1457-1460.
6. Chen, S.; Bommer, J. G.; van der Wiel, W. G.; Carlen, E. T.; van den Berg, A., Top-Down Fabrication of Sub-30 nm Monocrystalline Silicon Nanowires Using Conventional Microfabrication. *ACS Nano* **2009**, 3, (11), 3485-3492.
7. Bae, S. E.; Lee, J. S.; Lee, I. C.; Song, M. B.; Lee, C. W. J., Behavior of hydrogen-terminated Si(111) surface in oxygen-dissolved NH₄F solution with or without Cu(II) ions. *Bull Korean Chem Soc* **2005**, 26, (11), 1891-1894.
8. Wade, C. P.; Chidsey, C. E. D., Etch-pit initiation by dissolved oxygen on terraces of H-Si(111) (vol 71, pg 1679, 1997). *Appl Phys Lett* **1998**, 72, (1), 133-133.
9. Snow, E. H.; Grove, A. S.; Fitzgerald, D. J., Effects of ionizing radiation on oxidized silicon surfaces and planar devices. *Proc IEEE* **1967**, 55, (7), 1168-1185.
10. Kimukin, I.; Islam, M. S.; Williams, R. S., Surface depletion thickness of p-doped silicon nanowires grown using metal-catalysed chemical vapour deposition. *Nanotechnology* **2006**, 17, (11), S240-S245.
11. Scott, S. A.; Peng, W.; Kiefer, A. M.; Jiang, H.; Knezevic, I.; Savage, D. E.; Eriksson, M. A.; Lagally, M. G., Influence of Surface Chemical Modification on Charge Transport Properties in Ultrathin Silicon Membranes. *ACS Nano* **2009**, 3, (7), 1683-1692.
12. Fink, C. K.; Nakamura, K.; Ichimura, S.; Jenkins, S. J., Silicon oxidation by ozone. *J Phys Cond Matter* **2009**, 21, (18).

Chapter 5

Selective biofunctionalization of all-(111) surface silicon nanowires

Here we demonstrate the utilization of carbon-silicon (C-Si) alkyl and alkenyl monolayers covalently linked to all-(111) surface silicon nanowire (Si-NW) for selective functionalization for biosensing. Commercially available protected amines were used for this purpose. Terminal amine groups on the functional monolayer surfaces were used for conjugation of biotin n-hydroxysuccinimide ester. The monolayer was characterized by contact angle and X-ray photoelectron spectroscopy (XPS). The selective functionalization on Silicon nanowires was demonstrated by high-resolution scanning electron microscopy (SEM) of 5 nm diameter thiolated Au nanoparticles linked with streptavidin and conjugated to the biotinylated all-(111) surface Si-NWs. Electrical measurements of monolayer passivated Si-NWs show improved device behavior and performance.¹

¹*This chapter has been modified from a published paper:
Masood, M. N.; Chen, S.; Carlen, E. T.; Van den Berg, A. ACS Appl Mater Interfaces, 2010, 2,(12), 3422.*

5.1. Introduction

Si-NW FET biosensors have been reported extensively for the highly sensitive, label-free, and real time detection of biomolecular binding of ssDNA, proteins, and viruses.^{1, 2, 3, 4} The high detection sensitivity of Si-NW biosensors has been attributed to the large surface-to-volume ratio and the three-dimensional multi-gate structure; both contribute to the improved sensitivity compared to conventional planar devices.⁵ In this chapter, we present a new Si-NW biosensor platform consisting of our recently reported all-(111) surface Si-NWs⁶ with a heterogeneous alkyl and alkenyl monolayer interfaces that are suitable for functionalization with any biomolecular moiety,⁷ and therefore, provides improved selectivity and sensitivity compared to conventional Si-NW biosensors. Figure 5.1a shows an example of the Si-NW biosensor measurement configuration. The front-gate voltage V_{fg} with reference electrode and back-gate voltage V_{bg} control the operating point of the sensor. The Si-NW channel conductance is defined as $G_c = \partial i_{ds} / \partial v_{ds} |_{V_{fg}, V_{bg}}$, where i_{ds} and v_{ds} are the NW drain-to-source current and applied voltage, respectively. Biosensing is achieved when molecular binding at the sensing surface induces a surface potential change $\Delta\psi_o$ that results in a measurable conductance change ΔG_c via a field-effect across the dielectric layer (Fig. 5.1a). The transformation of a nanowire (FET) into a biosensor requires surface functionalization, such that biologically active ligands⁸ are conjugated to the sensor surface.^{9, 10} Conventional Si-NW biosensors have the ligand attached directly to the SiO₂ sensor surface using silane-based attachment chemistry. However, conjugating to the SiO₂ layer reduces the sensor selectivity because the entire substrate surface is most often a homogeneous oxide surface. Figure 1b shows a cross-section (A-B, Figure.5.1a) of a triangular Si-NW with conventional non-selective functionalization as the ligands cover the entire homogeneous surface, which drastically reduces the number of analyte that are available to bind to the sensing surface. Figure 5.1c shows a selectively

functionalized Si-NW biosensor where the ligands are conjugated exclusively to the silicon surface and the entire surface is heterogeneously functionalized.

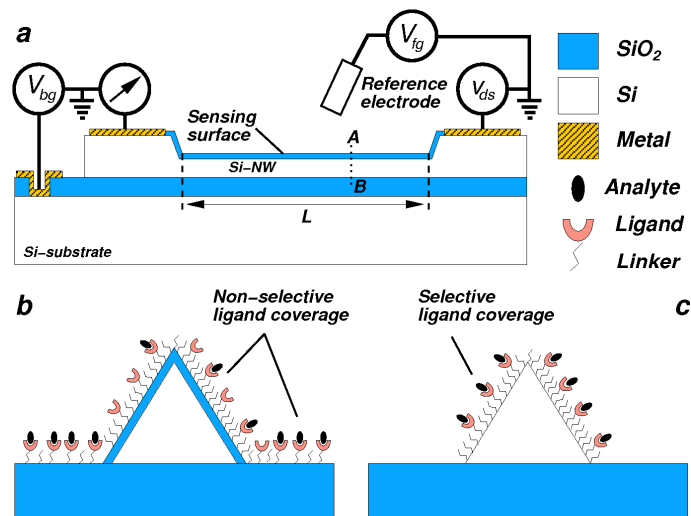


Figure 5.1 Si-NW biosensor configurations. (a) Biosensor with control voltages and current measurement, (b) Conventional non-selective homogeneous surface, (c) Selective heterogeneous functionalization with ligands conjugated exclusively to the Si-NW sensor.

It is well known that the Si (111) surface is preferred for the covalent alkylation of organic monolayers due to the surface atomic arrangement, which leads to densely packed layers and low density of dangling bonds.^{11, 12, 13, 14} However, existing reports of alkyl monolayer formation on Si-NWs have been conducted on a mixture of surface orientations due to limitations in fabrication technology.² Figures 5.2a-5.2d show cross-sections of commonly reported Si-NW shapes and the corresponding surface crystal orientation of the exposed facets, which is dependent on the fabrication technology. Bottom-up vapor-liquid-solid (VLS) synthesis of Si-NWs has been reported to have hexagonal cross-sections consisting of a mixture of surface orientations (Fig. 5.2a).¹⁵

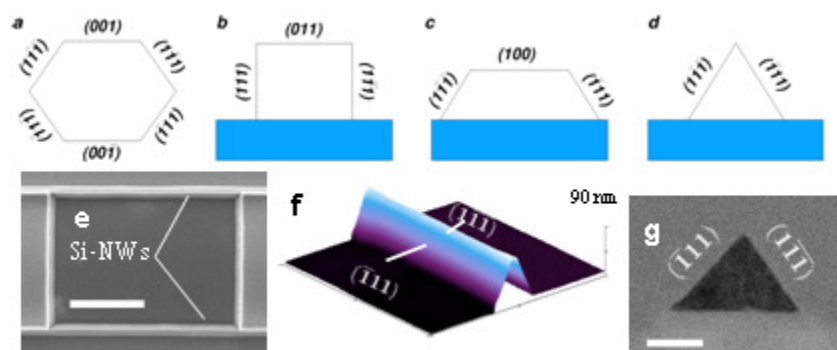


Figure 5.2 Ideal Si-NW fabrication dependent cross-section shapes (a-d). (a) Bottom-up VLS synthesized, (b) Top-down rectangular, (c) Top-down trapezoidal, and (d) Top-down triangular. Fabricated all-(111) surface Si-NWs (e-f). (e) High-resolution scanning electron microscopy (HRSEM) image of triangular Si-NWs (scale bar: 1 μm) (f) Tapping-mode atomic force microscopy image of single Si-NW (NW height: 90 nm) (g) High-resolution transmission electron microscopy image of Si-NW cross-section (scale bar: 20 nm).

Direct covalent bonding of organic molecules to reconstructed silicon surfaces can be done using ultra-high vacuum (UHV) or via wet methods using hydrogen and halogen terminated surfaces.¹⁶ Carbon-silicon coupling reactions performed using wet chemistry methods are very attractive due to the simple apparatus required and the high reaction rates due to the presence of high reactant fluxes in solution; however, careful control of surface oxidation and cleanliness is required. The first step in forming a covalent C-Si bond is the formation of stable H-Si surfaces, which is most often done by removing the native oxide on the silicon surface with hydrofluoric acid (HF) and followed by ammonium fluoride (NH_4F) etching the silicon surface. Once a stable H-Si surface has been formed, the C-Si monolayer can be formed with an appropriate precursor and a free radical initiation using ultraviolet (UV) irradiation, heating, electrochemical reaction, transition metal complexes, or Lewis acid catalysts.¹⁷ There are many reports of C-Si monolayer formation on H-Si surfaces using different methods, such as a refluxed precursor solution of 1-hexadecene in mesitylene,¹⁸ neat solution and UV-irradiation,¹⁹ and a two-step hydrosilylation reaction with Grignard reagents. Monolayers formed with Grignard reagents may impart unwanted metal

contaminants to the surface. Monolayers formed by Lewis acid catalysis involve lower surface coverage as compared to the coverage obtained by heating, photochemical irradiation and Grignard reaction schemes.

5.2. Experimental

5.2.1. Surface preparation and monolayer formation

The samples were first cleaned to remove organic and metal impurities. The p-type planar Si (111) samples were cleaned with acetone and sonicated (10-20 min) and etched in 1% HF (1-2 min) to remove the native oxide. Etched silicon samples were rinsed with deionized H₂O and further cleaned with piranha solution (H₂O₂ 30%, H₂SO₄ in 1:1 ratio) at 90 °C for 10 min and rinsed thoroughly with dH₂O. This procedure was repeated three times. The contact angle of the resultant surface was found to be zero, for contact angle of different surfaces see Table 5.1.

Table 5-1 Measured contact angles of Si (111) surfaces after various treatments.

Surface	Contact angle (°)
piranha treated silicon	~0
hydrogen terminated silicon	84±4
alkyl-phthalimide monolayer	75±5
amine terminated monolayer	60±4
native oxide (new wafer)	50±5
1-octadecene (C ₁₈) monolayer	109±2

The p-type Si-NW samples were first cleaned with methanol, isopropanol, acetone and acetonitrile with low power sonication (5-20 min). The Si-NW samples were further cleaned with oxygen plasma (100 W, 10 min). Silicon nanowire and planar samples were etched with 1% HF and NH₄F for 4-5 min and then rinsed thoroughly with

deionized H₂O and placed into a custom-made vacuum vessel and the surface dried with a combination of vacuum (~1 mTorr) and heating with an infrared lamp (Scheme 5.1a). The vacuum vessel, Figure 5.3 continuously purged with argon during the drying step.

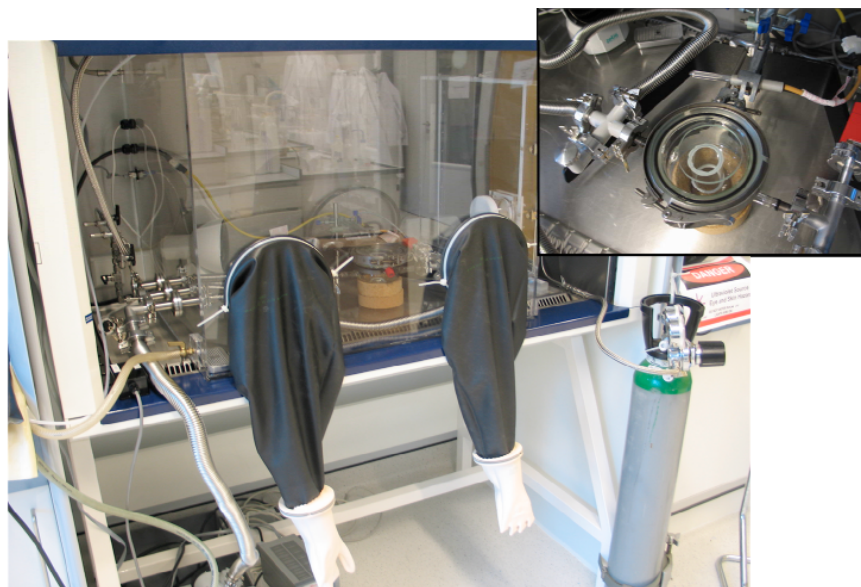


Figure 5.3 Monolayer reaction Apparatus. Glove box with positive pressure (N₂). Upper inset: Vacuum Chamber backfilled with Ar for low oxygen content monolayer formation.

A thin layer of precursor solution was deposited onto the samples and irradiated for 4 hours with a UV lamp (4.4 mW/cm² at 254 nm, Jelight Co., USA). The 40% NH₄F etchant and 0.2 M precursor solution in mesitylene were bubbled with pure argon gas for 1 hour before the hydrosilylation reaction. After the hydrosilylation reaction, the samples were exposed to ambient air and sonicated with dichloromethane, chloroform, methanol, and acetonitrile.

5.2.2. AFM imaging

A Digital Instruments Dimension 3100 was used for all AFM images. All AFM images performed in tapping mode with ultra sharp (average tip diameter ~2 nm) single crystal silicon tips (SSH-NCH-10, NanoandMore, GmbH).

5.2.3. XPS characterization

XPS characterization has been conducted with a monochromatic X-ray beam (Al K α , 1486.6 eV, 100W, Quantera, Physical Electronics). Mapping was done at 3×10^{-9} Torr and detector angles of 70° and 45° . XPS spectra were taken just after monolayer formation or after storage in a dry nitrogen box.

5.2.4. HRSEM imaging

For deprotection of the phthalimide groups, samples were placed in a 30% methylamine solution in ethanol for 3-6 hr (Scheme 5.1c). Following the reaction, the samples were rinsed with triethylamine and ethanol, and subsequently nitrogen dried. Activated biotin (Sigma Aldrich) was conjugated to the amine-terminated surfaces by placing the samples in a 3 mM solution of activated biotin/DMF for two hours at room temperature. After the reaction they were sonicated in DMF, ethanol, and acetone (5-10 min.). Gold nanoparticles conjugated with streptavidin (0.25 ml streptavidin conjugated Au nanoparticles in solution (5 nm average diameter, Ted Pella, Inc. USA) was diluted to 100 ml of solution by adding 20 mM Tris buffer, 154 mM NaCl, and deionized H₂O. The biotinylated surfaces were immersed with the labeling solution for 12 hours at room temperature. Monolayers prepared by 1-octadecene do not include a deprotection step and biotinylation.

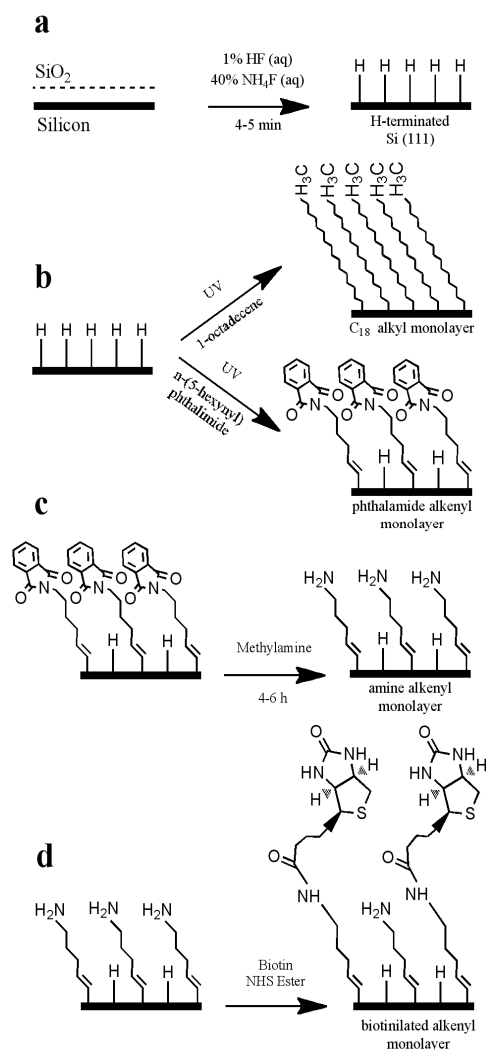
5.2.5. Electrical measurements

Si-NW devices were first encapsulated with a polyimide layer (thickness: 2 μ m), followed by wire-bonding to a custom printed circuit board and finally all electrical

wires and contacts were sealed with an epoxy (Hysol, Henkel Corporation). Following encapsulation, the Si-NW oxide surfaces were cleaned with UV ozone (UV/Ozone Pro Cleaner, Bioforce, Inc.). The monolayers were formed as previously described following the removal of the gate oxide. Electrochemical measurements were done in a 10 mM universal buffer mixture (UBM) (0.1 M citric acid, 0.1 M sodium dihydrogen phosphate, 0.2 M boric acid, and 0.1 M NaCl) at pH 2.8. The CV measurements were recorded with an impedance analyzer (Hewlett-Packard 4194A Impedance Gain-Phase Analyzer) at a frequency of 10 kHz and the front-gate voltage, using a reference electrode (REF200 Ag/AgCl, Radiometer Analytical) was swept from $-5 \text{ V} \leq V_{fg} \leq +2 \text{ V}$. The IV characteristics of the Si-NWs was measured with a lock-in amplifier (SR830, Stanford Research Systems) with $v_{ds}=50 \text{ mV}$, 30 Hz modulation frequency and $V_{bg}=0$. A reference electrode (REF200 Ag/AgCl, Radiometer Analytical) in 10 mM UBM at pH 2.8 buffer solution and the applied the front-gate voltage and was swept from $-1.5 \text{ V} \leq V_{fg} \leq 0 \text{ V}$ for oxide passivated devices and swept from $-0.4 \text{ V} \leq V_{fg} \leq 0 \text{ V}$ for the alkenyl monolayer passivated Si-NW devices.

5.3. Results and discussion

Two types of C-Si monolayers on H-Si (111) surfaces were formed using photochemical UV hydrosilylation based on the high reactivity of the C=C bond to the hydrogen terminated silicon promoted by the cleavage of the H-Si at room temperature.



Scheme 5.1 C-Si (111) monolayer formation. (a) Si-H surface formation: remove native SiO₂ with 1% HF (aq) followed by surface preparation with 40% NH₄F (aq) (b) Hydrosilylation UV reaction forming C₁₈ alkyl and phthalimide alkenyl monolayers (c) Deprotection of amine terminal groups (d) Conjugate biotin to amine groups.

First, a C₁₈ alkyl monolayer with methyl end groups was formed from a 1-octadecene precursor. The second monolayer consists of amine-terminated (-NH₂) alkenyl monolayer from an n-(5-hexynyl) phthalimide precursor. The H-Si surface is

first formed followed by the UV initiated hydrosilylation with 1-octadecene and n-(5-hexynyl) phthalimide precursors to form the different monolayers. Following removal of the phthalimide groups (deprotection) with a methylamine solution, an amine terminal group (NH_2) was released for further conjugation.

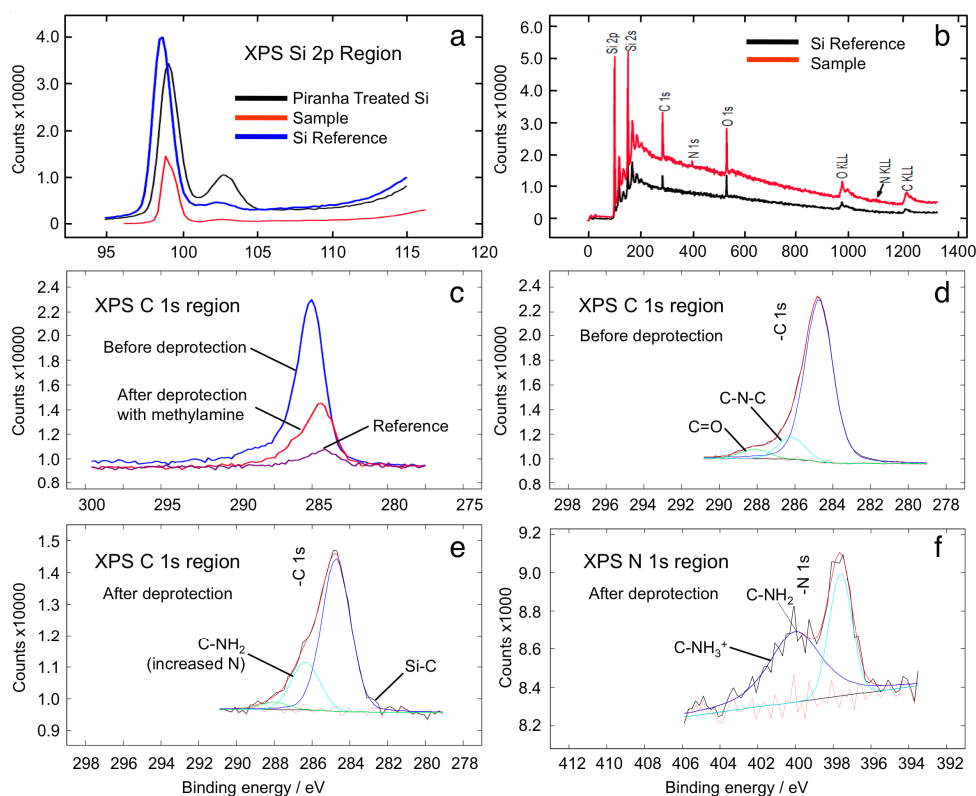


Figure 5.4 XPS results. (a) Si 2p region (peak at 103 eV) shows oxidation of the silicon surface (b) Survey spectrum of phthalimide monolayer on Si (111) surface (red) and silicon reference sample (black) (c) C1s region of the spectrum showing a comparison before and after deprotection (d, e) C1s region shows fit for different functional bonds in the monolayer before and after deprotection (f) N1s region after deprotection.

The quality of the as-prepared monolayers was verified by using sessile drop contact angle measurements Table 1, and XPS on planar samples. A measured contact angle of 109° for the C18 alkyl monolayer indicates a high quality ordered monolayer on our

planar and Si-NW surfaces. The XPS spectra were taken just after monolayer formation or after storage in dry nitrogen. Figure 5.4 shows representative XPS data for experimental samples. An etched piece of silicon was used as a reference. Figure 5.4a shows that the oxidation (peak at 103 eV) of the silicon surface exposed to UV irradiation for monolayer formation (red) comparable to the H-Si reference (blue) and sufficiently lesser than native oxide of piranha treated sample (black) respectively. A survey spectrum of a phthalimide alkenyl monolayer on Si (111) (Fig. 5.4b) shows the expected elements (Si, C, N, and O) indicating a clean contamination free surface. The silicon reference shows a small amount of carbon deposited on the surface, however, not the N1s peak (at 400 eV) thus discriminating the Phthalimide monolayer. Figure 4c shows XPS spectra of the C1s region before and after deprotection where deprotection of the surface Phthalimide moieties exposes the NH₂ functional groups for further conjugation (Fig. 5.4c). The monolayer following deprotection shows that the overall area percentage of C-N peak (286.57 eV) increases compared to the area of C-C (284.77 eV) as the carbon number decreased from 14 to 6 (Figs. 5.4d, before and 5.4e, after deprotection). The peak at 288.55 eV (C=O) is expected to disappear after deprotection, but shows a decrease in percent area due to partial deprotection or some physically adsorbed C=O moieties on the surface (Fig. 5.4e). Figure 5.4f shows XPS results from the N1s region of the spectrum following deprotection showing amine groups NH₂ and in the ammonium form NH³⁺ from the monolayer. High resolution scanning electron microscopy was used to image the selective conjugation of thiolated Au nanoparticles coupled to the biotinylated Si-NW surfaces.

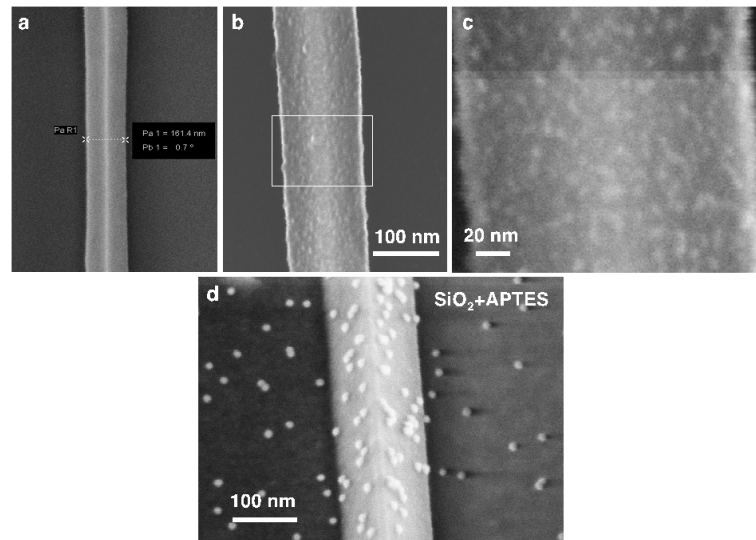


Figure 5.5 HRSEM images. (a) Blank Si-NWs (b) Si-NW surfaces following the conjugation of 5 nm diameter Au nanoparticles (scale bar: 100 nm) (c) zoomed image of Si-NW surface (scale bar: 20 nm). (d) Si-NW surfaces following the conjugation of 15 nm diameter nanoparticles after an APTES (3-aminopropyl triethoxy silane) monolayer showing non-selective functionalization.

As previously described, this step requires the removal of the phthalimide protection groups to provide access to the NH_2 functional groups. Activated biotin was then conjugated to the NH_2 -terminated surfaces. Gold nanoparticles conjugated with thiolated-streptavidin were then coupled to the biotinylated surfaces. Figure 5.5a shows an HRSEM image of a non-conjugated Si-NW. Figure 5.5b shows the selective conjugation of the Au nanoparticles to biotinylated all-(111) Si-NWs, and Fig. 5.5c a zoomed image of the Si-NW surface. Figure 5.5d shows a silicon nanowire with thermally grown oxide conjugated with 3-amino propyl triethoxy Silane (APTES) monolayer. Amine terminal of APTES layer was further conjugated with activated biotin and streptavidin–gold (15 nm). Electrical characteristics have been measured using two different device configurations: capacitance-voltage (*CV*) characteristics of monolayer passivated electrolyte-insulator-silicon (EIS) structure with (111) surface planar silicon samples (Fig. 5.6a) and current/front-gate voltage (*IV*) characteristics of

Si-NWs with oxide and alkenyl monolayer dielectric layers (Fig. 5.6b). The high frequency CV measurements demonstrate that the monolayer surfaces are uniformly passivated with an estimated monolayer thickness $t_m \approx 3 \text{ nm}^{20}$, where $\epsilon_m \approx 2$ is the relative permittivity of the monolayer²¹ and A_c is the capacitor area. The most striking device performance improvement of monolayer passivated Si-NWs, compared to oxide passivated surfaces, is that the monolayer interfaces have improved electrical performance (Fig. 5.6b), where device conductance can be modulated with very small front-gate voltages for $N_a \sim 10^{17} \text{ cm}^{-3}$, which is not possible with the oxidized Si-NWs without back-gating. The monolayers do not completely eliminate the interface effects as the measured device current with $V_{fg}=0$ is $i_{ds} \approx 2 \text{ nA}$, which is lower than the ideal current $i_{ds} \approx 6 \text{ nA}$.²² The alkenyl monolayer passivated devices also show improved transconductance of $g \approx 63 \text{ pA mV}^{-1}$ compared to 36 pA mV^{-1} for a 10 nm oxide passivated Si-NW surface. The detection sensitivity is $\Delta G/G_o \approx 0.32$ for the alkenyl monolayer passivated Si-NWs with $h=100 \text{ nm}$ compared to 0.04 for the oxidized Si-NW, a $\sim 10\times$ increase.²²

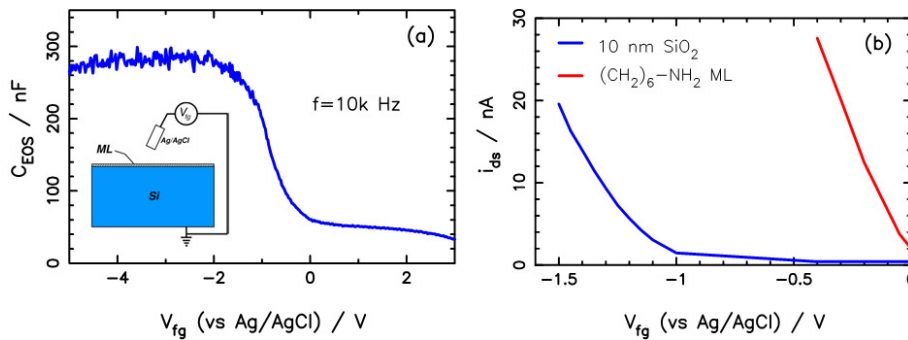


Figure 5.6 Electrical measurements (a) high frequency CV behavior of EIS structure with C_{18} monolayer passivation (b) IV characteristics of Si-NWs with oxide (blue) and alkenyl monolayer (red) dielectric layers.

5.4. Conclusion

The selective functionalization of C-Si monolayers on all-(111) surface Si-NWs has been demonstrated, which offers a new Si-NW sensing platform with several advantages for biosensing compared to conventional Si-NW biosensor geometries and silicon dioxide (SiO₂) passivation layers, which includes: 1. Ligands conjugated exclusively on the nanowire surface eliminates ligand conjugation in non-sensor regions, 2. Improved detection sensitivity due to selective functionalities, 3. Si-(111) surfaces support the highest quality C-Si monolayers. 4. Elimination of fixed SiO₂ charge, and 5. Si (111) surfaces can have low interface trap densities for H-Si and C-Si interfaces.

5.5. Bibliography

1. Cui, Y.; Wei, Q.; Park, H.; Lieber, C. M., Nanowire nanosensors for highly sensitive and selective detection of biological and chemical species. *Science* **2001**, 293, (5533), 1289-1292.
2. Bunimovich, Y. L.; Shin, Y. S.; Yeo, W. S.; Amori, M.; Kwong, G.; Heath, J. R., Quantitative real-time measurements of DNA hybridization with alkylated nonoxidized silicon nanowires in electrolyte solution. *J Am Chem Soc* **2006**, 128, (50), 16323-16331.
3. Gao, Z.; Agarwal, A.; Trigg, A. D.; Singh, N.; Fang, C.; Tung, C. H.; Fan, Y.; Buddharaju, K. D.; Kong, J., Silicon nanowire arrays for label-free detection of DNA. *Anal Chem* **2007**, 79, (9), 3291-3297.
4. Patolsky, F.; Lieber, C. M., Nanowire nanosensors. *Mater Today* **2005**, 8, (4), 20-28.
5. Wanekaya, A. K.; Chen, W.; Myung, N. V.; Mulchandani, A., Nanowire-based electrochemical biosensors. *Electroanalysis* **2006**, 18, (6), 533-550.
6. Chen, S.; Bomer, J. G.; Van der Wiel, W. G.; Carlen, E. T.; Van Den Berg, A., Top-down fabrication of sub-30 nm monocrystalline silicon nanowires using conventional microfabrication. *ACS Nano* **2009**, 3, (11), 3485-3492.
7. Buriak, J. M., Organometallic chemistry on silicon and germanium surfaces. *Chem*

Rev **2002**, 102, (5), 1271-1308.

8. A ligand refers to a receptor biomolecule attached to the sensor surface. An analyte refers to the complementary biomolecule in the solution. A ligand-analyte pair is a selectively hybridized biomolecular conjugate.

9. Van Der Voort, D.; McNeil, C. A.; Renneberg, R.; Korf, J.; Hermens, W. T.; Glatz, J. F. C., Biosensors: Basic features and application for fatty acid-binding protein, an early plasma marker of myocardial injury. *Sens and Actuat, B: Chemical* **2005**, 105, (1), 50-59.

10. Bunimovich, Y. L.; Ge, G.; Beverly, K. C.; Ries, R. S.; Hood, L.; Heath, J. R., Electrochemically programmed, spatially selective biofunctionalization of silicon wires. *Langmuir* **2004**, 20, (24), 10630-10638.

11. Samares, K.; Miramond, C.; Vuillaume, D., Properties of electronic traps at silicon/1-octadecene interfaces. *Appl Phys Lett* **2001**, 78, (9), 1288-1290.

12. Weldon, M. K.; Queeney, K. T.; Eng Jr, J.; Raghavachari, K.; Chabal, Y. J., The surface science of semiconductor processing: Gate oxides in the ever-shrinking transistor. *Surf Sci* **2002**, 500, (1-3), 859-878.

13. Leao, C. R.; Fazio, A.; Da Silva, A. J. R., Si nanowires as sensors: Choosing the right surface. *Nano Lett* **2007**, 7, (5), 1172-1177.

14. Scheres, L.; Giesbers, M.; Zuilhof, H., Organic monolayers onto oxide-free silicon with improved surface coverage: Alkynes versus alkenes. *Langmuir* **2000**, 16, (24), 4790-4795.

15. Wu, Y.; Cui, Y.; Huynh, L.; Barrelet, C. J.; Bell, D. C.; Lieber, C. M., Controlled growth and structures of molecular-scale silicon nanowires. *Nano Lett* **2004**, 4, (3), 433-436.

16. Bent, S. F., Organic functionalization of group IV semiconductor surfaces: Principles, examples, applications, and prospects. *Surf Sci* **2002**, 500, (1-3), 879-903.

17. Puniredd, S. R.; Assad, O.; Haick, H., Highly stable organic monolayers for reacting silicon with further functionalities: The effect of the C-C bond nearest the silicon surface. *J Am Chem Soc* **2008**, 130, (41), 13727-13734.

18. Sieval, A. B.; Linke, R.; Zuilhof, H.; Sudholter, E. J. R., High-quality alkyl monolayers on silicon surfaces. *Adv Mater* **2000**, 12, (19), 1457-1460.

19. Cicero, R. L.; Chidsey, C. E. D.; Lopinski, G. P.; Wayner, D. D. M.; Wolkow, R. A., Olefin additions on H-Si(111): Evidence for a surface chain reaction initiated at isolated

dangling bonds. *Langmuir* **2002**, 18, (2), 305-307.

20. The monolayer thickness has been estimated with $t_m \approx \epsilon_m \epsilon_o A_c / C_{EOS}$, with $A_c = 0.5 \text{ cm}^2$.

21. Gorostiza, P.; de Villeneuve, C. H.; Sun, Q. Y.; Sanz, F.; Wallart, X.; Boukherroub, R.; Allongue, P., Water exclusion at the nanometer scale provides long-term passivation of silicon(111) grafted with alkyl monolayers. *J Phys Chem B* **2006**, 110, (11), 5576-5585.

22. The maximum ideal current in the undepleted triangular is $i_{ds} \approx q \mu_b N_a v_{ds} L^{-1} w h / 2$ with $\mu_b \approx 300 \text{ cm}^2 \text{ V}^{-1} \text{ s}^{-1}$, $N_a = 10^{17} \text{ cm}^{-3}$, $v_{ds} = 100 \text{ mV}$, $L = 10 \text{ }\mu\text{m}$, $h = 100 \text{ nm}$, and $w = 2h / \tan(54.74^\circ)$ where μ_b is the concentration dependent hole mobility.

Chapter 6

Mathematical modeling of thin gate dielectrical layers of silicon nanowires and their sensitivity

An analytical model is presented to demonstrate the improvement in detection sensitivity of the alkyl and alkenyl passivated all-(111) Si-NW biosensors compared to conventional nanowire biosensor geometries and silicon dioxide passivation layers as well as interface design and electrical biasing guidelines for depletion-mode sensors. Mathematical analysis revealed that thin dielectric layers result in higher detection sensitivities and three important conclusions can be drawn from this analysis. First, thin ($t_f \sim 1$ nm) dielectric layers in combination with low channel doping ($N_a = 10^{17} \text{ cm}^{-3}$) results in the largest detection sensitivity, however, over a small range of surface potential ψ_o (or surface charge σ_o), and therefore, requires precise front-gate biasing for full utilization. Second, thin dielectric layers and larger channel doping ($N_a = 10^{18} \text{ cm}^{-3}$) results in slightly lower and more uniform sensitivities. Lastly, a reference electrode is important for providing a well-defined gate potential for device biasing and operation. It should be noted that higher sensitivities can be obtained by moderately accumulating the front surfaces.²

² *This chapter has been modified:*
Masood, M. N.; Chen, S.; Carlen, E. T.; Van den Berg, A. *ACS Appl Mater Interfaces*, 2010, 2,(12), 3422.

6.1. Introduction

Silicon nanowire-field effect transistor (SiNW-FET) devices have been used as highly sensitive and efficient biosensors^{1,2} and interface between silicon nanowire and analyte solution (dielectric material, oxide) is the most crucial element in this regard. Silicon nanowires having diameter in nanometer ranges have very high sensitivity to surface charges as at such a nanoscale level most of the atoms are surface atoms due to high surface to volume ratios and all interactions are essentially surface interactions.³ Down scaling of silicon/semiconductor devices thus improves the sensitivity of detection but in order to improve the sensor performances further, addressing a good interface between active body of the sensor and aqueous environment is also very important. Detection sensitivity of ligand-analyte binding is dependent on the distance from the charged analyte to the silicon surface, which includes analyte, ligand, and linker (on an oxide in the conventional case).⁴ We have developed an analytical model of a depletion-mode Si-NW with triangular cross-section that is used to quantitatively estimate the detection sensitivity. The body of the depletion-mode Si-NW device (Fig. 6.1) doped with impurities results in a quiescent channel conductance $G_c = \mu_b L^{-1} Q_c$, where μ_b is the carrier mobility, L the length, and Q_c the charge per unit length ($Q_c > 0$ for p-type and $Q_c < 0$ for n-type).⁵

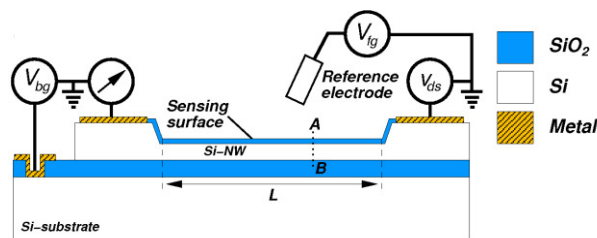


Figure 6.1 Biosensor with control voltages and current measurements.

6.2. Experimental

2D finite element simulations were performed using commercial simulation packages Tsuprem-4 Version C-2009.06 and Medici Version A-2007.12, Synopsys, Inc.

6.3. Results and Discussion

We have developed an analytical model of a depletion-mode Si-NW with triangular cross-section that is used to quantitatively estimate the detection sensitivity. As previously described, a surface potential change $\Delta\psi_0$ on the sensing surface induced by an electrical charge density change $\Delta\sigma_0$ near the sensing surface during molecular binding results in the field-effect modulation of the conduction cross-sectional area A_c (red hashed region, Fig. 6.2), and the channel conductance is modulated $G_c \pm \Delta G_c$ where $Q_c = qN_a A_c$, N_a is the doping concentration, which is assumed to be uniformly distributed.

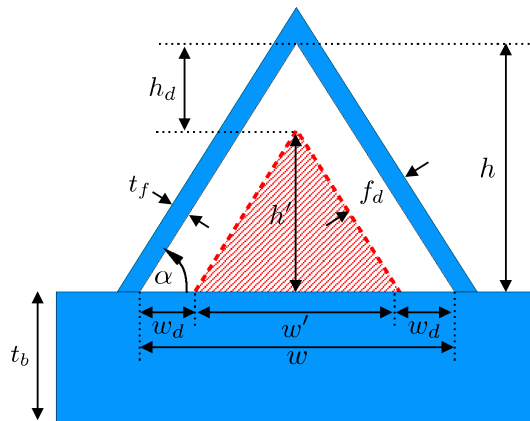


Figure 6.2 Ideal cross-section with conduction area A_c (red hashed) used to estimate the depletion-mode p-type Si-NW transconductance and sensitivity.

The conduction cross-sectional area A_c as a function of ψ_o can be derived by considering the triangular Si-NW cross-section, shown in Fig. 6.2, with width w , height h , base angle α , front oxide thickness t_f , buried oxide thickness t_b and depletion width f_d , which is a function of the oxide surface potential ψ_o . From Fig. 6.2, $A_c = w'h'/2$, where $w' = w - 2w_d$ and $h' = h - h_d$. The distances w_d and h_d are related to f_d using the geometry of the device cross-section: $w_d = f_d/\sin\alpha$ and $h_d = f_d/\cos\alpha$. The conductance cross-sectional area can then be written as a function of the depletion distance $A_c(f_d) = (w - 2f_d/\sin\alpha)(h - f_d/\cos\alpha)/2$. The depletion function can be approximated assuming a flat surface and the depletion approximation. From Fig. 6.1, we can apply Kirchoff's voltage law and sum the voltage drops across the device structure: $V_{fg} = V_{fb} + Q_s/C_d + \psi_s$, where V_{fb} is the flatband voltage, which is the potential required to completely undeplete the silicon layer, Q_s is the total charge in the silicon layer, C_d is the capacitance due to the dielectric layer on the silicon surface and ψ_s is the potential at the silicon surface. The depletion layer is $f_d = (2\epsilon_{si}\epsilon_o\psi_s/qN_a)^{1/2}$, which results in $\psi_s = f_d^2 qN_a / 2\epsilon_{si}\epsilon_o$. Since $Q_s = (2\epsilon_{si}\epsilon_o qN_a)^{1/2} f_d$, then we can write the general expression again as $V_{fg} = V_{fb} + (\epsilon_d\epsilon_o/t_f)(2\epsilon_{si}\epsilon_o qN_a)^{1/2} f_d + f_d^2 qN_a / 2\epsilon_{si}\epsilon_o$, which can be rewritten in terms of the depletion distance as $f_d^2 + 2(\epsilon_{si}/\epsilon_d)f_d t_f = 2(\epsilon_{si}\epsilon_o/qN_a)(V_{fg} - V_{fb})$ where the solution to the quadratic equation results in the depletion distance as a function dielectric thickness $f_d = [(t_f\epsilon_{si}/\epsilon_d)^2 + 2\epsilon_{si}\epsilon_o(V_{fg} - V_{fb})/qN_a]^{1/2} - t_f\epsilon_{si}/\epsilon_d$. The front-gate V_{fg} (Fig. 6.1) is used to set the operating point of the sensor and V_{fb} is the flat band voltage necessary to achieve flat energy bands at the silicon surface. Note that the back-gate control voltage V_{bg} does not appear in the conduction expression because we have assumed that the lower surface of the NW is not depleted and not electrostatically coupled to the front-gate. The flat band voltage is $V_{fb} = E_{ref} - \phi_{Si}/q - \psi_o - Q_i/C_i - \chi^{sol} - \Delta\chi$, where E_{ref} is the potential drop due to the reference electrode, ϕ_{Si} is the silicon work function, Q_i and C_i represent the insulator effective charge per unit area and capacitance, χ^{sol} is the surface dipole potential, and $\Delta\chi$ represents various potential drops at the interface. For

this analysis, we assume that V_{fg} completely compensates for the various potential drops and $V_{fg} - V_{fb} \approx \psi_o$ and the effects of interface states have been neglected. Figure 6.3 depicts hole depletion contours from a two-dimensional finite element simulation as the oxide surface potential is varied $\psi_o > 0$.

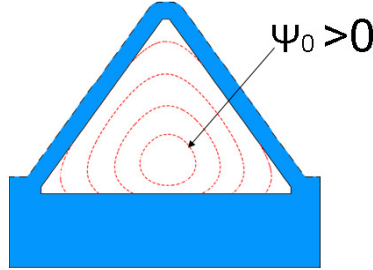


Figure 6.3 2D finite element simulation result of depletion region contours (red dashed lines the edge of depletion region) as $\psi_o > 0$.

Despite rounding of the potential contours near the sharp corners, the area modulation function $A_c(f_d)$ reasonably well approximates the triangular depletion shape. The surface potential transconductance can be estimated as $g_{\psi_o} = \partial G_c / \partial \psi_o \big|_{V_{ds}, V_{fg}, V_{bg}}$, which is used to determine the operating point ψ_{o_s} (set with V_{fg}) where g_{ψ_o} is maximum. The commonly used relative detection sensitivity can then be calculated $\Delta G / G_o = |G(\psi_{o_s}) - G_o| / G_o$, where $G_o = G(\psi_{o_b})$, and ψ_{o_s} is the surface potential following the sensing event. This behavior has been previously described for depletion-mode silicon nanowires.⁶

Figure 6.4 shows the normalized transconductance $\|g_{\psi_o}\|$ ⁷ as a function ψ_o for dielectric layer thicknesses $t_f = 1$ nm and 10 nm with $N_a = 10^{17}$ cm⁻³ and 10¹⁸ cm⁻³. The transconductance with a 1 nm layer is ~10x larger than the 10 nm thick layer for the same dopant concentration, however, only for small ψ_o and all transconductances become comparable for $\psi_o > 100$ mV.

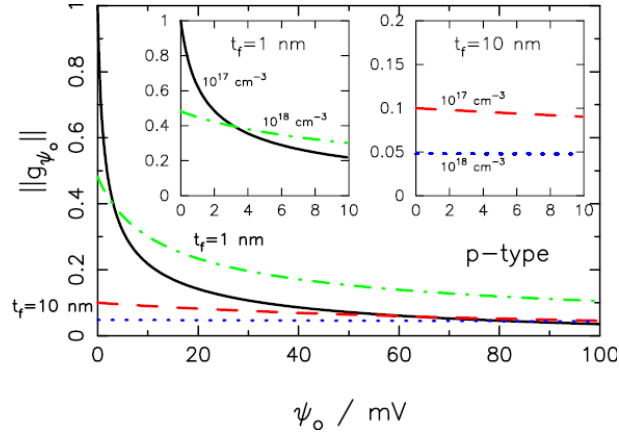


Figure 6.4 Normalized transconductance-surface potential for $t_f = 1 \text{ nm}$: $N_a = 10^{17} \text{ cm}^{-3}$ (black, solid) and 10^{18} cm^{-3} (green, dot-dash); $t_f = 10 \text{ nm}$: $N_a = 10^{17} \text{ cm}^{-3}$ (red, dashed) and 10^{18} cm^{-3} (blue, dotted).

The surface charge transconductance $g_{\sigma_o} = \partial G_c / \partial \sigma_o |_{V_{ds}, V_{fg}, V_{bg}}$ can also be estimated with use of the Grahame equation $\sigma_o = (8\epsilon_w \epsilon_o k T c_o)^{1/2} \sinh[q\psi_o / 2kT]$, for small values of ψ_o , which relates the surface charge density to the surface potential in a monovalent electrolyte, where ϵ_w is the permittivity of water and c_o is the ionic concentration of the electrolyte. The surface charge detection transconductance has similar behavior (Figure 6.5).

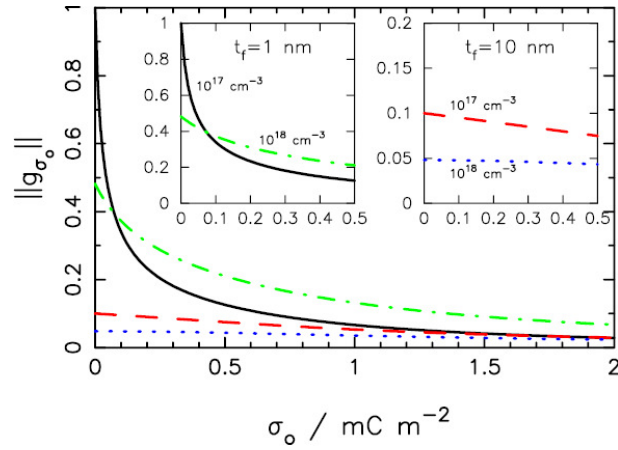


Figure 6.5 Normalized transconductance-surface charge density for $t_f=1$ nm: $N_a=10^{17}$ cm^{-3} (black, solid) and 10^{18} cm^{-3} (green, dot-dash); $t_f=10$ nm: $N_a=10^{17}$ cm^{-3} (red, dashed) and 10^{18} cm^{-3} (blue, dotted).

The $|\Delta G/G_o|$ can then be estimated, where $G_o = G(\psi_{o_b} = 0)$. Figure 6.6 shows the characteristics of $|\Delta G/G_o|$ as a function of t_f and N_a for $\Delta\psi_o = 10$ mV, typical for small analyte concentrations.⁹

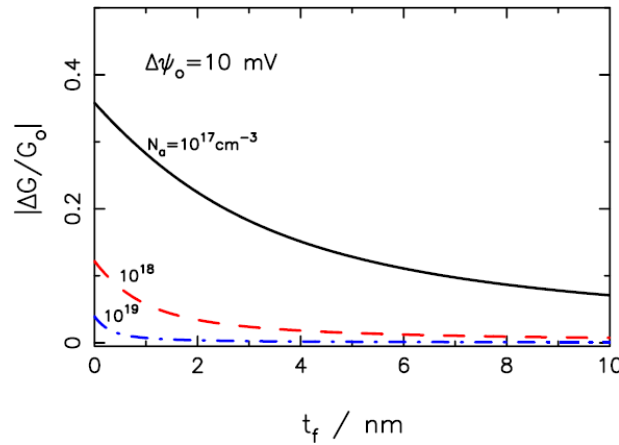


Figure 6.6 $|\Delta G/G_o|$ as a function of dielectric thickness for different N_a with $h=100$ nm and $\Delta\psi_o=10$ mV.

Figure 6.7 shows the strong dependence of $|\Delta G/G_o|$ on h and N_a for fixed $t_f=1$ nm. The sensitivity behavior is similar to previously reported measurements.

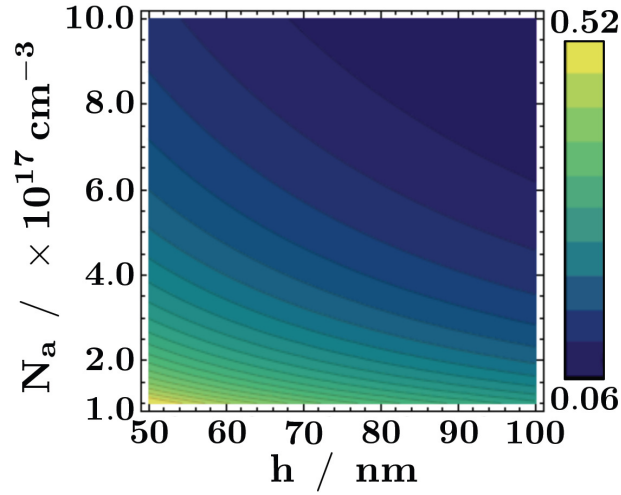


Figure 6.7 Contour map of $|\Delta G/G_o|$ for $t_f=1$ nm showing the N_a and h dependence.

6.4. Conclusion

Figures 4, 5, 6 and 7 clearly show that thin dielectric layers result in higher detection sensitivities and three important conclusions can be drawn from this analysis. First, thin ($t_f \sim 1$ nm) dielectric layers in combination with low channel doping ($N_a=10^{17} \text{ cm}^{-3}$) results in the largest detection sensitivity, however, over a small range of ψ_0 (or σ_o), and therefore, requires precise front-gate biasing for full utilization. Second, thin dielectric layers and larger channel doping ($N_a=10^{18} \text{ cm}^{-3}$) results in slightly lower and more uniform sensitivities. Lastly, a reference electrode is important for providing a well-defined gate potential for device biasing and operation. It should be noted that higher sensitivities can be obtained by moderately accumulating the front surfaces.

6.5. Bibliography

1. Stern, E.; Klemic, J. F.; Routenberg, D. A.; Wyrembak, P. N.; Turner-Evans, D. B.; Hamilton, A. D.; LaVan, D. A.; Fahmy, T. M.; Reed, M. A., Label-free immunodetection with CMOS-compatible semiconducting nanowires. *Nature* **2007**, 445, (7127), 519-522.
2. Patolsky, F.; Zheng, G.; Lieber, C. M., Fabrication of silicon nanowire devices for ultrasensitive, label-free, real-time detection of biological and chemical species. *Nat Protoc* **2006**, 1, (4), 1711-1724.
3. Elfstrom, N.; Juhasz, R.; Sychugov, I.; Engfeldt, T.; Karlstrom, A. E.; Linnros, J., Surface charge sensitivity of silicon nanowires: Size dependence. *Nano Lett* **2007**, 7, (9), 2608-2612.
4. Zhang, G. J.; Zhang, G.; Chua, J. H.; Chee, R. E.; Wong, E. H.; Agarwal, A.; Buddharaju, K. D.; Singh, N.; Gao, Z.; Balasubramanian, N., DNA sensing by silicon nanowire: Charge layer distance dependence. *Nano Lett* **2008**, 8, (4), 1066-1070.
5. Doping concentration dependent carrier mobility has been included in all calculations.
6. Chen, S.; Bommer, J. G.; Van der Wiel, W. G.; Carlen, E. T.; Van Den Berg, A., Top-down fabrication of sub-30 nm monocrystalline silicon nanowires using conventional microfabrication. *ACS Nano* **2009**, 3, (11), 3485-3492.
7. The calculated sensitivity data is normalized to the maximum sensitivity occurring for $t_f = 1 \text{ nm}$ and $N_a = 10^{17} \text{ cm}^{-3}$ at $\phi_o = 0$, for the surface charge sensitivity calculation $\epsilon_w = 80$ and $C_0 = 10 \text{ mM}$.
8. Israelachvili, J. *Intermolecular and Surface Forces*, 2nd ed.; Academic Press: London; 1992.
9. Fritz, J.; Cooper, E. B.; Gaudet, S.; Sorger, P. K.; Manalis, S. R., Electronic detection of DNA by its intrinsic molecular charge. *P. Nat. Acad. Sci USA* **2002**, 99, (22), 14142-14146.

Chapter 7

Multifunctional symmetric precursor: selective functionalization with Si-N bonded monolayer

Multifunctional symmetric molecules having the same reactive groups on the both ends can avoid the use of bulky functional groups; can give well packed functional monolayers with reduced processing time. In this chapter ethylene diamine ($C_2H_4(NH_2)_2$) has been explored as a precursor compound to make functional monolayers via the Si-N bond. X-ray photoelectron spectroscopy (XPS) studies were carried out to check the bond formation and monolayer stability. Subsurface oxidation caused by the amine group on the silicon sub-surface retains the Si-N bond and free amine groups on the surface remain available for further functionalization. Selective bioimmobilization is demonstrated on Si (111) surface silicon nanowires using fluorescence spectroscopy. These monolayers were also been tested with biosensing experiments using capacitance-voltage measurements of biotin-streptavidin binding.¹

¹ Manuscript in preparation.

7.1. Introduction

Silicon based biosensors and biochips require surface functionalization of biomolecules onto the active inorganic areas of the sensors/chips, which necessitates the use of self-assembled monolayers (SAM).¹ Amine or carboxylic acid/aldehyde terminated monolayers on thermally grown silicon oxide using silane-based attachment chemistry are well established to immobilize biomolecules in a straight forward way, however, selectivity and reproducibility issues remain.² Silicon-alkyl monolayers on hydrogen terminated silicon utilizing the Si-C bond are potential candidates for surface passivation of semiconductors for molecular electronics³ and bioimmobilization for biosensors.⁴ However, the long term stability of these layers under harsh acidic and basic environments,^{5,6} surface oxidation⁷, the nature of the oxide formed after exposure to ambient, and its effect on surface quality remain active research areas. The main draw back with the silicon-alkyl monolayers is the number of atop silicon atoms remaining unsubstituted after the chemical process because of steric hindrance caused by long chain hydrocarbon and the surface coverage is typically only ~50%.⁸ However, while considering the remaining bonds on the surface, they are shown to be terminated with hydrogen and/or hydroxyl (-OH) groups. Consistently, no silicon oxide is detectable by surface sensitive XPS on such initially prepared alkylated Si surfaces. Although the rate of surface oxidation is sufficiently impeded, where core level XPS studies of the Si 2p region of the alkylated silicon surface has shown very small but detectable levels of oxide formation after a number of weeks in an ambient environment.⁹ Hydrogen terminated/alkyl surfaces get oxidized by the presence of an oxidant O₂ (g) and a nucleophile i.e. H₂O.¹⁰ Surface oxidation also involves insertion of an oxygen atom into the back-bond of silicon, i.e. Si-O-Si bond formation, also known as subsurface oxidation, which has been shown to enhance the stability of the Si-C bond in the case of Si-alkyl monolayers by relaxing the Van der Waals repulsion forces among the grafted alkyl chains as a consequence of an increased inter-silicon distance while the Si-alkyl monolayer remains intact. Apart from surface uniformity

and stability of the grafted monolayers, a more basic and practical issue is the possibility of further modification of these surfaces.¹¹ Amine terminated groups attached to the Si-alkyl monolayer can be further conjugated with biomolecules.¹² Such surfaces can be fabricated by using *t*-butyloxycarbonyl (*t*-BOC) protected ω -unsaturated aminoalkane, such as *t*-BOC (10-aminodec-1-ene),^{13,14} N-1-BOC-amino-3-cyclopentene(BACP),¹⁵ tert-Butyl Allylcarbamate¹⁶ or a Phthalimide protected aminoalkane such as N-Vinyl Phthalimide¹⁷ and N-(5-hexynyl) Phthalimide¹² using either a photochemical UV or a heating hydrosilylation reaction on hydrogen terminated silicon surfaces. Utilization of surface amine groups for further biomolecular conjugation in this case involves a deprotection step making the immobilization process longer and in many cases damaging to the monolayer.¹⁸ Steric hindrances due to bulky protection groups might involve lower surface coverage¹⁹, inefficient passivation and higher leakage current in electrical solution based measurements can lead to improper biosensor device operation.²⁰ A ω -unsaturated aminoalkane, if used without a protection group, results in non-uniform monolayers due to competition between head and tail groups towards the hydrogen terminated silicon. Higher amounts of surface oxidation have also been monitored on these surfaces.¹⁵ One solution to the problem of covalently linking organic molecules to the silicon surface with an bio-active end group in a single step is to use multifunctional precursor molecules that can be grafted to the silicon surface at one end and can be reacted chemically at the other end provided that only end group reacts with the silicon surface.¹¹ Symmetric bifunctional molecules are superior compared to asymmetric molecules in developing molecular assemblies where chemical disorder produced by two different groups is eliminated. Ethylene diamine reactivity with silicon (001) surfaces has been investigated under ultra-high vacuum (UHV).²¹ The preparation of the Si-N bonded alkyl monolayer on Si (100) has also been demonstrated via chemical vapor deposition and in solution at low temperatures using chlorine terminated silicon (Si-Cl).²² Silicon surface monolayers using the Si-N and Si-O bonds has already been reviewed.²³ Successful Si-N bonded monolayers on hydrogen terminated silicon has also been demonstrated using vapor phase reaction under UV-irradiation.²⁴ In this

chapter, we use a symmetric multifunctional molecule, such as ethylene diamine to form a functional monolayer on hydrogen terminated Si(111) surfaces and demonstrate the selective immobilization of biomolecules onto the surface of all (111) surface Si-NW devices. Si-C bonded monolayers fabricated via 1-Octadecene and 1-Undecanoic acid are used as a reference to check the extent of sub-surface oxidation caused by carbon and/or carboxylic group to the silicon surface and the preferential reactivity of doubly bonded carbon atom towards silicon. We studied the prepared monolayer on planar surfaces by XPS and studied the biomolecular recognition ability of the surface by the Si-ethylene diamine monolayer (NH-(CH₂)₂-NH)-biotin²⁵ binding event using an electrolyte-insulator-semiconductor (EIS) sensor configuration.

7.2. Experimental

7.2.1. Materials

All chemicals were used as received. Ethylene diamine (bioanalytical grade), 1, 10-dodecane diamine (98%), biotin succinimidyl ester, Tween 20, sulphuric acid (98%), H₂O₂ (30%), HF (1%), NH₄F (40%) and standard phosphate buffer saline tablets were purchased from Sigma Aldrich. Streptavidin Alexa Fluor 488 was purchased from Invitrogen. Silicon (111) wafers used were p-type with doping levels between 10¹⁵ and 10¹⁸ cm⁻³ were used. Milli-Q deionized (DI) water (18.2 MΩ-cm) was used for rinsing glassware and for dilutions. A custom quartz reactor was made to carry out the hydrosilylation reaction under an inert nitrogen atmosphere.

7.2.2. Surface preparation

7.2.2.1. Cleaning and hydrogen termination of planar samples

Single-side polished silicon chips were used once and discarded. Si (111) planar chips were cleaned by sonication for 15 minutes in a mixture of ethanol, acetone, isopropanol

and DI water and were dried under a stream of nitrogen. A few samples were further treated with air/oxygen plasma (100 W) for 20 minutes, or with UV-Ozone; a similar procedure used for surface cleaning Si-NW devices (section 7.2.2.2). These chips were then etched with 1% HF. Most of the chips were cleaned with a piranha solution (1:1) (H_2SO_4 (98%): H_2O_2 (30%)) at 90 °C for 30 minutes and subsequent etching of the chemically grown oxide with 1 % HF solution for 10 minutes and followed by rinsing with DI water. The solutions of 40% NH_4F were purged with nitrogen for 1 hour. These chips were etched in 40% NH_4F for 20 minutes under bubbling nitrogen and were rinsed with DI water and blown dry under nitrogen before further reaction.

7.2.2.2. Cleaning and hydrogen termination of silicon nanowire devices

Silicon nanowire biosensor devices are typically encapsulated in an insulating polymer layer to avoid contact between the metallic conducting material and ion-containing aqueous solutions. The Si-NW devices have windows opened in the polymer encapsulation layer (Durimide) leaving the Si-NW gate regions exposed. The exposed Si-NW gate regions were cleaned with UV-Ozone and air plasma for 10 minutes. The gate oxide was removed with 1% HF and thoroughly rinsed with DI water and nitrogen dried.

7.2.2.3. Monolayer formation

The clean solutions of ethylene diamine were purged with pure argon gas for at least one hour prior to use. Freshly cleaned samples of silicon or silicon nanowire devices were placed immediately, after etching, rinsing with water and drying with nitrogen, in a quartz reactor containing freshly deoxygenated ethylene diamine. The quartz tube was exposed with UV light ($\lambda = 254$ nm, 4.4 mW cm^{-2}) for two hours. After the reaction, the silicon chip was rinsed with methanol, ethanol, iso-propanol and DI water three times each in order to remove any adsorbed material. 1-Octadecene and 1-Undecynoic monolayers were prepared using the same procedure.

7.2.2.4. *Surface characterization*

XPS studies/surface characterization has been conducted with a monochromatic X-ray beam (Al KR, 1486.6 eV, 100W, Quanter, Physical Electronics). Mapping was done at 3×10^{-9} Torr and a detector angle of 45° . XPS spectra were taken just after monolayer formation or after storage in a dry nitrogen box. Either the carbon peak at 284.3 or silicon (Si 2p 3/2) was taken as a reference for peak fitting.

7.2.2.5. *Bioconjugation and fluorescence microscopy*

Prepared amine terminated surfaces were used as soon as possible for further bioconjugation. For the immobilization of biotin, biotin succinimidyl ester (Biotin-NHS) in dimethyl formamide (DMF) 3-9 mM/ml was used for two hours at room temperature. After curing, surfaces were rinsed three times with DMF (the solvent), methanol, ethanol, acetone and DI water to remove any physically adsorbed material. Samples were dried with nitrogen and were used further for either fluorescence studies or electrical measurements. Streptavidin conjugated Alexa-Fluor 488 (Invitrogen) was first diluted to 2 ml with a 1x PBS (pH 7.4) buffer. 100 μ l of as-diluted stock was further diluted to 1 ml with the same buffer and was used to bind with surface immobilized biotin for one hour. After curing, the samples were washed thoroughly to remove physically adsorbed material with the same buffer for a number of times. For the samples used in electrical measurements, after biotin immobilization, samples were washed thoroughly with ethanol and DI water and were soaked in 0.1% Bovine Albumin serum in 1 x PBS pH 7.4 (0.05% Tween) buffer to prevent non-specific binding.

7.2.2.6. *Electrical measurements*

Capacitance-voltage (CV) measurements were recorded with an impedance analyzer (Hewlett-Packard 4194A Impedance Gain-Phase Analyzer) at an AC frequency of 10

kHz (amplitude 20 mV) and the front-gate voltage scan, using a platinum wire as a reference electrode. A custom cell was used for the measurements. EIS capacitors were prepared in the MESA+ clean room. Test devices have an active surface area of $1.96 \times 10^{-5} \text{m}^2$. Back contacts were made in the clean room by aluminum (Al) e-beam evaporation and sometimes a drop of Gallium-Indium eutectic was used to make an electrical contact after scratching back side oxide layer. A parallel capacitance-resistance model was used for data collection with a Labview program.

7.3. Results and discussions

7.3.1. XPS characterization

Si-N bonded monolayers were fabricated using hydrogen terminated Si (111) surfaces as the substrate and ethylene diamine as the precursor molecule in solution phase under inert atmosphere and UV irradiation. XPS was used to characterize the sample surface regarding type of bond, nature of oxide formed and stability of the as-prepared monolayers. Figure 7.1 shows survey spectra of as-prepared monolayers consisting of conventional Si-C bonded layers (Figure 7.1a & 7.1b) and a Si-N bonded layer (Figure 7.1c). Figure 7.1c shows a substantially higher amount of oxygen (532 eV) on the sample surface (Si-N bonded layer) as compared to the reference (Si-piece, blank) which was etched with 1% HF/40% NH_4F prior to XPS measurements. The survey spectrums of 1-Octadecene and 1-Undecanoic acid modified surfaces are also compared with the reference under the same experimental conditions (Figures 7.1a, b). Substantially high amounts of oxygen shown in the survey spectrum (Figure 7.1c) might be due to two reasons: i) nucleophilic nature of amine groups which might act as a catalyst to oxidize the silicon surface utilizing traces of oxygen in solution, ii) physisorbed (hydrogen bonded) water on the surfaces increase the oxygen content in XPS spectrum. Probably both of these factors are involved here.

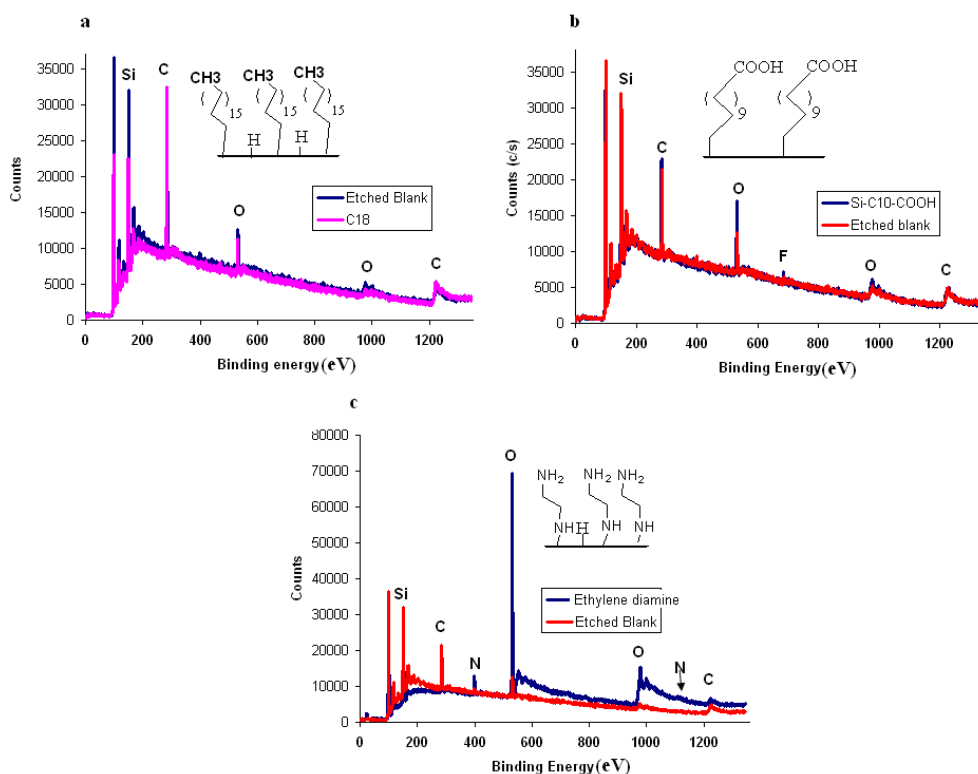


Figure 7.1 XPS Survey spectrum: a) 1-Octadecene (C18) modified surface prepared under the same conditions compared with Blank. b) 1-Undecenoic acid monolayer prepared on Si (111) surface. c) Ethylene diamine modified silicon surface compared with etched blank, showing substantial amount of oxygen present on the surface. Blank has higher content of non-specifically adsorbed carbon.

The survey spectrum of the 1-Octadecene monolayer fabricated on planar Si (111) surface under nearly identical conditions as that of the ethylene diamine monolayer shows relatively small amounts of oxide which is approximately equal to that for freshly etched blank sample (Figure 7.1a). Figure 7.2a shows the Gaussian fitted Si 2p region of the XPS spectrum for the 1-Octadecene bonded monolayer where the oxide peak at 103 eV is nearly absent, however, in contrast, the O 1s region of the same spectrum (Figure 7.2b) shows sufficiently prominent oxygen peak.

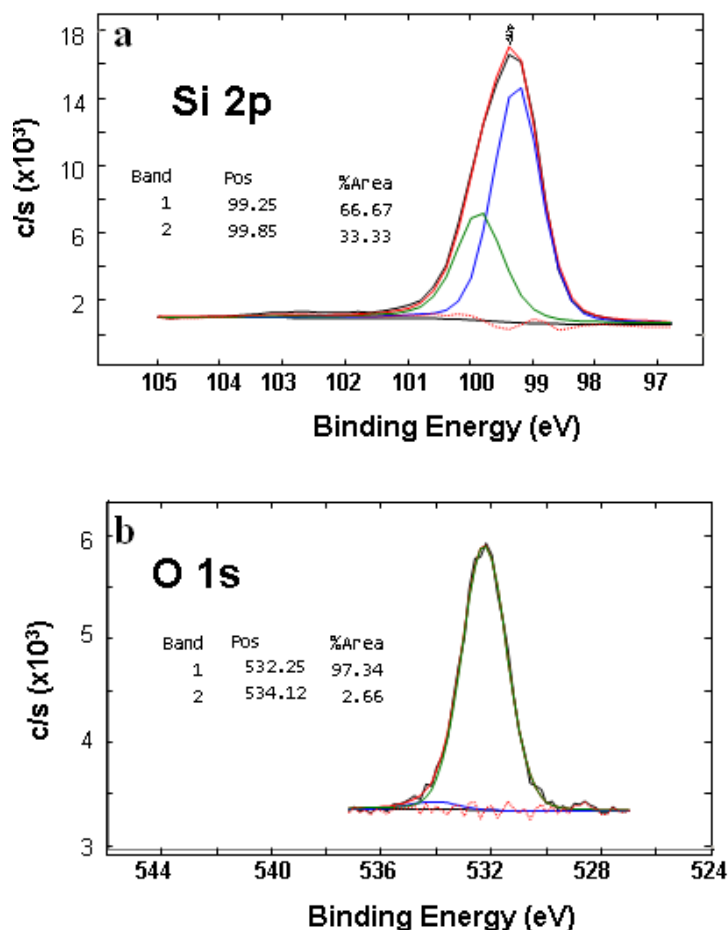


Figure 7.2 High resolution (XPS) spectra of C18 monolayer a) silicon 2p region showing very small or negligible amount of silicon in the form of silicon oxide (SiO_x) b) Oxygen 1s region of the high resolution spectrum showing negligible fraction of oxygen in fully developed oxide (SiO_2) at 534 eV where as most of the oxygen (532 eV, 97%) is either from physically adsorbed moieties on the surface during washing or a small fraction from sub-surface oxidation. The colored peaks fits represent different oxidation states or duplets.

Only a very small region of the oxygen peak at 534 eV might be due to the fully developed surface silicon dioxide where as a fit at 532 eV is probably due to a small amount of sub-surface oxidation,²⁶ but mostly from the top surface impurities getting adsorbed onto the monolayer during wash process.²⁷ The O 1s XPS signal could arise from a number of sources, including adsorbed solvent from the wet chemical preparation techniques, adsorbed pump oil vapor introduced in the quick-entry load

lock, or contaminating dust particles covered with oxygen-containing organic molecules that were not possible to avoid when working in standard laboratory conditions.²⁸ Figure 7.3 shows the high resolution XPS Si 2p region of the octadecyl-silicon surface before and after a month in ambient environment. Surface oxidation is substantially suppressed due to monolayer formation via the Si-C chemistry route even after a month. A small rise in the silicon peak (99.7 eV) as well as the silicon oxide peak (103 eV) can be observed indicating an increased surface oxidation.

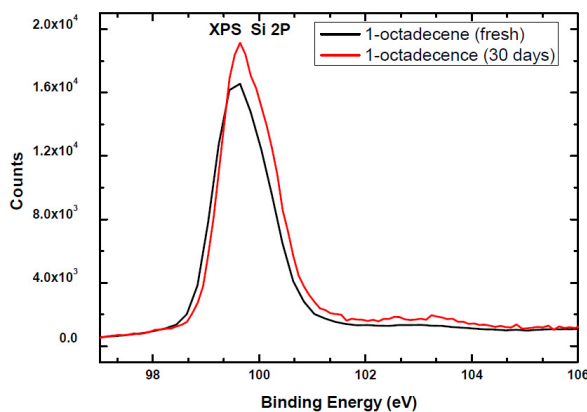


Figure 7.3 XPS Si 2p region of a Si (111) sample with a 1-Octadecene monolayer, comparing a fresh sample and the same sample after one month.

Carboxylic monolayers can be prepared by using ω -carboxylic-1-alkene without protecting the tail group (-COOH) under optimal reaction conditions. Figure 7.4 compares the Si 2p regions of freshly modified silicon surfaces by 1-Octadecene and 1-Undecanoic acid. The small amount of surface oxidation can be seen in the case of the undecylenic monolayer that might be due to the interaction of the carboxylic acid group with the silicon surface inducing small subsurface oxidation.

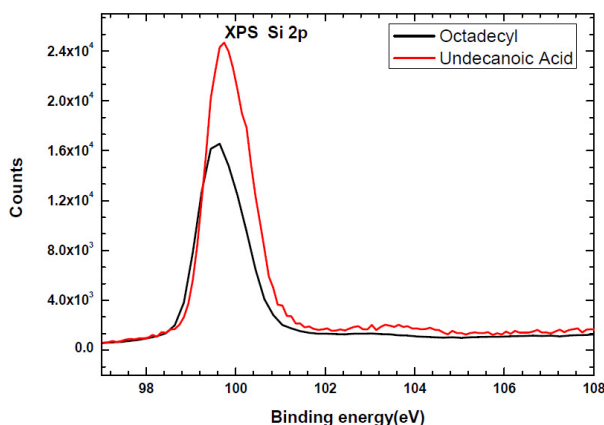


Figure 7.4 XPS Si 2p region for fresh Octadecyl and Undecanoic acid.

That was why, while correlating the high resolution XPS spectra of Si-C bonded monolayers, it can be proposed that though the oxidation peak in survey spectrum for ethylene diamine monolayer (Figure 7.1c) is high but it is mostly due to; i) adsorbed water and oxygen containing impurities attached to free pendant amine terminated surface; ii) extensive sub-surface oxidation caused by amine groups attached to silicon in the presence of trace aqueous oxygen where the back-bond of silicon is only oxidized and not the surface silicon atoms leaving Si-H bond or Si-N bonds intact and any functionality on the monolayer will remain available for immobilization^{2, 8} as proved later by XPS, fluorescence and biosensing measurements; and iii) a small amount of fully developed surface oxide.

The ethylene diamine surface has more carbonaceous contents as shown by the survey spectra (Figure 7.1c) probably because of the fact that the amine terminated surfaces are more susceptible towards adventitious carbon impurities from the environment²⁹ as well as over exposure to UV radiation might cleave the C-N bond in the amine groups of the ethylene diamine resulting in Si-C attachment.²¹ Figure 7.5 shows high resolution XPS spectra of planar Si (111) surfaces modified with the ethylene diamine precursor. The high resolution XPS spectra show two major peaks in the C 1s region (Figure 7.6a), one at 285 eV is most probably due to the Si-C attached chains^{21, 30} after cleavage of the C-N bond due to over-exposure with UV irradiation where as the

second and third peaks, 286 and 288 eV, are carbon peaks representing carbon that we assume are attached to nitrogen atoms ($-\text{NH}_2$, $-\text{NH}-$), which have two different chemical environments, the intensity of the peak at 288 eV might be attenuated due to adventitious carbon.^{31, 32} The high resolution XPS spectrum of nitrogen (Figure 7.6b) shows two sets and types of nitrogen peaks due to their chemical states; one set is 398.2 eV and 402.3 eV with a peak for the bond of nitrogen with silicon known as a dissociative bond ($\text{Si}-\text{NH}-\text{C}$)^{21, 33, 34} and one for the protonated or dative bond ($\text{Si}-\text{NH}_2^+-\text{C}$)²¹, respectively. The peaks at 399.79 eV and 401.3 eV represent the free amines ($-\text{NH}_2$)³⁵ and protonated free amines ($\text{C}-\text{NH}_3^+$),^{29, 32} respectively. The peak at 289 eV in the carbon 1s (Figure 7.5a) region represents some carbonyl groups from adventitious

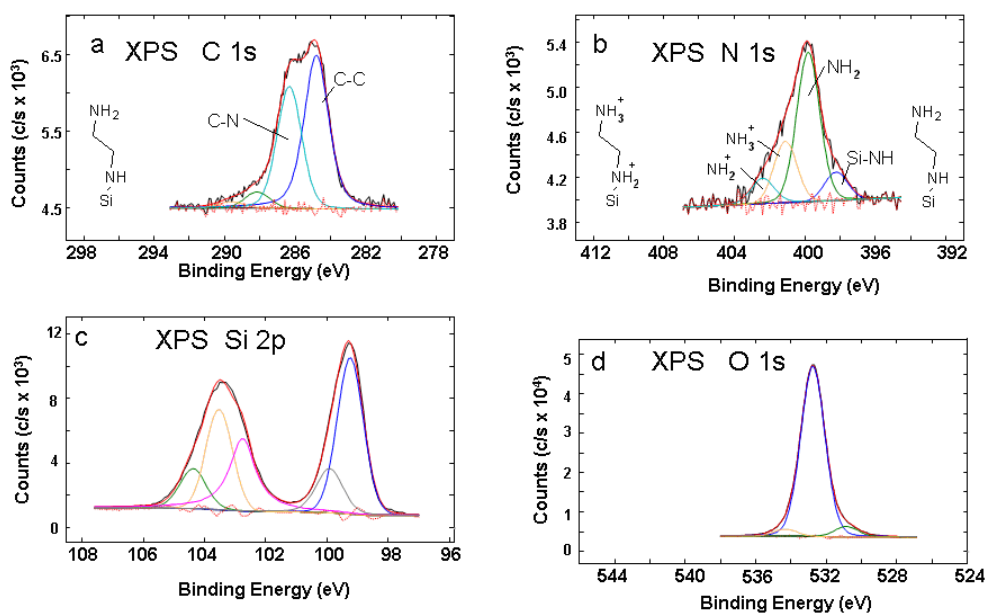


Figure 7.5 High resolution XPS spectrum of the ethylene diamine monolayer on planar Si (111) surface.

contaminants.³⁶ The Si 2p region of the spectrum (Figure 7.5c) shows a continuum

including fitted peaks at 99.7 eV, 100 eV, 103.8 eV and 104 eV. The silicon oxidation state for the Si-N bond should be at 101.78 eV,³³ however, it is difficult to distinguish in all samples from the Si-C and Si-O regions. The Si 2p region starting from 101 eV to 104 eV can be fitted with two major peaks one at 102.76 eV due to (O₃Si—N)³⁴ and the second at 103.5 eV representing the (O₃Si—O) bond which is fully developed SiO₂; and a third fit at 104 eV is most probably due to a Si-N dative bond (Si⁻NH₂) due to higher energy requirements to remove an electron. However, the Si-N remains intact, N 1s in Figure 7.5b compared with N 1s²¹ and a monolayer of adsorbed ethylene diamine with free amine groups remain available for further conjugation of biomolecules on the sub-oxide (O₃ Si) surface. Figure 7.6 shows the fits in the XPS N 1s peaks for a freshly prepared sample and after three days in ambient conditions.

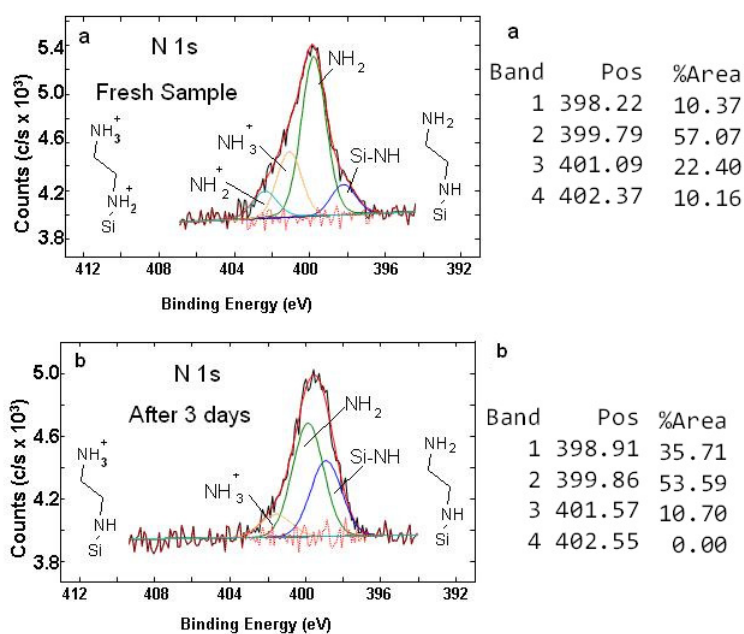


Figure 7.6 Ethylene diamine monolayer in ambient laboratory conditions: a) freshly prepared, b) after 3 days.

The peak intensity at 398.3-398.7 eV becomes more than double after three days where

as peak at 402.3 eV (dative bond, Si-NH_2^+) reduces nearly to zero most probably due to the transformation of all Si-NH_2^+ bonds at the surface to Si-NH showing more stability for a Si-NH configuration and better stability of the monolayer. Figure 7.7 shows the comparison between the high resolution XPS plots of a freshly prepared ethylene diamine monolayer and the sample sample after three days in ambient laboratory conditions. An adventitious amount of carbon deposited onto the surface can be seen by the rise of the C 1s signal in Figure 7.7a. The N 1s signal from the amine was suppressed consequently as shown in Figure 7.7b where as surface oxide peak at 103 eV and oxygen (O 1s Peak 532 eV) are suppressed probably due to the deposition of extra material.

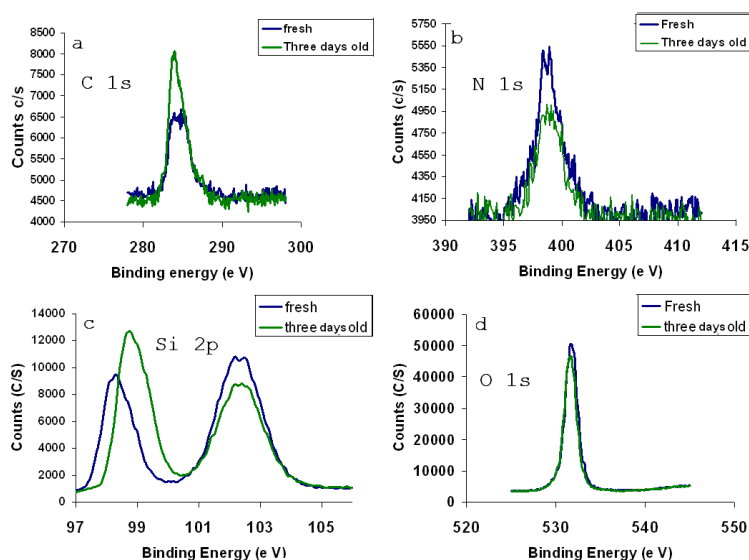


Figure 7.7 Stability of the ethylene diamine monolayer on planar Si (111) samples after three days in ambient laboratory conditions.

Figure 7.8 shows a possible mechanism for subsurface oxidation during ethylene diamine layer formation. Oxidation of the silicon surface usually proceeds by the involvement of a trace amount of oxygen in the solution and availability of a nucleophile such as ethylene diamine.⁸ Few reports are available to date dealing with

the reaction of ethylene diamine with hydrogen terminated silicon in solution phase under UV exposure. Eves et. al.²⁴ carried out a UV reaction with an alkyl amine in gas phase and proposed that a hydrogen atom dissociates from the amine group creating a free dissociated amine radical that reacts with the hydrogen terminated silicon surface. According to their proposed reaction mechanism, a surface is not necessarily exposed directly for amine adsorption avoiding degradation of the monolayer by extraneous UV exposure.

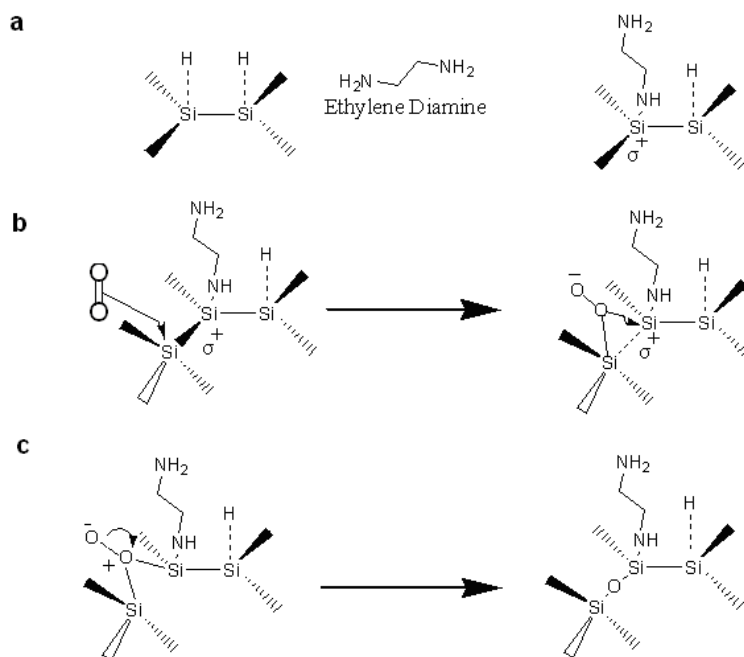


Figure 7.8 Proposed mechanism of subsurface oxidation for silicon with ethylene diamine monolayer.^{2, 8, 37, 38}

In contrast, most of the hydrosilylation reactions in solution phase involve creation of a dangling bond after Si-H bond cleavage and electrophilic attack of doubly bonded alkene to make a Si-C bond.³⁹⁻⁴² In Figure 7.8a, under UV exposure and in solution phase, the reaction might proceed by the dissociation of a hydrogen atom from the

silicon surface which probably interacts with an ethylene diamine molecule resulting in a Si-N bond after another hydrogen atom cleaved from the amine group ($-\text{NH}_2$),³⁰ or it might involve only the dissociation of the N-H bond. The electronegativity of the $-\text{NH}$ group, in case of the Si-N bond, is high and renders the silicon atom positively charged, however, cannot be attacked directly by aqueous oxygen due to steric hindrance⁴³ but renders oxidation at the subsurface silicon atom favorable due to an inductive effect (Figure 7.8b). This attack is more favorable in the case of a dative bond (Si^+NH_2) and leads to a weakening of the Si-Si bond, while increasing its length and makes the oxygen atom to bridge between two silicon atoms possible (Figures 7.8b & 7.8c).

7.3.2. Fluorescence studies

Despite the fact that the XPS studies show extensive sub-surface oxidation on the silicon surface of the ethylene diamine monolayer, the free (pendant) amine groups at the top of the Si-N bonded monolayer remain available for further functionalization of biomolecules. Selective biofunctionalization of silicon nanowires only onto the active nanowire area is important for better sensitivity of the detection as described in chapter 2.¹² In order to check the selective biofunctionalization of silicon nanowires via Si-N bounded monolayers, biotin was immobilized onto the nanowires by using succinimidyl ester derived biotin and was reacted subsequently with Alexa-Fluor conjugated streptavidin. The oxide on the surface of silicon nanowire was thin (~10 nm) as compared to the oxide layer on the other parts of the chip. Si-NW surfaces were modified after etching the Si-NW surface oxide and by UV reaction with ethylene diamine.

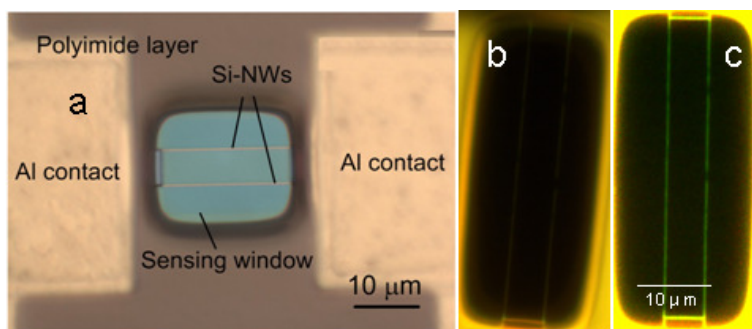


Figure 7.9 Selective functionalization of silicon nanowire surfaces via Si-N bounded monolayers a) pair of silicon nanowire devices prepared in our lab⁴⁴ b) fluorescence microscope image before modification (a control blank was also the same even after modification and subsequent bioimmobilization), c) modified silicon nanowire after modification and bioimmobilization.

Figure 7.9a shows a pair of Si-NW FET devices prepared and encapsulated in the MESA+ clean room, Figure 7.9b shows a fluorescence image of a pair of UV ozone cleaned Si-NWs before surface modification (a blank sample was similar) where as Figure 7.9c shows the selective bioimmobilization of the Si-NWs with biomolecules (biotin-streptavidin-Alexa Fluor 488 conjugate).

7.3.3. Electrical measurements

7.3.3.1. Biosensing by capacitance-voltage measurements

EIS sensors were used to test the ethylene diamine monolayers for biosensing experiments in using C-V measurements. C-V measurements are routinely used in universities and in semiconductor industry for a number of applications including characterization of gate dielectric layers.⁴⁵

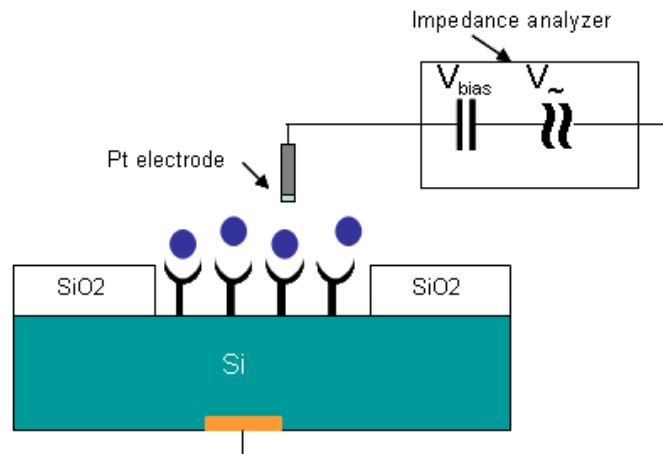


Figure 7.10 Biosensing on surface modified electrolyte-insulator-semiconductor EIS structure in capacitance-voltage readout.

It is due to the fact that the technique is simple and is able to characterize the device under test in an efficient way if properly used. On the other hand, can also be used in biosensing applications using the EIS sensor configuration as shown in Figure 7.10.^{46, 47} Figure 7.10 shows the EIS biosensor configuration which was operated by varying the DC bias in order to induce accumulation, depletion and inversion regions in the semiconductor body where as a small AC voltage of amplitude 15-20 mV was superimposed onto the DC bias to readout capacitance and resistance values at each portion of the C-V curve (accumulation, depletion, inversion). Biomolecules are usually immobilized onto the surface of the EIS capacitor on oxide or Si-alkyl functional monolayer after etching and hydrosilylation reaction.¹² In an ideal C-V measurement the capacitance in accumulation equals the insulator (oxide or monolayer/biomolecules immobilized) capacitance and hence thickness or dielectric constant of the insulator can be calculated via the well known formula:

$$C_{layer} = \epsilon_r \epsilon_0 A / t_{layer} \quad (1)$$

Where C_{layer} is the capacitance of the layer ϵ_r is the dielectric constant of the layer, ϵ_0 is the permittivity of free space ($8.85 \times 10^{-12} \text{ F m}^{-1}$), t is the thickness of the layer and A is

the surface area of the EIS capacitor. An increase in the thickness of the top layer causes a decrease in the capacitance provided that the surface charge remains constant. An EIS surface modified with an ethylene diamine monolayer, and subsequently immobilized with biotin succinimidyl ester, should be able to detect a streptavidin binding event by a change in capacitance in the accumulation region. The flat band voltage V_{fb} is another characteristic of a semiconductor which can be calculated from Mott-Schottky plots for thin insulators. Hence, binding events can be monitored by using capacitance change as well as shift in flat band voltage of the device. That is why C-V measurement technique can be very sensitive for detection of bioanalytes due to two dimensional responses in capacitance as well as in voltage by the changes in bio-density, thickness and charge distribution. The basic principal of charge detection allows charged biomolecules to exert an electric field effect on the silicon substrate to create or modify a dense layer of charges already present in the silicon called depletion layer or “space charge region”. The depletion layer is created when a field applied near the surface of the semiconductor repels the majority carriers from the surface, resulting in a region that is depleted of majority carriers. This region contains a large portion of fixed immobile ions that appear as an added dielectric to the silicon dioxide/insulating monolayer. The overall capacitance is determined by combining the series capacitances of insulator and depletion layer capacitance. Since the insulator (oxide, monolayer) capacitance is a fixed quantity, the change in capacitance is determined primarily by the thickness of depletion layer (modulated by surface charges as biomolecules). The strength and density of biomolecules determines the strength of the field penetrating the insulator (oxide, monolayer), and therefore, the thickness of the underlying depletion layer. The capacitance is inversely proportional to the thickness of the space charge region (modulated by biomolecules). A thicker space charge region correlates to a smaller measured capacitance and vice versa.⁴⁸

Figure 7.11a shows the detection of a streptavidin binding event on APTES modified surface after subsequent biotin immobilization. There was no sufficient change in the capacitance after binding of streptavidin or shift in flat band voltage along x-axis. Figure 7.11b shows a blank measurement with an EIS capacitor processed entirely in

the same way as sample without an ethylene diamine monolayer on the surface and probably is covered with a native oxide. The small change in the capacitance is due to the field effect of streptavidin charges (negative at pH 7.4) non-specifically on the blank surface. There is a slight shift in the flat band voltage for the blank sample (Figure 7.11b) compare to the sample with SiO₂ gate oxide (Figure 7.11a). Figure 7.11c shows the streptavidin binding on ethylene diamine modified surface where an increase in the capacitance $\Delta C \approx 35$ nF and a shift in the curve to the positive side of x-axis after streptavidin binding. There is a significant increase in the accumulation capacitance to near 120 nF due to thin monolayer as expected. There is a substantial shift in the flat band voltage $\Delta V_{fb} \approx 0.5V$. The reason for an increase in capacitance is due to the net charge that accumulates on the sensor surface as compare to the thickness of the adsorbed layer and therefore, the capacitance increases due to additional charge $Q = C V$ for a fixed applied gate voltage.

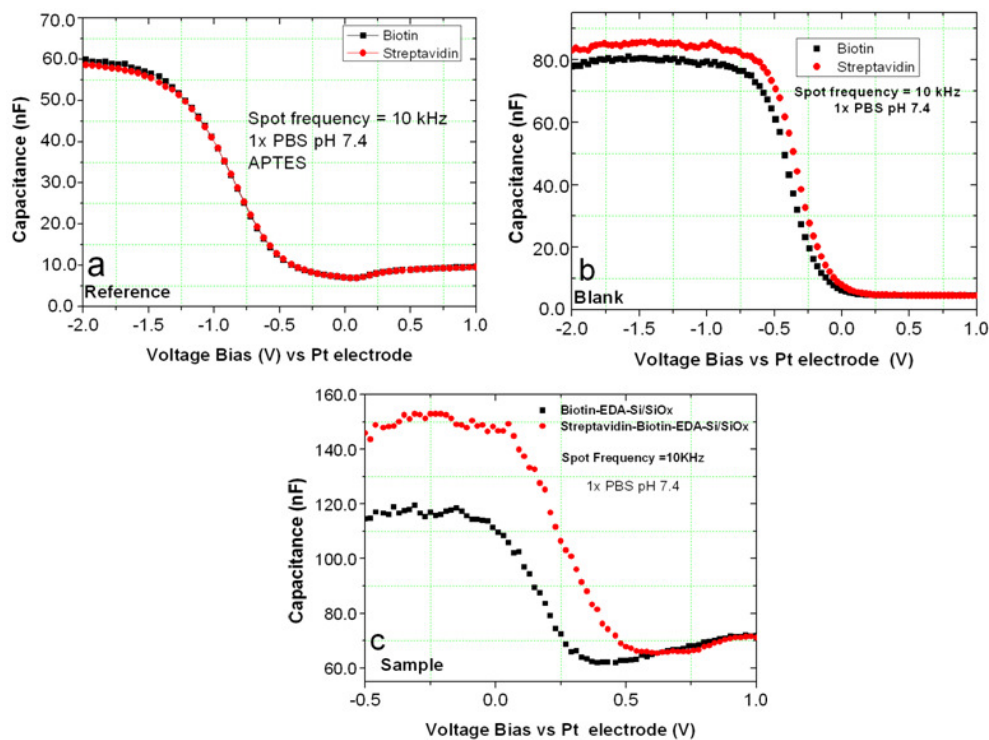


Figure 7.11 Capacitance-voltage measurements for monitoring biotin-streptavidin binding event in 1 x PBS buffer a) biotin-streptavidin binding on native oxide-3-amino propyl triethylsilane (APTES)-biotin (streptavidin) b) Etched, UV irradiated (under argon, without ethylene diamine), and biotin adsorbed blank (streptavidin binding), c) Ethylene diamine modified surface after biotin immobilization and streptavidin binding.

According to the equation (1) the thickness of the layer on the surface of the capacitor can be calculated as $t \approx [3.9 \times 8.85 \times 10^{-12} \text{ (F/m)} \times 1.96 \times 10^{-5} \text{ m}^2] / C_{\text{layer}}$ which is nearly equal to 6 nm with the APTES monolayer (Figure 7.11a)

7.4. Conclusion

Ethylene diamine molecules were used as a precursor compound to make Si-N bonded monolayers on hydrogen terminated silicon surface. XPS, fluorescence and electrical measurements were carried out on as prepared surfaces. It was realized by repeated

experiments and with controls samples that the Si-N chemistry works well in selective functionalization of patterned surfaces such as silicon nanowires as well showed improved detection capability of biomolecules in electrolyte insulator semiconductor sensor configuration.

7.5. Bibliography

1. Yang, M.; Teeuwen, R. L. M.; Giesbers, M.; Baggerman, J.; Arafat, A.; de Wolf, F. A.; van Hest, J. C. M.; Zuilhof, H., One-step photochemical attachment of NHS-terminated monolayers onto silicon surfaces and subsequent functionalization. *Langmuir* **2008**, 24, (15), 7931-7938.
2. Li, M., Modification of Silicon by self-assembled monolayers for Application in nano-electronics and biology, PhD Thesis, Graduate School—New Brunswick Rutgers, The State University of New Jersey, New Jersey, USA, **2007**.
3. Aswal, D. K.; Lenfant, S.; Guerin, D.; Yakhmi, J. V.; Vuillaume, D., Self assembled monolayers on silicon for molecular electronics. *Anal Chim Acta* **2006**, 568, (1-2), 84-108.
4. Arafat, A.; Daous, M. A., A short route of covalent biofunctionalization of silicon surfaces. *Sens and Actuat, B: Chemical* **2011**, 152, (2), 226-234.
5. Aureau, D.; Morailion, A.; De Villeneuve, C. H.; Ozanam, F.; Allongue, P.; Chazalviel, J. N.; Rappich, J. In Electronic properties and pH stability of Si(111)/alkyl monolayers, *ECS Trans*, **2009** 19, 373-379.
6. Gorostiza, P.; de Villeneuve, C. H.; Sun, Q. Y.; Sanz, F.; Wallart, X.; Boukherroub, R.; Allongue, P., Water exclusion at the nanometer scale provides long-term passivation of silicon(111) grafted with alkyl monolayers. *J Phys Chem B* **2006**, 110, (11), 5576-5585.
7. Popoff, R. T. W.; Asanuma, H.; Yu, H. Z., Long-term stability and electrical performance of organic monolayers on hydrogen-terminated silicon. *J Phys Chem C* **2010**, 114, (24), 10866-10872.
8. Juarez, M. F.; Soria, F. A.; Patrito, E. M.; Paredes-Olivera, P., Influence of subsurface oxidation on the structure, stability, and reactivity of grafted Si(111) surfaces. *J*

Phys Chem C **2008**, 112, (38), 14867-14877.

9. Webb, L. J.; Michalak, D. J.; Biteen, J. S.; Brunschwig, B. S.; Chan, A. S. Y.; Knapp, D. W.; Meyer, H. M.; Nemanick, E. J.; Traub, M. C.; Lewis, N. S., High-resolution soft X-ray photoelectron spectroscopic studies and scanning auger microscopy studies of the air oxidation of alkylated silicon(111) surfaces. *J Phys Chem B* **2006**, 110, (46), 23450-23459.
10. Miura, T. A.; Niwano, M.; Shoji, D.; Miyamoto, N., Initial stages of oxidation of hydrogen-terminated Si surface stored in air. *App Surf Sci* **1996**, 100-101, 454-459.
11. Leftwich, T. R.; Teplyakov, A. V., Chemical manipulation of multifunctional hydrocarbons on silicon surfaces. *Surf Sci Rep* **2008**, 63, (1), 1-71.
12. Masood, M. N.; Chen, S.; Carlen, E. T.; van den Berg, A., All-(111) Surface Silicon Nanowires: Selective Functionalization for Biosensing Applications. *ACS Appl Mater Interfaces* **2010**, 2, (12), 3422-3428.
13. Strother, T.; Hamers, R. J.; Smith, L. M., Covalent attachment of oligodeoxyribonucleotides to amine-modified Si (001) surfaces. *Nucl Acid Res* **2000**, 28, (18), 3535-3541.
14. Tian, F. Y.; Ni, C. Y.; Teplyakov, A. V., Integrity of functional self-assembled monolayers on hydrogen-terminated silicon-on-insulator wafers. *Appl Surf Sci* **2010**, 257, (4), 1314-1318.
15. Lin, Z.; Strother, T.; Cai, W.; Cao, X. P.; Smith, L. M.; Hamers, R. J., DNA attachment and hybridization at the silicon (100) surface. *Langmuir* **2002**, 18, (3), 788-796.
16. Bunimovich, Y. L.; Shin, Y. S.; Yeo, W. S.; Amori, M.; Kwong, G.; Heath, J. R., Quantitative real-time measurements of DNA hybridization with alkylated nonoxidized silicon nanowires in electrolyte solution. *J Am Chem Soc* **2006**, 128, 16323-16331.
17. Ara, M.; Tsuji, M.; Tada, H., Preparation of amino-terminated monolayers via hydrolysis of phthalimide anchored to Si(111). *Surf Sci* **2007**, 601, (22), 5098-5102.
18. Ofir, Y.; Zenou, N.; Goykhman, I.; Yitzchaik, S., Controlled amine functionality in self-assembled monolayers via the hidden amine route: Chemical and electronic tunability. *J Phys Chem B* **2006**, 110, (15), 8002-8009.
19. Scheres, L.; Rijksen, B.; Giesbers, M.; Zuilhof, H., Molecular Modeling of Alkyl and Alkenyl Mono layers on Hydrogen-Terminated Si(111). *Langmuir* **2011**, 27, (3), 972-

980.

20. Lu, M.-P.; Hsiao, C.-Y.; Lai, W.-T.; Yang, Y.-S., Probing the sensitivity of nanowire-based biosensors using liquid-gating. *Nanotechnology* **2010**, 21, (42), 425505.
21. Mathieu, C.; Bai, X.; Gallet, J. J.; Bournel, F.; Carniato, S.; Rochet, F.; Magnano, E.; Bondino, F.; Funke, R.; Kohler, U.; Kubsy, S., Molecular Staples on Si(001)-2 x 1: Dual-Head Primary Amines. *J Phys Chem C* **2009**, 113, (26), 11336-11345.
22. Zhu, X. Y.; Mulder, J. A.; Bergerson, W. F., Chemical vapor deposition of organic monolayers on Si(100) via Si-N linkages. *Langmuir* **1999**, 15, (23), 8147-8154.
23. Shirahata, N.; Hozumi, A.; Yonezawa, T., Monolayer-derivative functionalization of non-oxidized silicon surfaces. *Chem Record* **2005**, 5, (3), 145-159.
24. Eves, B. J.; Fan, C. Y.; Lopinski, G. P., Sequential reactions with amine-terminated monolayers and isolated molecules on H/Si(111). *Small* **2006**, 2, (11), 1379-1384.
25. Fischer, M. J. E., Amine Coupling Through EDC/NHS: A Practical Approach. *Surface Plasmon Resonance: Methods and Protocols* **2010**, 55-73.
26. Borman, V. D.; Gusev, E. P.; Lebedinski, Y. Y.; Troyan, V. I., Mechanism of submonolayer oxide formation on silicon surfaces upon thermal oxidation. *Phys Review B* **1994**, 49, (8), 5415.
27. Lin, Z.; Strother, T.; Cai, W.; Cao, X.; Smith, L. M.; Hamers, R. J., DNA Attachment and Hybridization at the Silicon (100) Surface. *Langmuir* **2002**, 18, (3), 788-796.
28. Webb, L. J.; Michalak, D. J.; Biteen, J. S.; Brunschwig, B. S.; Chan, A. S. Y.; Knapp, D. W.; Meyer, H. M.; Nemanick, E. J.; Traub, M. C.; Lewis, N. S., High-Resolution Soft X-ray Photoelectron Spectroscopic Studies and Scanning Auger Microscopy Studies of the Air Oxidation of Alkylated Silicon(111) Surfaces. *J Phys Chem B* **2006**, 110, (46), 23450-23459.
29. Sugimura, H.; Hozumi, A.; Kameyama, T.; Takai, O., Organosilane self-assembled monolayers formed at the vapour/solid interface. *Surf Interf Anal* **2002**, 34, (1), 550-554.
30. Cao, X.; Hamers, R. J., Silicon Surfaces as Electron Acceptors: Dative Bonding of Amines with Si(001) and Si(111) Surfaces. *J Am Chem Soc* **2001**, 123, (44), 10988-10996.
31. Wagner, C. D.; Muilenberg, G. E., *Handbook of x-ray photoelectron spectroscopy: a reference book of standard data for use in x-ray photoelectron spectroscopy*. Perkin-

Elmer Corp., Physical Electronics Division: 1979.

32. Beamson, G.; Briggs, D., *High resolution XPS of organic polymers: the Scienta ESCA300 database*. Wiley: Chichester [England]; New York, 1992.
33. Yamamoto, K.; Koga, Y.; Fujiwara, S., XPS studies of amorphous SiCN thin films prepared by nitrogen ion-assisted pulsed-laser deposition of SiC target. *Diam & Rel Mater* **2001**, 10, (9-10), 1921-1926.
34. Wong, C. K.; Wong, H.; Filip, V.; Chung, P. S., Bonding structure of silicon oxynitride grown by plasma-enhanced chemical vapor deposition. *Japan J Appl Phys, Part 1: Regular Papers and Short Notes and Review Papers* **2007**, 46, (5 B), 3202-3205.
35. Yegen, E.; Lippitz, A.; Treu, D.; Unger, W. E. S., Derivatization of amino groups by pentafluorobenzaldehyde (PFB) as observed by XPS and NEXAFS spectroscopy on spin coated 4,4'-methylenebis(2,6-diethylaniline) films. *Surf Interf Anal* **2008**, 40, (3-4), 176-179.
36. Cooper, S. L.; Bamford, C. H.; Tsuruta, T. Polymer biomaterials in solution, as interfaces and as solids festschrift honoring the 60th birthday of Dr. Allan S. Hoffman. <http://www.knovel.com/knovel2/Toc.jsp?BookID=1576>
37. Ogawa, H.; Ishikawa, K.; Inomata, C.; Fujimura, S., Initial stage of native oxide growth on hydrogen terminated silicon (111) surfaces. *J Appl Phys* **1996**, 79, (1), 472-477.
38. Wayner, D. D. M.; Wolkow, R. A., Organic modification of hydrogen terminated silicon surfaces. *Journal of the Chemical Society, Perkin Trans 2* **2002**, 2, (1), 23-34.
39. Zuilhof, H.; Rosso-Vasic, M.; Spruijt, E.; van Lagen, B.; De Cola, L., Alkyl-Functionalized Oxide-Free Silicon Nanoparticles: Synthesis and Optical Properties. *Small* **2008**, 4, (10), 1835-1841.
40. Sieval, A. B.; Linke, R.; Zuilhof, H.; Sudholter, E. J. R., High-quality alkyl monolayers on silicon surfaces. *Adv Mater* **2000**, 12, (19), 1457-1460.
41. Sieval, A. B.; Opitz, R.; Maas, H. P. A.; Schoeman, M. G.; Meijer, G.; Vergeldt, F. J.; Zuilhof, H.; Sudholter, E. J. R., Monolayers of 1-alkynes on the H-terminated Si(100) surface. *Langmuir* **2000**, 16, (26), 10359-10368.
42. Sun, Q. Y.; de Smet, L.; van Lagen, B.; Giesbers, M.; Thune, P. C.; van Engelenburg, J.; de Wolf, F. A.; Zuilhof, H.; Sudholter, E. J. R., Covalently attached monolayers on crystalline hydrogen-terminated silicon: Extremely mild attachment by

visible light. *J Am Chem Soc* **2005**, 127, (8), 2514-2523.

43. Perrine, K. A.; Teplyakov, A. V., Reactivity of selectively terminated single crystal silicon surfaces. *Chem Soc Rev* 39, (8), 3256-3274.

44. Chen, S.; Bomer, J. G.; Carlen, E. T.; van den Berg, A., Al₂O₃/Silicon NanoISFET with Near Ideal Nernstian Response. *Nano Lett* 11, (6), 2334-2341.

45. Stauffer, L., Fundamentals of semiconductor C-V measurements. *EE: Evaluation Engineering* **2008**, 47, (12), 20-24.

46. Maupas, H.; Saby, C.; Martelet, C.; Jaffrezic-Renault, N.; Soldatkin, A. P.; Charles, M. H.; Delair, T.; Mandrand, B., Impedance analysis of Si/SiO₂ heterostructures grafted with antibodies: An approach for immunosensor development. *J Electroanal Chem* **1996**, 406, (1-2), 53-58.

47. Souteyrand, E.; Martin, J. R.; Martelet, C., Direct detection of biomolecules by electrochemical impedance measurements. *Sens and Actuat: B. Chemical* **1994**, 20, (1), 63-69.

48. Taing, Meng-Houit. ; Charcaterisation and fabrication of a Multiarray Electrolyte-Insulator-Semiconductor Biosensor, A Phd thesis, Faculty of science, Enviornment, Engineering and Technology, Griffith University, Brisbane, Austraila, 2007.

Chapter 8

Conclusions and future recommendations

This chapter covers the conclusions drawn from the research work done during the last four years and some future recommendations.

I. Conclusions

Silicon-alkyl and Si-amine monolayers were fabricated selectively on (111) surfaces of triangular silicon nanowire field-effect transistor (Si-NW FET) devices to be used as biosensors after subsequent bioconjugations and immobilizations in aqueous solutions. Before tethering of monolayers of any kind on bare silicon surface, preparation of active gate regions of the devices was found to be a very crucial step because of the strong dependence of the monolayer qualities in terms of packing density, uniformity and ability to sustain the surface characteristics against surface oxidation and on surface morphology, and its chemistry and its stability for a reasonable length of time. After formation of the Si-C based or Si-N based monolayers, it was crucial as well to characterize the surface with the help of different techniques such as x-ray photoelectron spectroscopy, fluorescence spectroscopy, scanning electron microscopy, atomic force microscopy and electrical measurements. In chapters 2 and 3, the theoretical background of the work was described including an introduction to Si-NW FET devices, their fabrication, operation and different factors affect the detection sensitivity. Chapter 3 described Si-alkyl based monolayers, their fabrication procedures and effect on device operation. While reviewing these chapters it can be concluded that Si-NW FETs when used as biosensors can be very sensitive for cheap, efficient, label free, fast and real time screening of drugs, cancer biomarkers and viruses, and Si-alkyl monolayers can offer a substantial role in improving device characteristics by reducing limit of detection as a result of selective immobilization, strong field effect due to thin layers.

Chapter 4 described different aspects of cleaning and hydrogen termination of Si-NW FET with the help of different etchants have different resulting Si-NW surface morphologies as well as surface chemistries for planar samples which dictates the ultimate quality of surface modifications and sensing performances. 1% aqueous HF solution cleanly produce hydrogen terminated Si-NW surfaces however resistance to oxidation for a planar silicon surfaces is inferior most probably due to higher surface roughness as compare to nitrogen purged 40% NH_4F etched surface but a thorough

rinse with DI water is strongly recommended in order to get rid of concentrated salt crystals remaining on the surface. Oxygen rich solution can cause pit formation.

Chapter 5 described the selective functionalization of C-Si monolayers on all-(111) surface Si-NWs has been demonstrated, which offers a new Si-NW sensing platform with several advantages for biosensing compared to conventional Si-NW biosensor geometries and silicon dioxide (SiO₂) passivation layers, which includes: 1. Ligands conjugated exclusively on the nanowire surface eliminates ligand conjugation in non-sensor regions, 2. Improved detection sensitivity due to selective functionalities, 3. Si-(111) surfaces support the highest quality C-Si monolayers. 4. Elimination of fixed SiO₂ charge, and 5. Si (111) surfaces can have low interface trap densities for H-Si and C-Si interfaces.

Chapter 6 describes mathematical modeling that reveals that thin dielectric layers result in higher detection sensitivities and three important conclusions can be drawn from this analysis. First, thin ($t_f \sim 1$ nm) dielectric layers in combination with low channel doping ($N_a = 10^{17}$ cm⁻³) results in the largest detection sensitivity, however, over a small range of ψ_0 (or σ_o), and therefore, requires precise front-gate biasing for full utilization. Second, thin dielectric layers and larger channel doping ($N_a = 10^{18}$ cm⁻³) results in slightly lower and more uniform sensitivities. Lastly, a reference electrode is important for providing a well-defined gate potential for device biasing and operation. It should be noted that higher sensitivities can be obtained by moderately accumulating the front surfaces. Chapter 7 introduces a new multifunctional symmetric precursor that is used to form monolayers with a Si-N covalent bond and a pendant amine group for future bioimmobilization. It was realized by repeated experiments and with control samples that Si-N chemistry works well in selective functionalization of patterned surfaces such as silicon nanowires as well showed improved detection capability of biomolecules in electrolyte insulator semiconductor sensor configuration.

II. Future recommendations

A sensing platform constructed out of bottom-up molecular assemblies, crystalline in nature having perfect passivation of dangling bonds and interface states giving flexibly tunable surface properties and selective chemical handles is promising, however, dealing with conventional chemical labs and wet benches is cheaper at one hand and compromise surface qualities on the other hand. Treating surfaces in an nitrogen purged glove box is both cleaner and safe but makes manipulations difficult. Si-NW FET biosensor for detection of trace bioanalytes such as DNA, proteins and viruses need Si-C based monolayer interface for highly sensitive detections. The following recommendation can be made:

- 1) A perfect hydrogen terminated interface free of native or sub-oxide is highly recommended for high quality monolayers. A thermal annealing step in hydrogen environment after etching removes the etch imperfection and non-reacted sites resulting into a relatively stable hydrogen terminated surface.
- 2) Functional monolayers fabricated out of precursor molecules without any protection group and capable of maximum surface coverage is needed. A mixed monolayer having small fraction of bulky functional precursor molecules and a large fraction of inert and small methyl terminated filling molecules is a clever approach.
- 3) Creation/generation of functionalities on the surface of a well packed methyl terminated monolayer with the help of controllable air plasma oxidation and/or UV-Ozone treatment is fruitful as well.
- 4) In-situ generation of hydrogen or chloride terminated surfaces along with exposure of small functional molecules such as azide ions can generate a surface with 100% surface coverage with ability to bind with linker groups and biomolecules.
- 5) It will be interesting to try electrochemical fabrication of Si-alkyl monolayers with the help of diazonium ions.

Summary

The research work was mainly focused on the surface modification/surface functionalization of active-gate areas of silicon nanowire field-effect transistor devices (Si-NW FET) using hydrogen terminated surfaces, Si-C and Si-N bonded monolayers and subsequent bioimmobilization for biosensor applications. Experiments were conducted on planar silicon samples for contact angle measurements and x-ray photoelectron spectroscopy (XPS) for the confirmation of step wise surface modification process. Efficiency of surface amendments/modification on Si-NW FET devices was tested and monitored by scanning electron microscopy (SEM), fluorescence spectroscopy, and atomic force microscopy (AFM) as well as electrical measurements by front and back gating the devices in air and in aqueous solutions. Contact angle measurements are very good to have an immediate idea of surface physical property in terms of hydrophobicity or hydrophilicity. Methyl terminated monolayers give a contact angle nearly equal to 109° where as functional monolayers involving deprotected surface amine groups or carboxylic acid groups show a decrease in contact angle by $20\text{-}40^\circ$ from the starting contact angle value of hydrogen terminated surfaces (84°) after successful surface modification. X-ray photoelectron spectroscopy (XPS) is a very powerful surface technique and is very simple to interpret the chemical environment and chemistry of the different surface groups, their oxidation states in terms of their binding energies as well as comparisons can be made with different binding energy regimes to get a rough guess of the chemical species present on the surface. For example, if a surface involves a monolayer with carbon chain and an amine group, all sort of chemical bonds can be counter checked by comparing the C 1s region with the N 1s region of the spectrum. All monolayers were characterized using XPS and extent of surface oxidation and the stability of monolayer was determined. Si-alkyl monolayers proved to be stable and prevent surface oxidation for a reasonable length of times. Si-C bond can be reasonably

detected via fitted peaks at 283-284 eV range below C-C peak bond energy at 285 eV, but more efficiently for alkyne head group. Well packed monolayers terminated with methyl groups are recommended for further bioimmobilization after generation of functional groups chemically or via UV-ozone or air plasma activation as compared to ones obtained via protected functional groups as bulky groups undermine the oxidative resistance of the surface due to steric hindrances. Mixture of monolayers is also good approach to obtain functional monolayers. XPS was able to reasonably characterize Si-N bonded layers as well. In contrast to ethylene diamine adsorption experiments on silicon under ultrahigh vacuum as reported in a few reports, where both amine groups get attached to neighboring silicon atoms in the form of a molecular staple, giving a single nitrogen peak at 398.7 eV, our results are unique in the solution phase, showing both amine groups have different chemical environments indicated by more than one peak fits where one nitrogen group is shown to attach with the surface and another amine group is free or pendant and ready for subsequent bioimmobilization as also confirmed by fluorescence and biosensing studies. Selective functionalization of Si-NW FETs after successful modification of surfaces and confirmation through contact angle and XPS studies was demonstrated by streptavidin-biotin binding where Streptavidin was conjugated either by gold nanoparticles or Alexa Fluor 488 label to see via SEM or fluorescence spectroscopy, respectively. Si-C and Si-N bonded monolayers showed successful selective bioimmobilization onto the Si-NW gate regions. Monolayers on Si-NW FET were characterized by electrical measurements and a mathematical model was proposed giving guidelines for improved sensitivity of Si-NW FET devices after modification via ultra thin layers and put light on the operation regime where maximum sensitivity can be obtained. Use of a reference electrode was shown to be crucial in order to control surface potential in a narrow potential window and to get perceivable results. Effect of doping level and uniformity of the response of the biosensor was taken into consideration and it has been shown that high sensitivity can be obtained in lower doped nanowires with thinner gate-dielectric films and operating the device at

smaller possible voltages, however, the sensor response is more uniform at higher doping levels. Biosensing via Si-N bonded monolayers was shown electrically in electrolyte-insulator-semiconductor (EIS) biosensor configuration and showed improved sensitivity of streptavidin-biotin binding event as compared to sensing on oxide surface via APTES based bioimmobilization.

Publications

- 1) M. Masood, S. Chen, E.T. Carlen, A. van den Berg, All-(111) Surface Silicon Nanowires: Selective Functionalization for Biosensing Applications, *ACS Appl. Mater. Interfaces*, 2010 2, 3422, DOI: [10.1021/am100922e](https://doi.org/10.1021/am100922e).
- 2) Shahid Bilal Butt, Muhammad Nasir Masood, FIA of Phenol and Pentachlorophenol at glassy Carbon electrode in Oxidative mode, *Journal of the Chemical Society of Pakistan*, 2008, 30, 75-80.

Conference Papers:

- 3) M. Masood, S. Chen, E.T. Carlen, A. Van den Berg, Selective Biofunctionalization all-Si (111) Surface Silicon Nanowires, in *Biosurfaces and Biointerfaces*, edited by J.A. Garrido, E. Johnston, C. Werner, T. Boland (Mater. Res. Soc. Symp. Proc. 1236E, Warrendale, PA, 2010), 1236-SS08-22.
- 4) Masood, M. N. Songyue, C. Carlen, E. T. Albert, Van. Berg, D13. (2010) MME2010 Abstracts: 21st Micromechanics and Micro systems Europe Workshop. University of Twente, Transducers Science and Technology, Enschede, the Netherlands. ISBN 978-9081673716 (<http://eprints.eemcs.utwente.nl/19346/01/MME2011.pdf>)

Acknowledgements

All worthy of praise is Allah Subhan-Wataala who has created all of the seven universes and the universe within which we live in is decorated with stars and each star and satellite has its own trajectory and they seldom collide with each other. He is He who made the human best of His creatures and granted him wisdom and passion to find the truth. He is Who granted man with mind to think, eyes to look, hands to work and billions of other blessings if man miss only one, he become arrogant and thankless but if gets all, forgets his creator at all!!

First of all I am thankful to my Allah who made me able to do all the things for my studies and these thanks will not be accepted completely in front of Allah if I should not pay thanks to my promoter prof. Dr. Albert van den Berg through whom Allah made my way to Netherlands for PhD. His kind behavior is like a brother, a vibrant leader and a guide in the group. We enjoyed barbeque parties at his home and it was a very nice platform for a yearly based talk and get-together. I will like to make special thanks to my daily supervisor Dr. Edwin Carlen as I shall not be able to complete this work without his encouragement and guidance. We had a lot of discussions on all the topics whether scientific or social during the last four years which were very informative and interesting and definitely I learned all aspects of research from him. I will like to pay special thanks to the graduation committee members who read the thesis for its evaluation and recommendations. Great thanks to Higher Education Commission (HEC) Pakistan for granting scholarship for four years and to PINSTECH for supporting my family at home. I will also like to pay a great thanks to Mrs. Wasim Yawar (Head Central Analytical Facility Division) and Dr. Shahid Bilal Butt (group leader chromatography) for allowing me to pursue a PhD degree and Yasir Arafat and Babar for looking after some of official matters. It is very necessary to pay special thanks to prof. Dr. Albert van den Berg and Dr. Edwin Carlen again for arranging scholarship for extra three months and made the completion of the thesis possible.

The last four years which I passed in the Bios group as well as in Netherlands was a

great experience of my life. I will like to pay thanks to all of my group fellows from whom I learned a lot in morning talks and technical discussion meetings. I will like to acknowledge specially Paul, Jan Nieuwkastele, Johan Bomer, and Hans de Boer for giving me all the technical help whenever required for my work. It will be also very important to make a word of thanks to Eddy de Weerd, Dr. Ad J. Sprenkeles, Dr. Mathieu Odijk, Dr. Lingling Shui, Dr. Wouter Sparreboom, Dr. Egbert, Dr. Ganeshram and Dr. Severine to help me at different occasions. I should also pay special thanks to Dr. Songyue Chen as I learned a lot at the start of my work from her. Thanks to my room mates Mingliang, Yanboo and Rerngchai for their co-operative behaviour all the time and company as well as nice discussions. I will like to pay special thanks to Arpita for her co-operation during work. Special thanks also to Dr. Iris and Verena Stimberg for managing Monday talks for various situations. I am thankful to Dr. Justyna, Dr. Egbert and Dr. Jan Eijkel and Dr. Wouter Olthuis for discussions/ talks at different occasions. I will like to pay thanks to workweek committees for Switzerland and USA. I will also like to acknowledge fully the XPS expert Gerard Kip who provided me a great help for all the XPS measurements. A special thanks to Mark Smither for SEM imaging. Glass blowing facility should also be acknowledged greatly for providing help. I will like to acknowledge all my group fellows in Bios as well as in whole of the EWI faculty for help and a very special acknowledgement for Hermine for helping me for official matters.

I will also like to acknowledge all the Muslim fellows who were here in Enschede and at the university for their company and help. Specially Hammad Nazir for cooking guidelines, Mudassir for giving company to visit masjid for prayers, Kazmi, Saqib, Rauf, Sohail Niazi, Zaigum Umer, Akram Raza, Sajid Khan, Naveed , Ahmad (Jordan), Muhammad Khateeb, and Ahmad (Hanbali), Hammad Fayyaz and all other PSA members. With Akram Raza I had many nice discussions and it was a good experience. Rashid Nazir was one of my friends in Amsterdam and we had nice talks via Skype off and on which was good to share ideas for which I am thankful to him. I am thankful to all the brothers in University of Twente Muslim group for arranging the facility of Jumma prayer at the campus and I should acknowledge university authorities for

providing prayer hall and ablution place for this purpose. I should acknowledge and pray to sheikh Omer khalil (May Allah rest his soul in peace and grant him paradise) for giving nice sermons in Jumma prayers. I am also thankful to all other fellow khateebis in this regard and U-Twente Muslim board for arranging different activities.

I will like to make great thanks to my all of the family members including my parents, wife, sisters, son and daughter for having so much patience and wait for me during four years. Special thanks to father in law and mother in law for helping me out and brother Zulqurnain during this time. Special acknowledgements to my uncle Hamid Saeed, Shahid Maqsood and Hamid Mehmood for looking after different matters at home during my absence. I am very thankful to my parents whose prayers remain always with me and after Allah subhan watalaa whatever I am, if I have some quality it is all due to my parents (by the will of Allah) and if I am bad, it is all due to myself. May Allah grant paradise to my late Father who was waiting for me however this is actually the fact of life and we all should all be ready for it.

Muhammad Nasir Masood

Curriculum Vitae

Muhammad Nasir Masood was born in Khair-Pur Mirs Sindh, Pakistan at 25th of November 1976. After finishing his higher secondary school education he started his undergraduate studies at Government College Shaiwal, where he got a two years bachelor degree in Science and went to Bahauud-din-Zakariya University Multan for further studies where he got masters degree in Chemistry with distinction in year 2000. In year 2001, he joined Pakistan Institute of Engineering and Applied Sciences Islamabad (PIEAS) as a fellow and did masters in Nuclear Engineering in 2003. He started to work as a junior scientist in a Chromatography lab in Islamabad and worked there for four years before starting PhD studies at University of Twente in September 2007.